

CHAPTER 4. SYNTHESIS OF NATURAL OLIGOMERIC STILBENOID AND ANALOGUES

As mentioned above, stilbene oxidation was carried out with two different techniques: electrochemical oxidation reported in Chapter 3 and *via* various chemical oxidants in different solvents. The objectives of using these two approaches are to be able to compare their respective merits and develop a biomimetic approach that would mimic what nature does as closely as possible. A comprehensive literature review will summarize published biomimetic oligostilbenoid syntheses based on the author's approaches as well as non-biomimetic syntheses. This is followed by the results obtained in this study and discussions on establishing the mechanisms involved in the oxidative formation of oligostilbenoids. A comparison will be made with results obtained in the preceding chapter. The structures of prepared oligostilbenoids are confirmed by spectroscopic measurements and/or by comparing with reported spectroscopic data in the literature. Finally, this chapter is completed with an overall conclusion and experimental procedures for oligostilbenoid preparation.

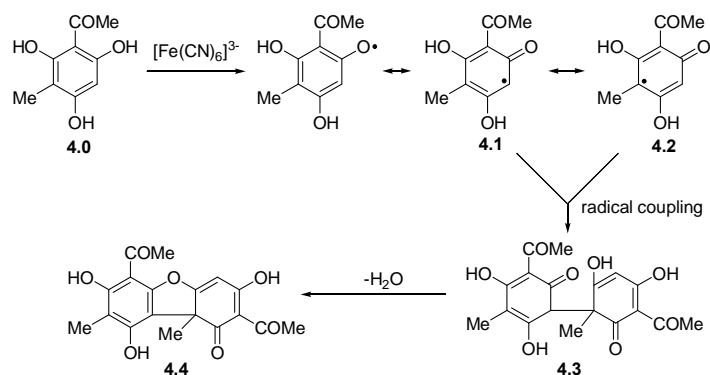
4.1. Oligostilbenoid biomimetic syntheses

The work presented below was initiated by the various chemists for different purposes. In some cases the objective was to obtain chemical correlations in order to support proposed structures for newly isolated oligostilbenes. In other instances, metabolic biotransformation of (oligo)stilbenoid alexins by pathogens and/or oxidases was the focus of the investigations. Finally, some groups attempted the biomimetic

synthesis of oligostilbenoids as an obvious preparative method. Notwithstanding their objectives, biomimetic syntheses will be presented below by the type of condensing agent, *i.e.* biological agents (cells or enzymes) or chemical reagents, including one electron oxidants and acid catalysts. Before we examine these works it might be useful, however, to concisely review oligostilbenoid biosynthesis.

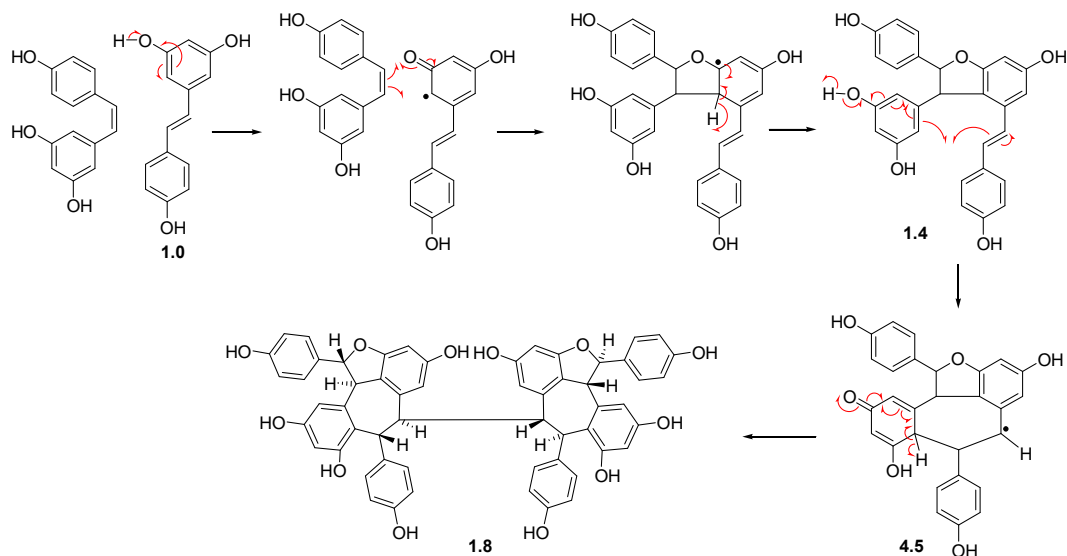
4.1.1. Biosynthesis of oligostilbenoids

The biosynthesis of oligostilbenoids has never been the subject of detailed investigation in spite of the fact that the structures of these compounds leave few doubts concerning the general mechanism of their biogenesis, which is likely to proceed through phenolic oxidative coupling. This fundamental mechanism, by which a number of natural compounds are believed to be constructed in plants *via* the coupling of phenolate radicals, was first described by D.H.R. Barton and co-workers in 1956.¹ In a seminal study illustrating this coupling, Barton *et al.* described the synthesis of usnic acid **4.4** (a secondary lichen metabolite) (Scheme 4.1). The *ortho*- and *para*-phenolic carbon radicals **4.1** and **4.2** respectively, generated by the action of one-electron oxidant ferricyanide on methylphloracetophenone **4.0**, dimerised to produce intermediate species **4.3**, thus generating new carbon-oxygen and carbon-carbon bonds.^{1,2}



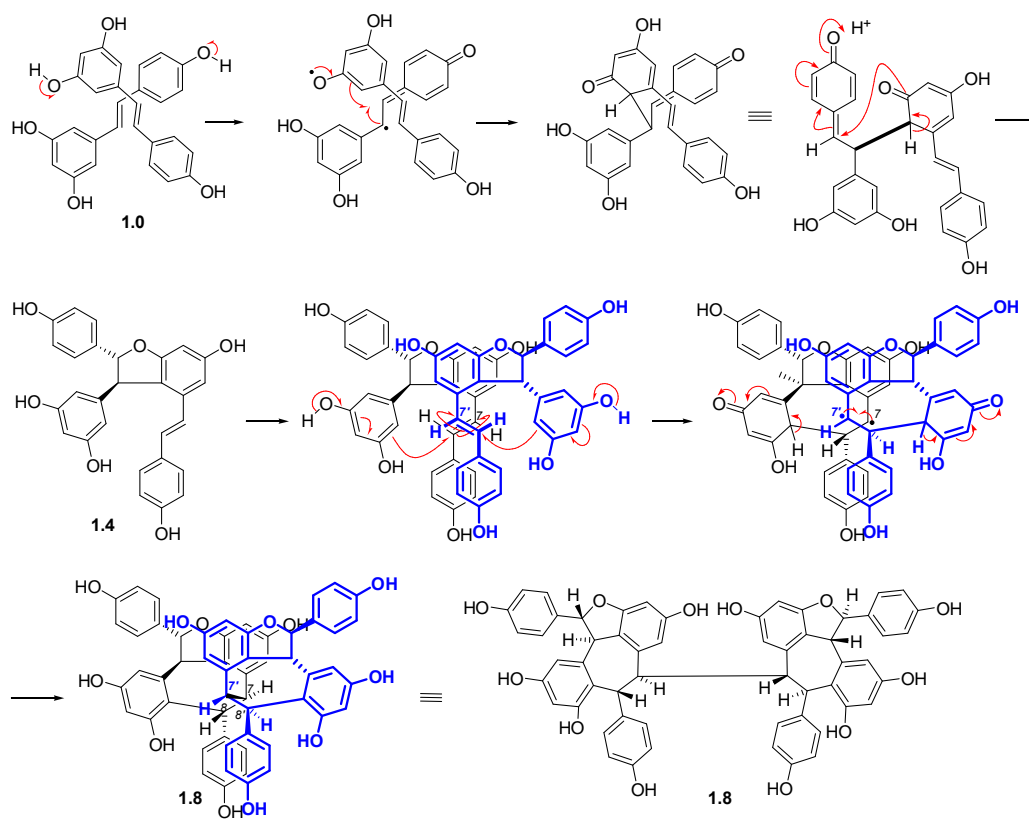
Scheme 4.1: Synthesis of usnic acid (adapted from references 1 and 2).

This concept can also be applied to the biosynthesis of oligostilbenoids. In their 1993 review, Sotheeswaran and Pasupathy proposed that tetrameric hopeaphenol **1.8** could result from a succession of radical couplings, the first occurring between two resveratrol units **1.0**.³ The resulting ϵ -viniferin **1.4** would then undergo an intramolecular coupling leading to dibenzocycloheptane radical species **4.5**. The coupling of two such radicals would lead to hopeaphenol **1.8** (Scheme 4.2).



Scheme 4.2: Sotheeswaran & Pasupathy's proposed biosynthesis of hopeaphenol **1.8** (adapted from reference 3).

It is known that oligostilbenes derive from monomeric stilbenes and that radicals are key intermediate species. It would be possible to present an improved version of Sotheeswaran and Pasupathy's Scheme on hopeaphenol biosynthesis in Scheme 4.3. Yet, whether the 7-membered rings are formed before or after the dimerisation of ϵ -viniferin radical species is an open debate. Similar approaches have been used to postulate on the biosynthetic pathways of various other stilbene oligomers.^{4,5}



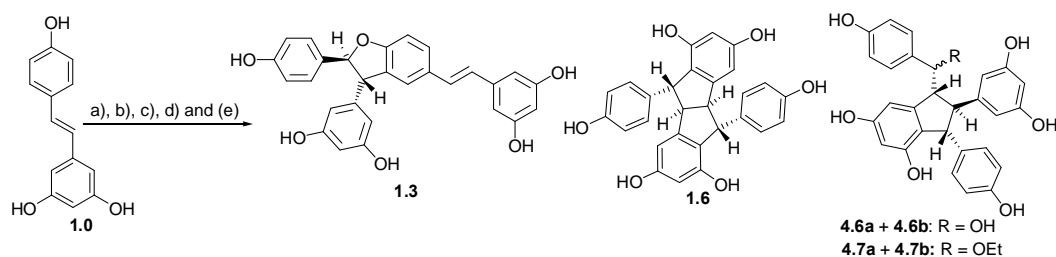
Scheme 4.3: Revised proposal for the biosynthesis of hopeaphenol **1.8** through ϵ -viniferin **1.4**.

4.1.2. Biotransformation and enzymatic coupling

Two types of enzymes, peroxidases and laccases, were used to biotransform resveratrol **1.0** and its analogues (inclusive of stilbene dimers). Peroxidases contain iron at their active site whereas copper is the cofactor in the case of the laccases.⁶ These ions function as mediators in electron transfer chains. How the enzyme type influences product formation is still not well understood. The work of the various investigators is therefore presented below according to the substrate.

4.1.2.1. Resveratrol, pterostilbene and their analogues

Two groups, led respectively by Niwa⁷ and Hou⁸, have subjected resveratrol **1.0** or its analogues to peroxidases. The approaches were different. Niwa had selected the ϵ -viniferin **1.4** as his target *via* resveratrol **1.0**, while Hou specifically targeted quadrangularin A **4.10** from a suitably modified resveratrol as starting material. Niwa treated **1.0** with several commercially available peroxidases from soybean, fungus and horseradish. It was hypothesized that **1.0** is dimerised in plant cells oxidatively by peroxidases or phenoloxidasases to produce ϵ -viniferin **1.4**. The above listed peroxidases were therefore used in mixtures of acetone/water as well as ethanol/water. In all cases (\pm)- ϵ -viniferin **1.3** and (\pm)-pallidol **1.6** were obtained as major products (Scheme 4.4). A mixture of (\pm)-leachianols F **4.6a** and G **4.6b** and a mixture of (\pm)-quadrangularins B **4.7a** and C **4.7b** were produced as minor compounds in presence of the fungal peroxidase.

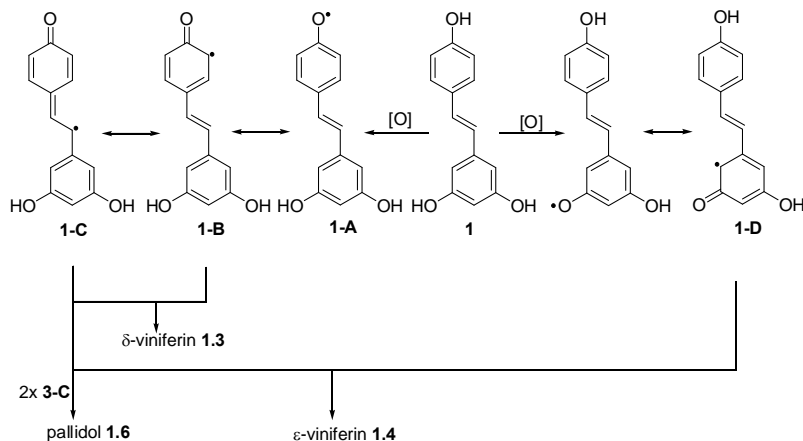


Reaction	Origin of peroxidases	Solvent	Yield (%)			
			1.3	1.6	4.6	4.7
a.	Horseradish	Acetone/0.5 M phosphate buffer (pH 6.0) (1:1, v/v)	12.6	10.2		
b.	Soya	Acetone/0.5 M phosphate buffer (pH 6.0) (1:1, v/v)	21.4	7.2	1.8	
c.	Soya	EtOH/0.5 M phosphate buffer (pH 6.0) (1:1, v/v)	12.1	9.5	5.2	8.6
d.	Fungus (<i>Arthromyces ramosus</i>)	Acetone/0.5 M phosphate buffer (pH 6.0) (1:1, v/v)	18.4	7.4	4.6	
e.	Fungus (<i>Arthromyces ramosus</i>)	EtOH/0.5 M phosphate buffer (pH 6.0) (1:1, v/v)	13.1	5.0	4.6	8.2

Scheme 4.4: Conversion of resveratrol into its dimers by peroxidases from different sources (adapted from reference 7).

In Niwa's opinion, resveratrol **1.0** oxidation can lead to three radical intermediates species **1-B**, **1-C** and **1-D** (Scheme 4.5). ϵ -Viniferin **1.4** would derive from intermediates **1-C** + **1-D**, pallidol **63** from **1-C** + **1-C**, while δ -viniferin **1.3**

would result from **1-B** + **1-C**. Since no ϵ -viniferin **1.4** was observed in his series of experiments, he concluded that intermediate **1-D** was not generated by these enzymes.



Scheme 4.5: Proposed radical intermediates involved in resveratrol oxidative coupling (adapted from reference 7).

In contrast to Niwa's work, Langcake *et al.*⁹ and Hirano *et al.*¹⁰ obtained not only (*E*)- δ -viniferin **1.3** but also its (*Z*)-isomer **1.3b** (Figure 4.1) when a combination of horseradish peroxidase-hydrogen peroxide was applied to resveratrol **1.0**. It could be argued that a (*Z*)-stilbene moiety would arise from photoisomerization as a result from excessive exposure of (*E*)-products to light.

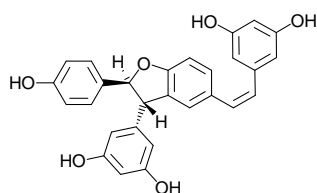
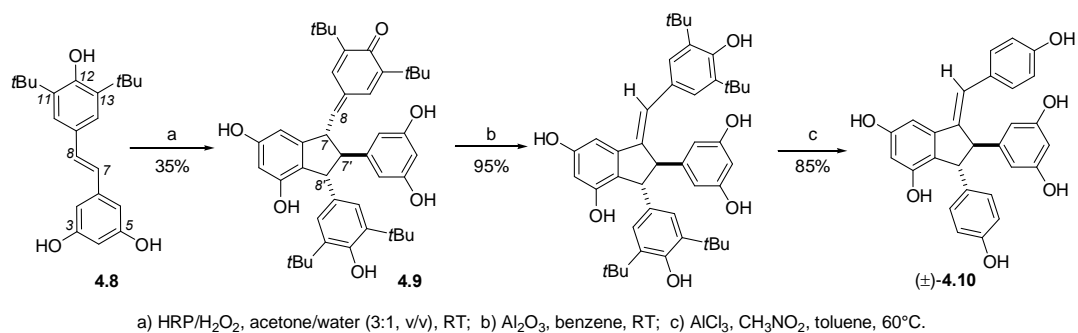


Figure 4.1: (*Z*)- δ -viniferin **1.3b**

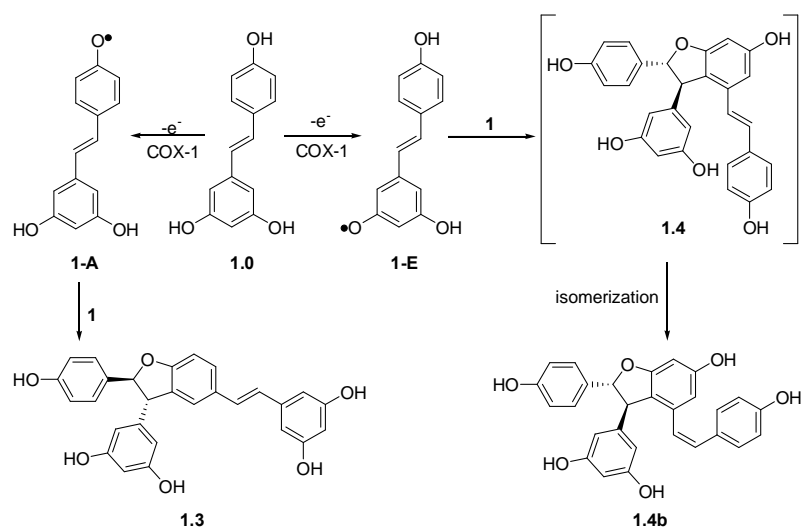
Hou's group reported the total synthesis of (\pm)-quadrangularin A **4.10** regioselectively in 11 steps with 15% overall yield (Scheme 4.6).⁸ These authors anticipated that regioselective oxidative coupling could be achieved by introducing

bulky substituents like *tert*-butyl groups at C11 and C13 of resveratrol in order to block these reactive sites. This would result in promoting the coupling of radicals C7-C7 ϕ instead of the undesired C11-C7 ϕ radical coupling that predominantly occurs and produces δ -viniferin type of product. Thus, **4.8** was prepared and subjected to horseradish peroxidase (HRP) and hydrogen peroxide in aqueous acetone to produce **4.9** (35% yield). (\pm)-Quadrangularin A **4.10** was finally obtained in two additional chemical steps.



Scheme 4.6: Synthesis of quadrangularin A **4.10** from substituted resveratrol **4.8** (adapted from reference 8).

Penning and co-workers (2005)¹¹ reported the oxidation of resveratrol **1.0** *via* COX-1 peroxidase (from mammalian cells). This resulted in the formation of two major resveratrol dimers possessing benzofuran moieties namely (*E*)- δ -viniferin **1.3** and (*Z*)- ϵ -viniferin **1.4b**. They believed that, during the oxidation process, two types of radicals are generated, **1-A** and **1-E** (Scheme 4.7), which are responsible for the formation of (*Z*)- ϵ -viniferin **1.4b** and (*E*)- δ -viniferin **1.3** respectively.



Scheme 4.7: Oxidation of resveratrol **1.0** via COX-1 peroxidase (adapted from reference 11).

Pezet¹² and three other groups, namely Breuil *et al.*,¹³ Cichewicz *et al.*,¹⁴ and Nicotra *et al.*,¹⁵ biotransformed resveratrol **1.0** and some unnatural stilbenes with help of laccases. These enzymes can be found in fungi, some bacteria and higher plants. They have an active site consisting of a metallic cluster of four copper atoms. All of them are believed to be involved in the redox process that promotes the radical cyclisation mechanism. As a result, various products were obtained with skeletons built around tetrahydrofuran, dihydrobenzofuran, benzodioxane and dihydronaphthalene scaffolds.

Botrytis cinerea was reported in 1991 to produce a laccase-like stilbene oxidase able to metabolize resveratrol.¹⁶ Pezet showed in 1998 that resveratrol **1.0** was dimerised to ϵ -viniferin **1.4** by a purified laccase from *B. cinerea*.¹² The result was obtained by comparing HPLC retention times of the biotransformation product and that of an authentic sample. The validity of these results could be questioned as this report is the only one to the best of our knowledge to mention ϵ -viniferin **1.4** as an enzymatic product. Identical retention times from a single chromatographic procedure

are not considered as a strong argument to positively identify compounds, especially when regioisomers are taken into account.

Breuil and co-workers incubated resveratrol in culture filtrates of *B. cinerea* for 15 days in ethanol to afford (*E*)- δ -viniferin **1.3** and its (*Z*)-isomer **1.3a**.¹³ Interestingly, the same results were obtained with HRP/H₂O₂-promoted dimerisation of resveratrol as reported by Langcake and Pryce.⁹

Cichewicz and co-workers subjected resveratrol **1.0** to growing incubations of *B. cinerea* and *B. allii* in DMF for two days.¹⁴ The most productive experiment was obtained with *B. cinerea* ATCC11542. This biotransformation produced three new metabolites, restrytisols A **4.11**, B **4.12** and C **4.13** (Figure 4.2), together with three known compounds, δ -viniferin **1.3** (major compound), pallidol **1.6** and leachianol F **4.6a**. The types of strain as well as culture conditions play however a major role in the biotransformation of hydroxystilbenes. This suggests that different laccases or laccase isoforms might participate to the resveratrol dimerisation.

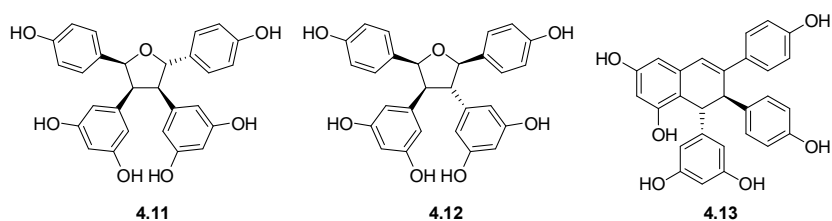
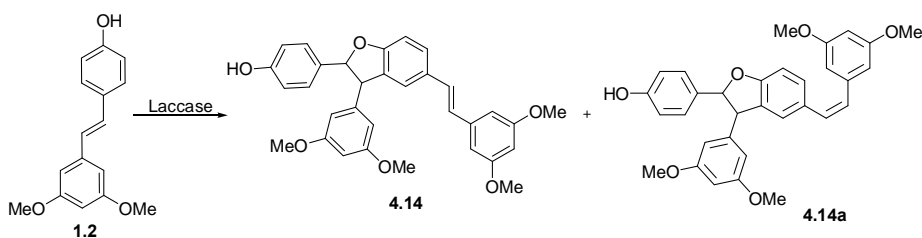


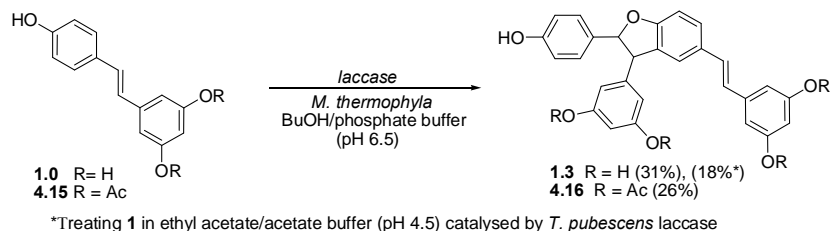
Figure 4.2: Structures of restrytisol A **4.11**, restrytisol B **4.12** and restrytisol C **4.13**.

Breuil and co-workers (1999) dimerised pterostilbene **1.2** with laccases providing a δ -viniferin type compound named pterostilbene *trans*-dehyrodimer **4.14** and as well as its *Z*-isomer **4.14a** (Scheme 4.8).¹⁷



Scheme 4.8: Dimerisation of pterostilbene **1.2** (adapted from reference 17).

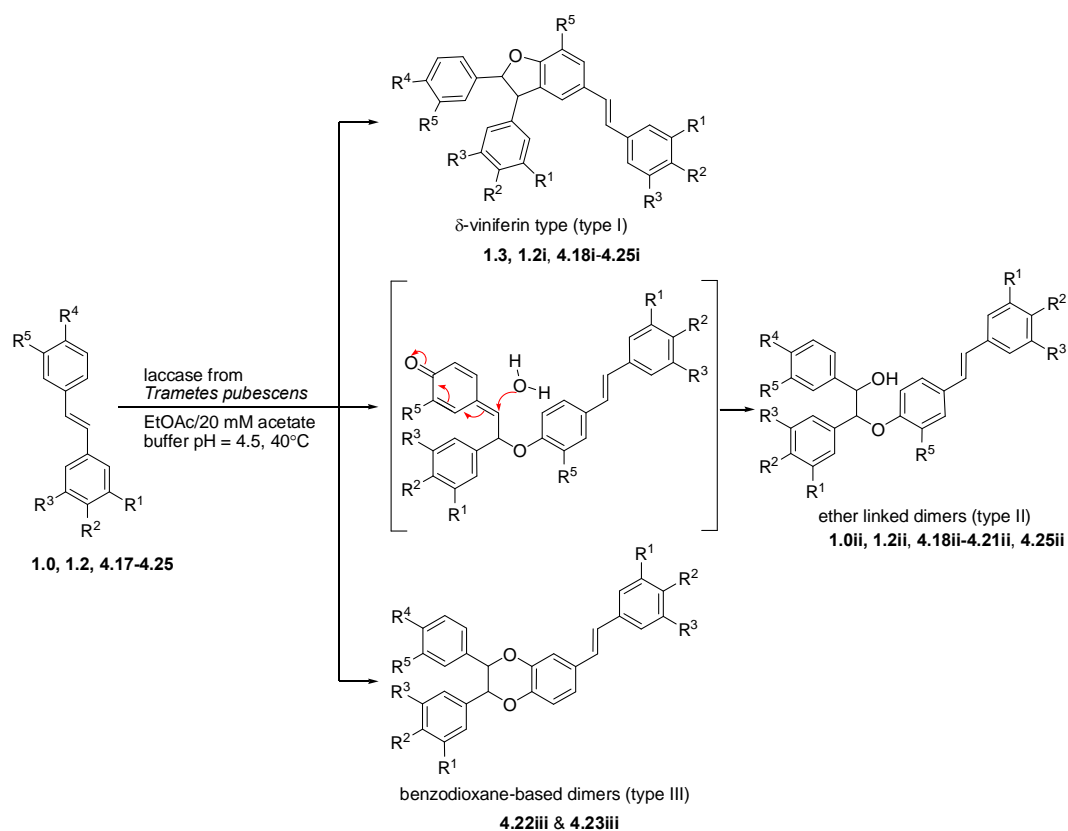
Fortiø group (2004) reported the laccase enzymatic oxidative coupling of resveratrol **1.0** into δ -viniferin **1.3** on a preparative-scale.¹⁵ Subjecting a resveratrol **1.0** solution in a butanol/phosphate buffer (pH 6.5) shaken for four days in presence of a laccase (from *Myceliophthora thermophila*) supported on glass beads resulted in δ -viniferin **1.3** in 31% yield. Tetraacetoxy- δ -viniferin analogue **4.16** is obtained (Scheme 4.9) when resveratrol **1.0** is replaced by its 3,5-diacetoxy derivative **4.15** (with free 12-OH group). However, using 12-*O*-methylresveratrol **4.17** did not lead to any biotransformation product. Logically, the authors concluded that the laccase-mediated oxidation of resveratrol takes place at the *para* 12-OH.



Scheme 4.9: Stilbene dimerisation by laccases from two different fungi *T. pubescens* and *M. thermophyla* (adapted from reference 15)

In 2007, the same group reported that the best reaction conditions were obtained in the presence of a laccase from *Trametes pubescens* in a biphasic system made of ethyl acetate containing the substrate and an aqueous phase (acetate buffer, pH 4.5).⁶ A series of hydroxystilbenes were tested affording three different types of

skeletons of substituted δ -viniferin type (type I), ether linked dimers (type II) and benzodioxane-based dimers (type III), (Scheme 4.10). Stilbenes **4.18**, **4.19**, **1.2**, **4.20** and **4.21** contain only one reactive phenolic OH group, which is responsible for the formation of types I and II structures. Stilbenes with catechol phenolic substitutions **4.22** and **4.23** are converted into type I and III structures. Compound **4.24** with two *para*-OH groups produced two different *trans*-dihydrofuran based dimers depending on which phenolic ring is involved in the benzofuran ring. The authors proposed that stilbene dimerisation occurred through a radical-radical coupling mechanism whereby the oxidation of the phenolic group takes place at the *para* 12-OH position of the stilbene and not through the radical addition to the double bond of a neutral species. In an attempt to verify this mechanism, mixtures of two different stilbenes were subjected to a series of laccase-mediated oxidation. As they expected, the reaction between equimolar amounts of the supposedly reactive resveratrol **1.0** and unreactive methoxystilbene **4.17** gave solely the dimeric products of resveratrol **1.3** and **1.0ii**. In the same manner, reacting **4.23** (quite reactive) and **4.19** (less reactive) in equimolar amounts produced only the dimeric product of the more reactive stilbene (**4.23i** and **4.23iii**). They proposed that the type I skeleton would derive from radical intermediates **1-B** + **1-C** (see Scheme 4.5), type II from species **1-A** + **1-C** followed by addition of a water molecule to the quinone intermediate and type III from the same species **1-A** + **1-C**. Even though the proposed mechanism was in agreement with most of the literature reports, it is in contrast to the hypothesis suggested by Penning and co-workers¹¹ by which dimerisation of resveratrol occurs *via* coupling between a radical and a neutral species.



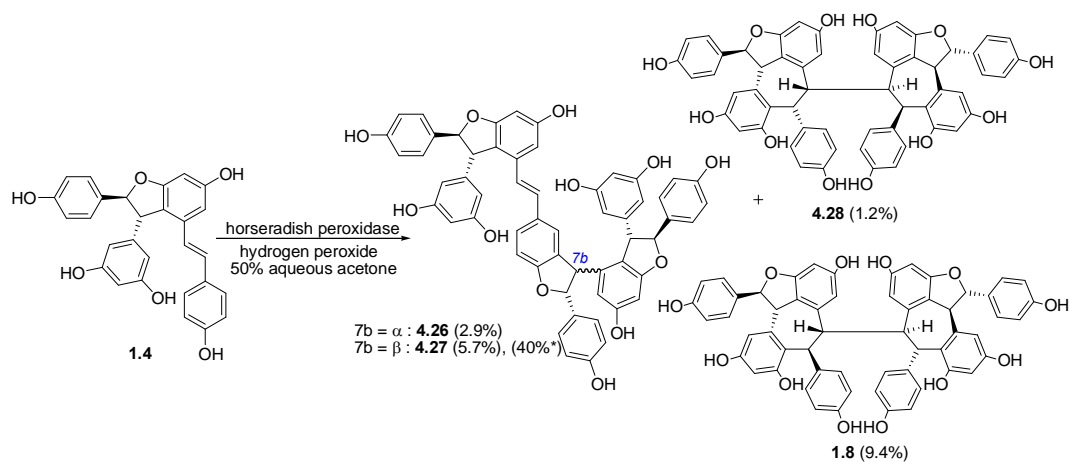
Substrate	R ¹	R ²	R ³	R ⁴	R ⁵	Products		
						Type I	Type II	Type III
1.0	OH	H	OH	OH	H	1.3	1.0ii	-
1.2	OCH ₃	H	OCH ₃	OH	H	1.2i	1.2ii	-
4.17	OH	H	OH	OCH ₃	H	-	-	-
4.18	H	OCH ₃	H	OH	H	4.18i	4.18ii	-
4.19	H	H	H	OH	H	4.19i	4.19ii	-
4.20	OCH ₃	OCH ₃	H	OH	H	4.20i	4.20ii	-
4.21	H	OCH ₃	H	OH	OCH ₃	4.21i	4.21ii	-
4.22	H	OH	H	OH	OH	4.22i	-	4.22iii
4.23	H	OCH ₃	H	OH	OH	4.23i	-	4.23iii
4.24	H	OH	H	OH	OCH ₃	4.24i	-	-
4.25	H	OH	H	OH	H	4.25i	4.25ii	-

Scheme 4.10: Stilbene dimerisation by laccase from *T. pubescens* (adapted from reference 6).

4.1.2.2. Oligostilbenoid/stilbene dimers

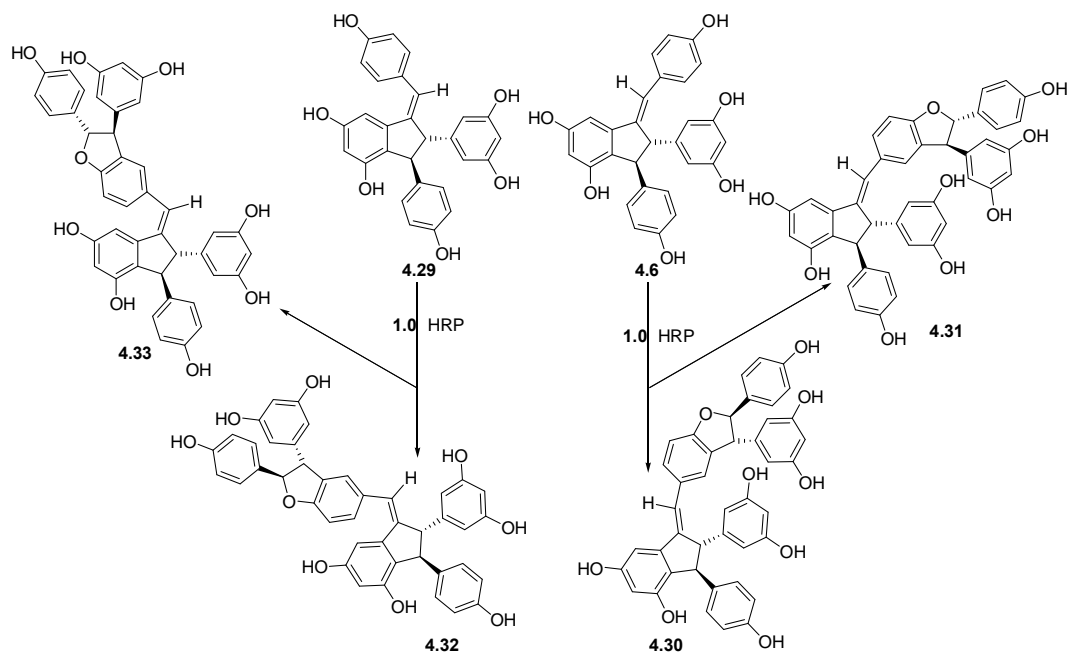
In view of establishing the absolute configuration of vitisin C **4.26** (a resveratrol tetramer) Niwaø group treated (+)- -viniferin **1.4** with HRP and hydrogen peroxide in 50% aqueous acetone for 15 minutes.¹⁸ (-)-Vitisin B **4.26** and (+)-vitisin C **4.27** were obtained in 5% and 4% yields respectively. Reinvestigation of the above

reaction under similar conditions gave (+)-hopeaphenol **1.8** (9.4%) and (-)-isohopeaphenol **4.28** (1.2%) in addition to (-)-vitisin B **4.26** and (+)-vitisin C **4.27** in 5.7% and 2.9% yields respectively (Scheme 4.11).⁴



Scheme 4.11: Biotransformation products of ϵ -viniferin by HRP/H₂O₂; ***1.4** was subjected to AgOAc in dry methanol, see section 3.4.5. (adapted from references 4 & 23*).

He *et al.* reported the biomimetic transformation of (-)-quadrangularin A **4.6** and its *cis* isomer (-)-parthenocissin A **4.29** via enzymatic oxidative coupling (Scheme 4.12) and their photocatalyzed cyclisation (see section 3.9).¹⁹ Treatment of **4.6** with **1.0**, HRP and H₂O₂ in aqueous acetone, afforded novel trimers (-)-laetevirenole D **4.30** and (+)-laetevirenole C **4.31** each in 14% yield (Scheme 4.12). Trimers (-)-parthenocissin B **4.32** and (+)-laetevirenole E **4.33** were obtained in the same conditions from **4.29** in 15% yield each. The above results were in agreement with the authors' biogenetic considerations, whereby the trimer was the product of the oxidative coupling of a dimer and a monomer, *e.g.* **1.0**.



Scheme 4.12: HRP-mediated condensation of stilbenoid dimers with resveratrol **1.0** (adapted from reference 19).

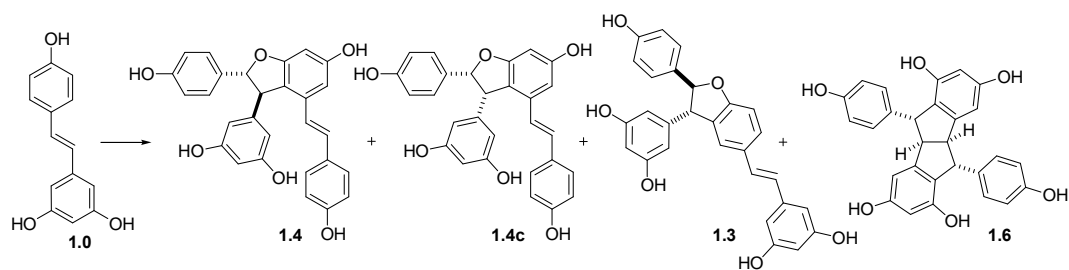
In summary, two types of enzymes, peroxidases and laccases, were used to biotransform resveratrol and its analogues inclusive of the stilbene dimers. When stilbene monomers are subjected to peroxidases, three different types of stilbene dimers consisting of benzofuran, indene and dibenzooctahydropentalene (pallidol type) moieties are produced. Stilbene trimers with benzofuran moieties are obtained by exposing dimers with an exocyclic tri-substituted olefin to resveratrol in presence of a peroxidase. However, 1,2-disubstituted olefin-containing dimers (ϵ -viniferin type) would condense into tetrameric species in the same conditions. In contrast, laccases convert resveratrol and analogues into dimers with furan, benzodioxane and tetralin ring systems in addition to benzofuran-based structures. Benzofuran seems to be a common scaffold obtained as a biotransformation product in all cases. Surprisingly, these enzymes produce only the δ -viniferin type, which does not occur in plants, and not its widespread natural regioisomer, ϵ -viniferin.

4.1.3. Oxidative coupling with Fe³⁺

Naturally occurring resveratrol and isorhapontigenin as well as synthetic protected stilbenoids were dimerised by the one electron oxidant Fe³⁺ {FeCl₃.6H₂O and K₃[Fe(CN)₆]} in different solvents. This resulted in the formation of different benzofuran regioisomers mainly of δ -viniferin and ϵ -viniferin type, pallidol- and restrytisol C-like skeletons.

4.1.3.1. Resveratrol

Lin and co-workers reported that ϵ -viniferin **1.4** was obtained in 30.2% yield in water/methanol mixture when subjecting resveratrol **1.0** to FeCl₃.6H₂O oxidative coupling.^{20,21} In another report in 2000, this group obtained not only **1.4** but also *syn*- ϵ -viniferin **1.4c** in FeCl₃/MeOH oxidation condition of **1.0**.²² Sako *et al.* treatment of **1.0** with K₃[Fe(CN)₆] in a phosphate buffer (pH 5.5)/MeCN mixture resulted solely in δ -viniferin **1.3** in 40% yield.²³ When Niwa's group exposed **1.0** to the same oxidant as above but in a mixture of methanol and water affording ϵ -viniferin **1.4** (21.9%), δ -viniferin **1.3** (22.5%) and pallidol **1.6** (15.7%).⁷ However, when they replaced K₃[Fe(CN)₆] by FeCl₃ in acetone, the yield of δ -viniferin **1.3** was increased to 97% (Scheme 4.13), while the yields of ϵ -viniferin **1.4** and pallidol **1.6** were reduced to 0.9% and 1.5% respectively.



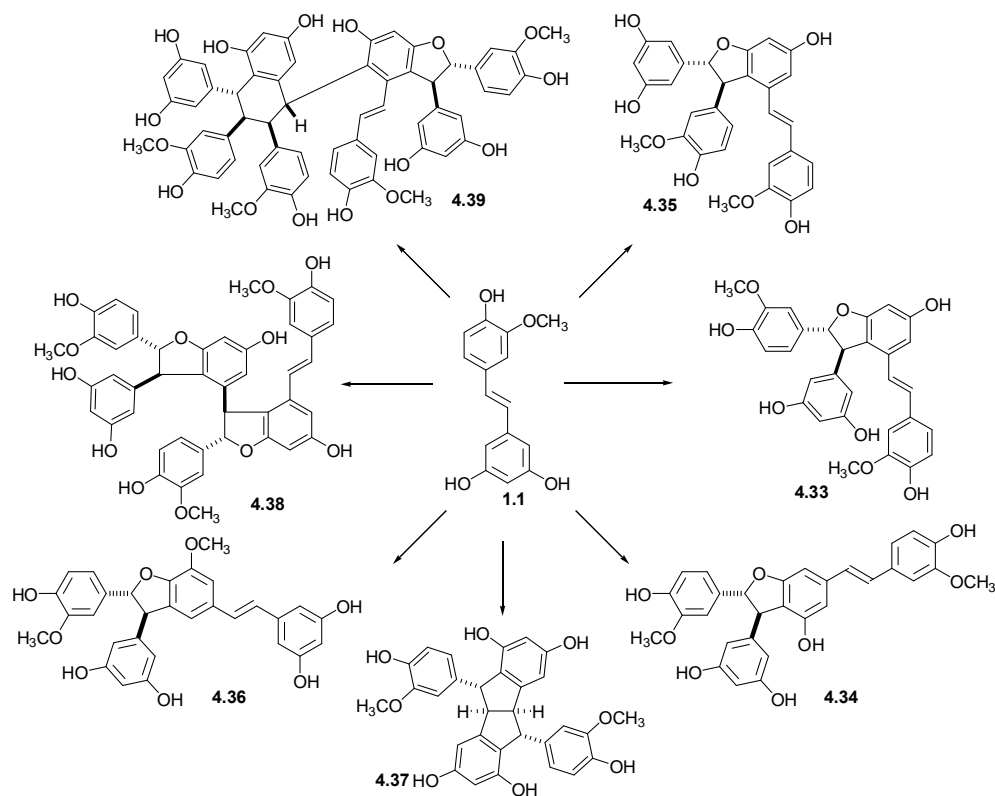
Reaction	Conditions	Yield (%)				Reference
		1.4	1.4c	1.3	1.6	
a.	FeCl ₃ ; acetone	0.9	-	97	1.5	[48]
b.	K ₃ [Fe(CN) ₆]; K ₂ CO ₃ ; MeOH/H ₂ O (2:1 v/v)	21.9	-	22.5	15.7	[48]
c.	FeCl ₃ ·6H ₂ O; MeOH/H ₂ O (1.3:1 v/v)	30.2	-	-	-	[61, 62]
d.	FeCl ₃ /MeOH	nr	nr	-	-	[63]
e.	K ₃ Fe(CN) ₆ ; 0.1 M phosphate buffer (pH 5.5)/MeCN (1:1, v/v); 50°C	-	-	40	-	[64]

Scheme 4.13: Fe³⁺ oxidative coupling of resveratrol (adapted from references 7, 21-23).

4.1.3.2. Isorhapontigenin

Lin and co-workers treated naturally available stilbene (*E*)-isorhapontigenin **1.1** with FeCl₃ in a mixture of acetone/water and obtained ten products: four of them were benzofuran based regioisomers, one pallidol-like skeleton **4.37** together with a trimer **4.38** and a tetramer **4.39** built on tetralin and on -viniferin scaffolds (Scheme 4.14).²⁴ The three benzofuran-based regioisomers bisisorhapontigenins A **4.33**, B **4.34** (major compounds) and C **4.35** (minor compound) involve the resorcinol ring for the formation of the benzofuran group while shegansu B **4.36** (major compound) is a δ -viniferin-like compound. Bisisorhapontigenin A **4.33** and C **4.35** are regioisomers whereby the *O* of the dihydrofuran ring is attached to C8 of the second unit in **4.33** as opposed to C7 in **4.35**. In contrast, C4 of the resorcinol ring of the stilbene was engaged in benzofuran ring formation of bisisorhapontigenin B **4.34** instead of C2 in **4.33** and **4.35**. The above oxidative couplings were rationalized by the authors through the involvement of phenoxy radical intermediates except for tetraisorhapontigenin A **4.39** where a Diels-Alder cycloaddition and radical couplings were proposed. The

structure of **4.39** and its plausible mechanism of formation are discussed in section 4.3.5.10.

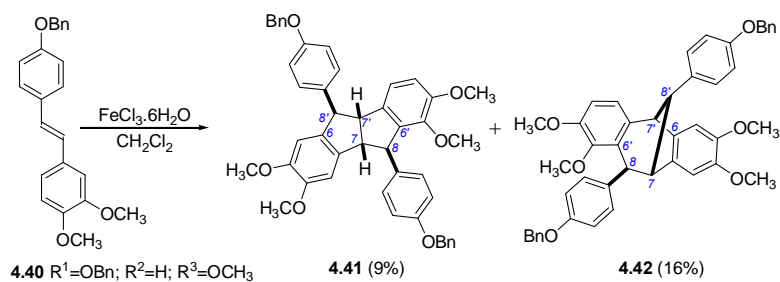


Reaction	Conditions	Yield (%)						Reference	
		4.33	4.34	4.37	4.36	4.37	4.38		4.39
a.	FeCl ₃ .6H ₂ O; acetone/H ₂ O (3:2, v/v)		0.9	0.54		0.6	0.34	0.36	[65]
b.	FeCl ₃ .6H ₂ O; acetone/H ₂ O (3:2, v/v)	major	major		major	-	22.5	15.7	[50]
c.	Ag ₂ O; acetone/H ₂ O (see section 4.1.4.2.)			-	30	-	40	-	[67]

Scheme 4.14: Oxidation of isorhapontigenin into its oligomers (adapted from references 9, 24 & 26).

4.1.3.3. Other stilbenes

Weberø group reported in 2008 stilbene oxidative coupling by means of one-electron oxidant in CH₂Cl₂.²⁵ Subjecting catechol substituted stilbene **4.40** to FeCl₃.6H₂O in CH₂Cl₂ produced pallidol and ampelopsin F analogues **4.41** and **4.42** respectively in a ratio of 1:1.5 (Scheme 4.15).

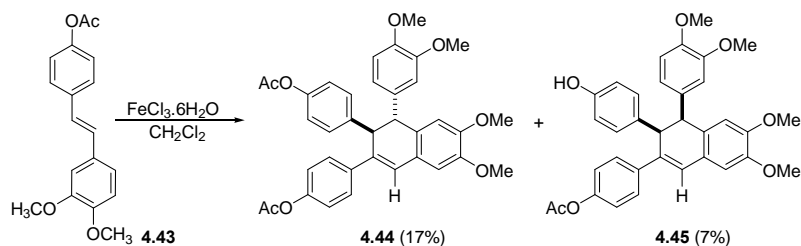


Scheme 4.15: Generation of pallidol and ampelopsin F analogues in FeCl₃.6H₂O/CH₂Cl₂ mixture (adapted from reference 25).

Various parameters, such as quantification and dilution of the FeCl₃ solution, effect of the solvent and reaction time, that influence the dimerisation of stilbene **4.40** were studied through HPLC chromatographic analysis. All starting materials were consumed within 5 hours in at least 1.5 eq of 60% FeCl₃ aqueous solution (w/v). However, diluting the FeCl₃ solution by half (30% w/v) resulted in lower yields of **4.41** and **4.42**. The dimerisation reaction was completely inhibited when carried out in the following solvents: water, methanol, ethanol, 2-propanol and DMF with low recovery of starting material. This suggests polymerization of **4.40**. Reactions carried out in acetone, ethylmethylketone (EMK), ethyl acetate, chloroform, diethyl ether, THF and acetonitrile show quite a high recovery of **4.40** and some common characteristics with appearance of two new peaks that is with retention times 16 and 17 minutes respectively that are intermediate between those of **4.41** and **4.42**. The yields of these latter products in these reactions were low. When the reaction was performed in non-polar solvents, xylenes, toluene and hexanes, the expected dimers were formed in moderate yields in addition to a number of unidentified compounds. The starting material was recovered in relatively low yield. Oxidative coupling of **4.40** in varying mixtures of dichloromethane and methanol was then examined. When dichloromethane is mixed with small portions of methanol (3-10% v/v), formation of additional products with retention times identical to those of the compounds obtained

from the reaction in chloroform (approximately 16 and 17 minutes) was observed. Small quantities of methanol considered as modifying the dichloromethane properties so as to make them similar to that chloroform. In summary, chloroform and dichloromethane appear to be the best solvents for generating small molecular weight products from stilbene the ferric chloride reactions.

Thomas's group previously reported (2002) that treating **4.43** with ferric chloride in dichloromethane gave catechol *anti*-isomer **4.44** and *syn*-isomer **4.45** (partially deprotected) in 17% and 7% yield respectively (Scheme 4.16).²⁶ The author proposed that the stilbene dimerisation undergoes thermally allowed pericyclic transformations, which would involve radical cationic species.



Scheme 4.16: Synthesis of dihydronaphthalene based stilbene dimers in $\text{FeCl}_3 \cdot 6\text{H}_2\text{O}/\text{CH}_2\text{Cl}_2$ mixture.²⁶

4.1.3.4. Summary

Two types of Fe^{3+} salts namely $\text{FeCl}_3 \cdot 6\text{H}_2\text{O}$ and $\text{K}_3\text{Fe}(\text{CN})_6$ are used in different solvents MeOH/ H_2O mixture, acetone/ H_2O mixture, $\text{CH}_2\text{Cl}_2/\text{MeOH}$ mixture, acetone, MeCN and CH_2Cl_2 to dimerise resveratrol, isorhapontigenin and protected stilbenes. It was observed that when resveratrol is subjected to a combination of $\text{FeCl}_3 \cdot 6\text{H}_2\text{O}/\text{acetone}$ or $\text{FeCl}_3 \cdot 6\text{H}_2\text{O}/\text{MeCN}$, the δ -viniferin type skeleton is produced (similar to silver salts effects), while $\text{FeCl}_3 \cdot 6\text{H}_2\text{O}/[\text{MeOH}/\text{H}_2\text{O}]$ complex produces only ϵ -viniferin type skeleton. A mixture of δ -viniferin type, ϵ -viniferin type and/or pallidol like skeletons are obtained when resveratrol is treated with $\text{K}_3\text{Fe}(\text{CN})_6$ in

MeOH/H₂O. Similar combinations of two types of skeletons (δ -viniferin and ϵ -viniferin types) are observed again in FeCl₃.6H₂O/[acetone/H₂O] complex when isorhapontigenin is used as the starting material. By contrast, subjecting protected stilbenes to FeCl₃.6H₂O in CH₂Cl₂ produce pallidol, ampelopsin F and dihydronaphthalene types skeletons based on the substitution pattern of the starting material.

4.1.4. Oxidative coupling with silver derivatives

Silver oxide and various salts were employed as one electron oxidants in oxidative coupling of resveratrol **1.0**, isorhapontigenin **1.1**, piceatannol **4.46**, pterostilbene **1.2** as well as resveratrol analogues and its dimer ϵ -viniferin **1.4**.

4.1.4.1. Resveratrol

Sako *et al.* treated resveratrol **1.0** in dry methanol with various one-electron silver oxidants Ag₂O, AgOAc, Ag₂CO₃ and AgNO₃ at 50°C to yield δ -viniferin **1.3** in 86%, 76%, 56% and 4% respectively. AgOAc, the best reagent of the list above, was then used with other solvents, dry acetone, MeCN and THF.²³ **1.3** was obtained in 90%, 86% and 19% yield respectively.

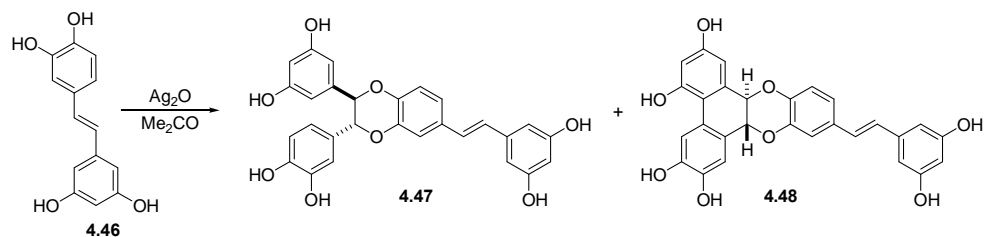
4.1.4.2. Isorhapontigenin

Zhou and Lin (2000) performed an oxidative coupling of isorhapontigenin **1.1** with Ag₂O in aqueous acetone to afford shegansu B **4.36** in 30% yield (it was also obtained with FeCl₃.6H₂O in acetone/water; see section 4.1.3.2 and Scheme 4.14).²⁷

The formation of **4.36** was hypothesized through 12-phenoxy radicals as intermediates.

4.1.4.3. Piceatannol

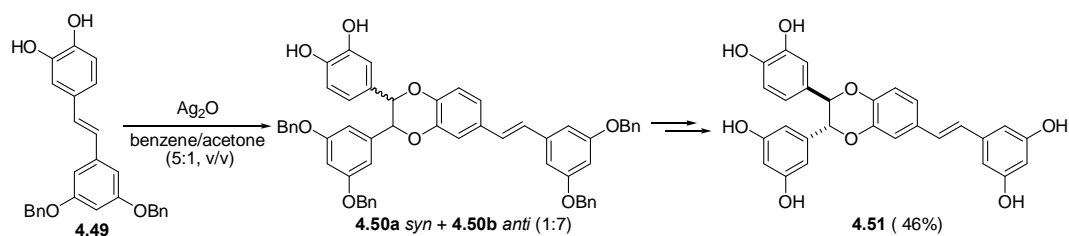
Baba K. *et al.* converted piceatannol **4.46** (another naturally occurring stilbenoid) to cassigarols E **4.47** and G **4.48** via Ag^+ (Ag_2O) coupling in acetone (Scheme 4.17).²⁸ Both benzodioxane type oligostilbenoids are found in *Cassia garrettiana*.



Scheme 4.17: Synthesis of cassigarols E and G (adapted from reference 28).

4.1.4.4. Other stilbenoids

Yang *et al.* reported the first total synthesis of (\pm)-maackin **4.51** in 2003 (Scheme 4.18).²⁹ To achieve this target, catechol substituted stilbene **4.49** was treated with Ag_2O in benzene/acetone mixture affording cyclised stilbene dimers as a mixture of isomers (*syn* **4.50a**/*anti* **4.50b**, 1:7). The *syn*-isomer **4.50a** was converted to **4.50b** with the *anti* configuration by treatment with anhydrous potassium carbonate in DMF. Eventually, the benzyl groups of **4.50b** were cleaved to give maackin **4.51**. The benzodioxane skeleton was also observed in laccases biotransformation of catechol stilbenes **4.22** and **4.23** (see section 4.1.2.1).



Scheme 4.18: Synthesis of (\pm)-maackin (adapted from reference 29).

4.1.4.5. Viniferins

Sako subjected δ -viniferin **1.4** to AgOAc in dry methanol at 50°C and obtained vitisin B **4.26** in 40% yield.²³ **4.26** was also obtained from reaction of HRP on ϵ -viniferin **1.4** (see section 3.2.2 and Scheme 4.11). In contrast, treatment of δ -viniferin **1.3** under the same conditions did not yield any reaction product.

4.1.4.6. Summary

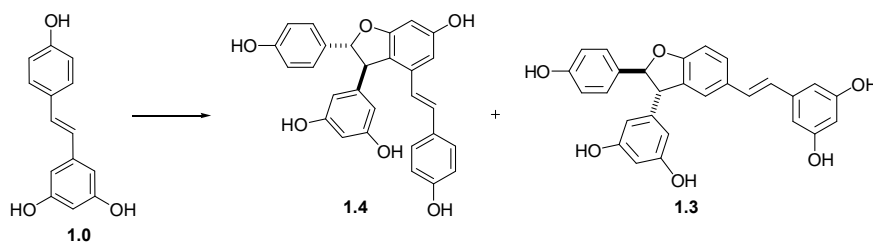
Silver oxide and salts (Ag₂O, AgOAc, AgNO₃ and Ag₂CO₃), one electron oxidants, couple oxidatively resveratrol **1.0**, isorhapontigenin **1.1** and other 12-hydroxystilbenes (including ϵ -viniferin **1.4**) in various solvents. The resulting dimeric species are restricted to only one type of skeleton, the δ -viniferin type, regardless of the solvent used. When a stilbene with 3,4-catechol substitution is treated with Ag₂O, a dimeric species with a benzodioxane moiety is afforded. From the above results, it seems that the presence of the 4-hydroxystyrene moiety is required in order to induce a regioselective coupling of the phenoxy radicals leading to 2,3-dihydrobenzofuran ring. In contrast, a free hydroxyl group at position 3 will not be involved in any benzofuran ring formation.

4.1.5. Dimerisation with other oxidants

A variety of other one-electron oxidants [Tl(NO₃)₃, Ce(SO₄)₂, PhI(OAc)₂, DDQ, MnO₂, Mn(OAc)₃, CuOAc, Cu(OAc)₂ and DPPH] were applied to resveratrol **1.0** and its analogues.

4.1.5.1. Resveratrol

Niwa and co-workers (2005) reported the formation of α -viniferin **1.4** and δ -viniferin **1.3** by means of one electron oxidants in methanol at -50°C (Scheme 4.19).⁷ Treating resveratrol **1.0** with thallium(III) nitrate produced **1.4** in 30% within 5 minutes but when the temperature was raised from -50° C to 0°C, only complex mixture was obtained. Replacing thallium(III) nitrate with cerium(IV) sulfate afforded **1.4** in low yield (3.7%) and **1.3** (8.4%). In this paper, Niwa indicated also that manganese(IV) oxide in dichloromethane induced the formation of **1.4** in high yield (91%) and pallidol **1.6** (9%). This last result seems quite untrustworthy as, from our experience, resveratrol is insoluble in dichloromethane. Furthermore this transformation is not reported in the experimental section. It will not be considered for further discussion.



Reaction	Conditions	Yield (%)		Reference
		1.4	1.3	
a.	Tl(NO ₃) ₃ , MeOH -50°C	30.1	-	[48]
b.	Tl(NO ₃) ₃ , MeOH -30°C	-	-	[48]
c.	Ce(SO ₄) ₂ , MeOH -50°C	3.7	8.4	[48]
d.	PhI(OAc) ₂ , dry MeCN, 50°C	-	25	[64]
e.	DDQ, dry MeCN, 50°C	-	7	[64]
f.	Mn(OAc) ₃ , MeOH 50°C	-	55	[64]
g.	CuOAc, MeOH 50°C	-	24	[64]
h.	Cu(OAc) ₂ , MeOH 50°C	-	22	[64]
i.	DPPH, MeOH, RT	-	18	[72]

Scheme 4.19: Synthesis of ϵ - and δ -viniferins in metallic and organic oxidative conditions (adapted from references 7, 23 & 31).

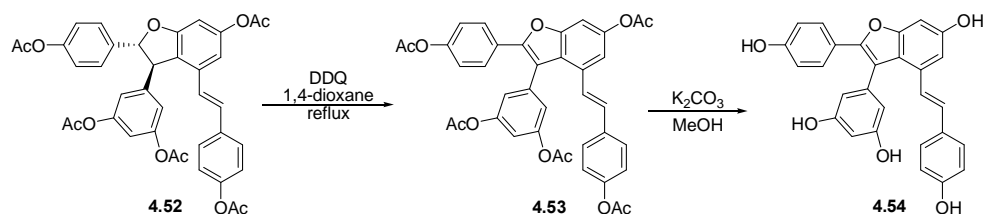
Sako *et al.* oxidized **1.0** using organic oxidants PhI(OAc)₂ and DDQ furnishing **1.3** in yield of 25% and 7% respectively (Scheme 4.19).²³ Oxidation of **1.0** with other metallic oxidants Mn(OAc)₃, CuOAc and Cu(OAc)₂ gave also **1.3** in moderate to low yields. Wang *et al.* obtained **1.3** as well (18%) as a major product of resveratrol **1.0** oxidation by DPPH.³⁰

4.1.5.2. Summary

MnO₂, Mn(OAc)₃, CuOAc, Cu(OAc)₂, PhI(OAc)₂, DPPH and DDQ mainly generate δ -viniferin type skeleton from resveratrol while Tl(NO₃)₃/MeOH complex produces solely its regioisomer, that is ϵ -viniferin skeleton. On the other hand, Ce(SO₄)₂/MeOH complex gives a combination of both δ -viniferin type and ϵ -viniferin type products.

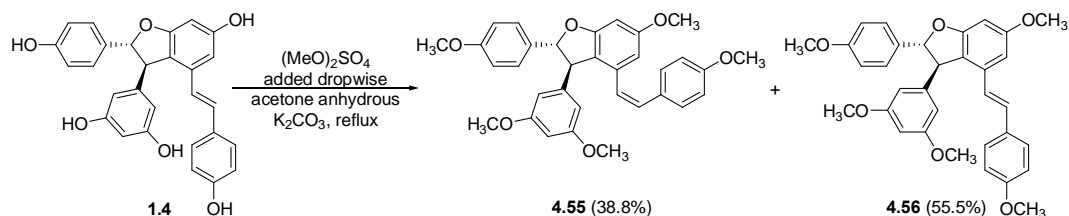
4.1.6. Chemical transformation of ϵ -viniferin and its derivatives

To prepare amurensin H **4.54**, Lin \AA s group performed a series of reactions including protection, oxidation and deprotection. ϵ -Viniferin **1.4** obtained by treating resveratrol **1.0** with FeCl_3 in MeOH as reported above (see section 4.1.3.1 and Scheme 4.13). This was followed by conventional acetylation of **1.4**. Oxidation of peracetylated ϵ -viniferin **4.52** by DDQ followed by deprotection afforded amurensin H **4.54** (Scheme 4.20).



Scheme 4.20: Oxidation of ϵ -viniferin pentaacetate **4.52** into amurensin H **4.54** (adapted from reference 20).

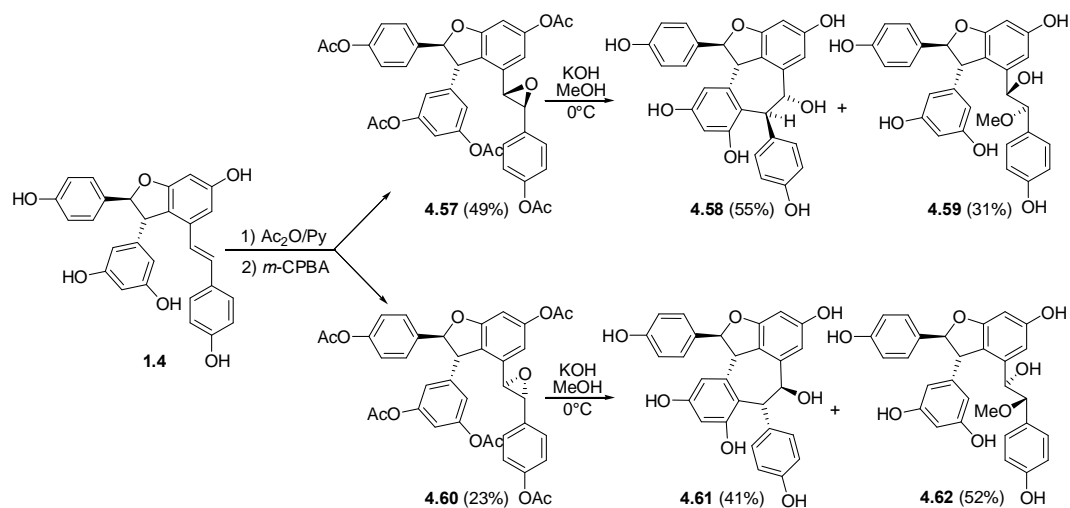
Lin \AA s group also reported that the permethylation of ϵ -viniferin **1.4** by $(\text{MeO})_2\text{SO}_4$ in anhydrous acetone led two methylated geometric isomers, *i.e.* (*Z*)-**4.55** and (*E*)-permethyl- ϵ -viniferin **4.56** in 38.8% and 55.5% respectively (Scheme 4.21).



Scheme 4.21: Protection and Isomerization of ϵ -viniferin (adapted from reference 21).

Niwa and co-authors³¹ protected and epoxidised ϵ -viniferin **1.4** with *m*-chloroperbenzoic acid (*m*-CPBA) in view of preparing (+)-ampelopsin A **4.58** (Scheme 4.22). Subjecting peracetylated (+)-epoxy- ϵ -viniferin **4.57** to acetate

hydrolysis and nucleophilic attack by resorcinolic ring of acetate indeed generated **4.58** as well as unnatural addition epoxide product **4.59**. Exposing diastereoisomeric (+)-*ε*-epoxy-*ε*-viniferin pentaacetate **4.60** to the above conditions led to the corresponding unnatural diastereoisomers **4.61** and **4.62**.



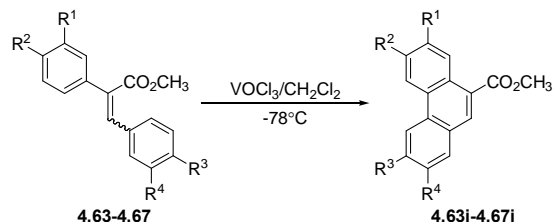
Scheme 4.22: Cyclization of ϵ -viniferin derivatives in basic medium (adapted from Takaya *et al.*).³¹

In summary, protected ϵ -viniferins are transformed into derivatives in three different chemical conditions. DDQ helps in the dehydrogenation process, permethylating agent, $(\text{MeO})_2\text{SO}_4$ facilitates *cis* Isomerization, while *m*-CPBA converts protected ϵ -viniferin into epoxides, which then readily undergoes intramolecular cyclisation leading to a seven-membered ring under basic conditions.

4.1.7. Stilbenes that fail to dimerise under oxidative conditions: (even though it is obvious)

Jin *et al.* (2004) subjected a series of mixtures of (*Z*)- and (*E*)- stilbene methyl esters (**4.63-4.67**) to vanadium oxytrichloride in dichloromethane at -78°C and

observed an intramolecular biaryl oxidative coupling leading to phenanthrene derivatives **4.63i-4.67i** (Scheme 4.23).³² Vanadium oxytrichloride was found to be the most effective oxidant to form biaryl units compared to many other oxidants like ferric chloride, PIFA, vanadium oxytrifluoride. Cyclization was observed only for *ortho*-3,4-substituted derivatives. Stilbenes *meta*-dimethoxy substituted or 2,3 substituted failed to cyclize.



No	Stilbene substrate [(Z)- and (E)-isomers mixtures]				Product	Yield (%)
	R ¹	R ²	R ³	R ⁴		
4.63	OCH ₃	OCH ₃	OCH ₃	OCH ₃	4.63i	98
4.64	OCH ₃	OCH ₃	OCH ₃	H	4.64i	82
4.65	OCH ₃	OCH ₃	H	H	4.65i	76
4.66	OCH ₃	H	OCH ₃	OCH ₃	4.66i	72
4.67	H	H	OCH ₃	OCH ₃	4.67i	54

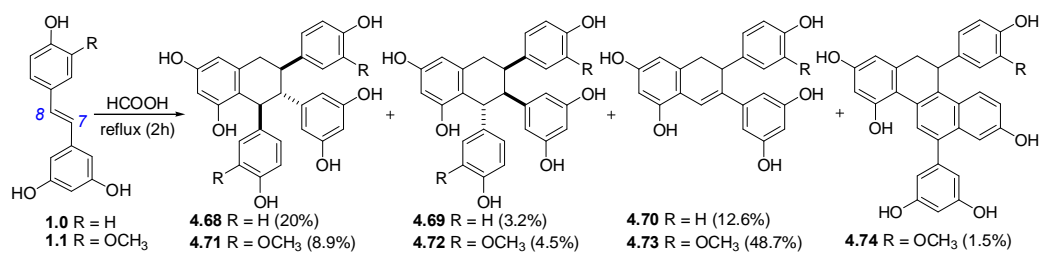
Scheme 4.23: Intramolecular oxidative coupling of stilbene analogues by VOCl₃ (adapted from reference 32).

4.1.8. Acid-catalysed dimerisation

Natural (resveratrol **1.0** and isorhapontigenin **1.1**) and unnatural stilbenes were subjected to different acidic conditions.

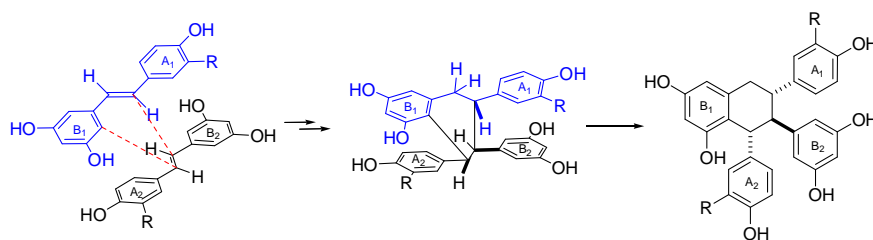
4.1.8.1. Resveratrol and isorhapontigenin

Resveratrol **1.0** and isorhapontigenin **1.1** were each treated with formic acid and refluxed for two hours to produce seven dimeric compounds with tetralin skeleton, named by the authors as resformicol A-C **4.68-4.70** and isorhaformicols A-D **4.71-4.74** respectively despite the fact that these compounds have not been isolated from natural resources (Scheme 4.24).³³



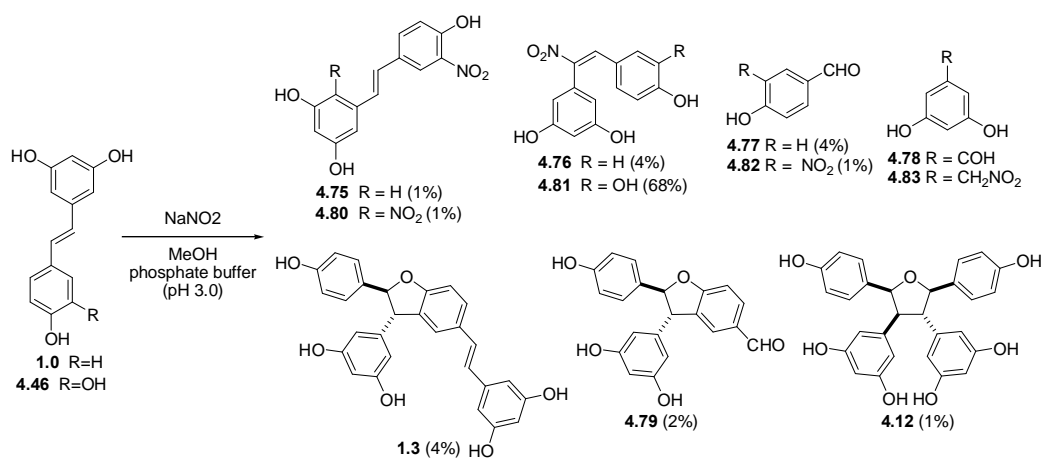
Scheme 4.24: Treatment of resveratrol and isorhapontigenin with formic acid (adapted from reference 33).

The authors proposed a mechanism that leads to two types of Diels-Alder adducts: a) normal [4+2] adducts forming a triaryltetralin system; b) derivatives of the former resulting from loss of rings or substituents. In their opinion the formation of **4.68** and **4.71** can be rationalized through the parallel approach in a head-to-tail manner of the two monomers where the overlap of the electric cloud of two aromatic rings A₂ and B₁ is to the maximum. As a result, a Diels-Alder type of reaction would be favored (Scheme 4.25). The authors believe that the starting point for cyclodimerization is the generation of the carbocation generated by acid treatment at position 8 of the stilbene. End products **4.68** and **4.71** (major products) have their three substituents of the cyclohexyl ring in the equatorial orientation, a relatively more stable configuration compared to **4.69** and **4.72** (minor products). Compounds **4.70** and **4.73** result from the loss of an aryl ring in the course of the re-aromatization of the dimerisation products. Compound **4.74** would derive from a second Diels Alder addition of isorhapontigenin **1.1** on **4.73** followed by subsequent losses of an aromatic ring and a methoxyl during the re-aromatization process. The absence of such product originating from resveratrol **1.0** could be due to the absence of methoxy group in the A₁ ring of **4.70**.



Scheme 4.25: Alignment of stilbenes leading to dimerisation (adapted from reference 33).

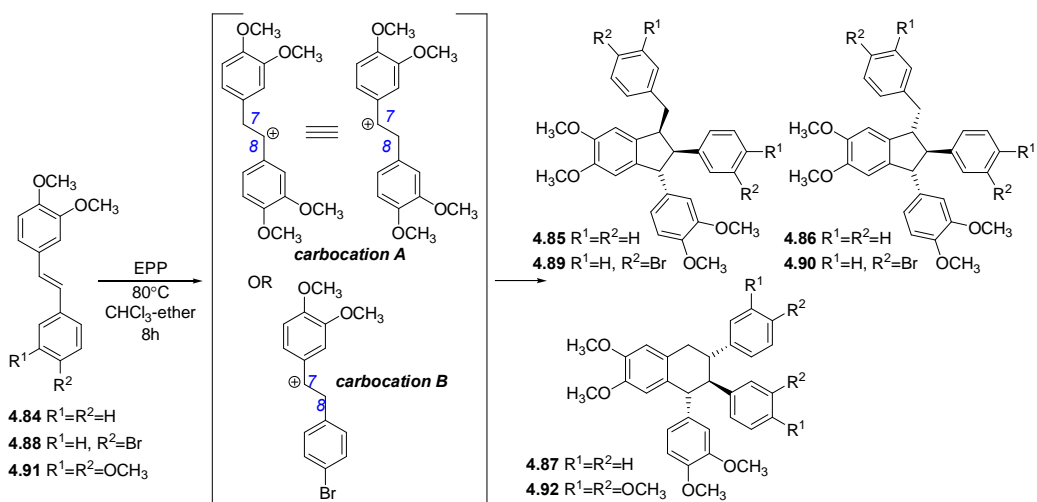
Panzella *et al.* (2006) reported the oxidation of resveratrol **1.0** at pH 3.0 (0.1 M phosphate buffer), by NaNO_2 in methanol at 37°C .³⁴ A variety of products were obtained in low yield resulting from nitration (**4.75**, **4.76**, **4.80**, **4.81**), oxidative breakdown (**4.77**, **4.78**, **4.82**, **4.83**) and dimerisation (**1.3**, **4.12**, **4.79**) as shown in Scheme 4.26. The proposed mechanism is based on phenoxyl radical intermediates. This acidic NO_2^- -promoted reaction gave only two dimers, δ -viniferin **1.3** and restrytisol B **4.12** and the partially cleaved dimer **4.79** in poor yields. Treatment of stilbene piceatannol **4.46** under similar conditions afforded mainly (*Z*)-nitrostilbene **4.81**.



Scheme 4.26: Treatment of resveratrol and piceatannol with NaNO_2 (adapted from reference 34).

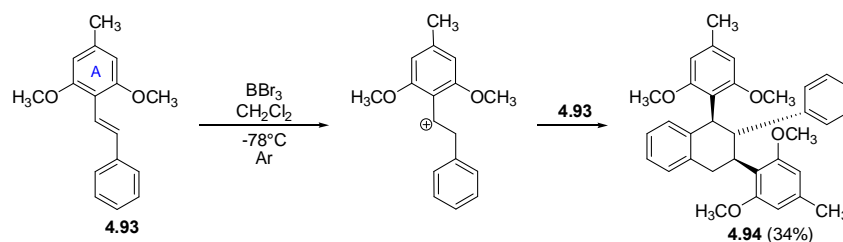
4.1.8.2. Unnatural stilbenes

J. M. Aguirre *et al.* (1999) reported the formation of indanes and tetralins *via* oxidation of (*E*)-stilbenes by ethyl polyphosphate (EPP) in a mixture of chloroform-ether at 80°C for 8 h (Scheme 4.27).³⁵ The authors were of the opinion that the preferential formation of the indane or tetralin skeleton was determined by the substituents in the stilbene precursor. The key factor for the cyclodimerization is the formation of a stable dimeric carbocation whereby the contribution of electron-donating substituents plays a major role in the stability of the intermediate. Compound **4.91** produced only tetralin **4.92** in 97% yield via the symmetrical and stabilized carbocation A leading to the formation of the more stable 6-membered ring. However, when bromine was introduced at a *para* position in stilbene precursor **4.88**, indanes **4.84** and **4.90** were formed in 65% yield via the more stable carbocation B. In contrast, compound **4.84** adopts behavior intermediate between **4.88** and **4.91** producing a mixture of indane and tetralin skeletons (**4.85-4.87**) in 41%.



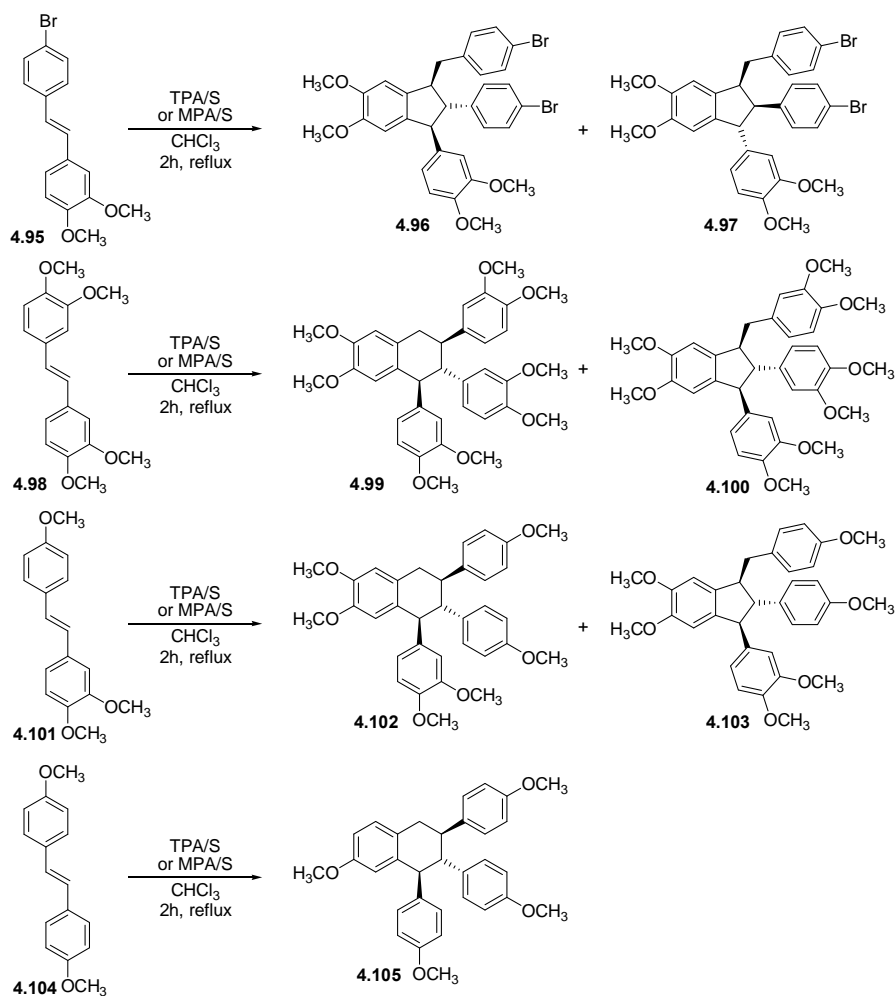
Scheme 4.27: Formation of indane and tetralin skeletons *via* EPP oxidative coupling (adapted from reference 35).

Li and Ferreira (2003) treated 2,6-dimethoxy-4-methylstilbene **4.93** with Lewis acid, $\text{BBr}_3/\text{CH}_2\text{Cl}_2$ to produce a sterically congested tetralin **4.94** in 34% yield (Scheme 4.28).³⁶ These authors proposed the formation of carbocation at the position to the more electron-rich aromatic ring, *i.e.* C7, followed by nucleophilic attack (by a second stilbene molecule) to give the observed product. The stereoselective cyclisation is considered to be directed by the nucleophilicity of the C2 and C6 of each aromatic ring determining the pathway that produces indanes and/or tetralins (as previously proposed by Aguirre *et al.*³⁵). This can be seen in the case of **4.93** where it produces only tetralin **4.94** as the C2 and C6 of the A ring are blocked by the methoxy groups.



Scheme 4.28: Synthesis of tetralin skeleton by BBr_3 (adapted from reference 36).

Alesso and co-workers (2002) reported the cyclodimerization of stilbenes using silica-supported molybdophosphoric acid (MPA/S) and tungstophosphoric acid (TPA/S) catalysts.³⁷ They obtained a mixture of indane and/or tetralin derivatives with remarkably high yields and short reaction time (Scheme 4.29). Treating **4.95** in TPA/S or MPA/S gave a mixture of diastereoisomeric indanes (**4.96** and **4.97**) in 98.5%. However, **4.98** and **4.101** each gave a mixture of tetralin and indane derivatives (**4.99/4.100** and **4.102/4.103**) in 90% and 77% respectively. In comparison with reactions carried out with EPP and with 50% sulphuric acid, silica-supported acid catalysts provided significantly better yields. For instance, compound **4.104** showed no reaction in the presence of EPP or 50% sulphuric acid but produced tetralin **4.105** in 99% yield when TPA/S or MPA/S was used.

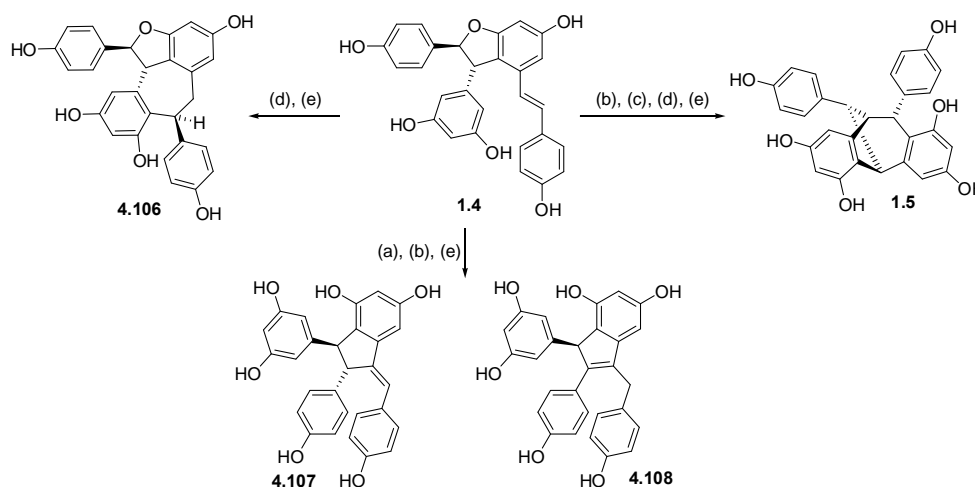


Scheme 4.29: Formation of tetralin and indane skeletons *via* MPA/S and TPA/S oxidative coupling (adapted from reference 37).

In summary, exposing natural resveratrol **1.0**, isorhapontigenin **1.1**, piceatannol **4.46** and unnatural stilbenes to different acidic reagents such as HCOOH, NaNO₂, BBr₃, ethyl polyphosphate (EPP), tungstophosphoric acid (TPA/S) and molybdophosphoric acid MPA/S provided stilbene dimers mainly of the tetralin and or indane type. The selectivity of these two types of skeletons is based on the stability of the generated carbocationic species.

4.1.9. Acid catalysed cyclisation of stilbene oligomers

Niwa and co-workers treated ϵ -viniferin **1.4** with three different types of acids in methanol, water and nitromethane to afford four different cyclization products comprising of five- and seven-membered rings (ampelopsin B **4.106**, ampelopsin D **4.107** and its regioisomer **4.108**, and ampelopsin F **1.5**) as shown in Scheme 4.30.^{31, 38} The generation of these different skeletons was explained by the variation in the position of the initial protonation of ϵ -viniferin either on the olefinic double bond or on the oxygen atom of the dihydrofuran ring followed by intramolecular nucleophilic attacks.

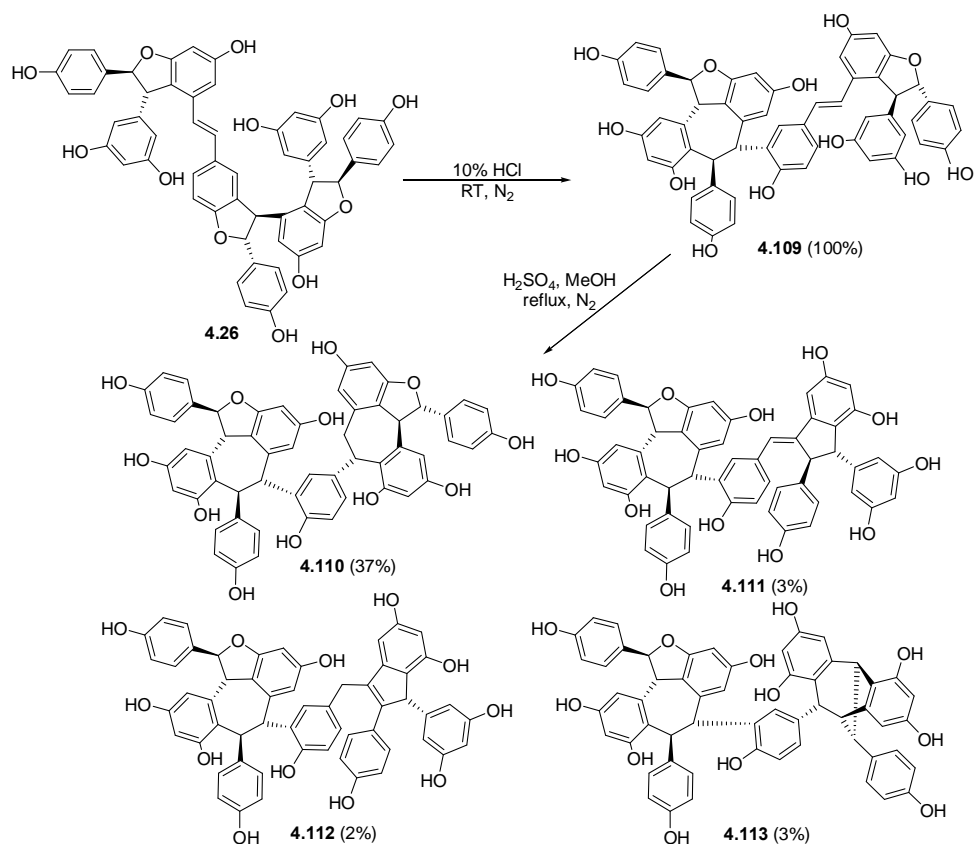


Reaction	Reagent	Solvent	Temperature	Yield (%)				Reference
				4.106	4.107	4.108	1.5	
a.	CF ₃ SO ₃ H	MeOH	reflux		14	8		[80]
b.	CF ₃ SO ₃ H	MeOH	reflux		14	10	21	[73]
c.	CF ₃ SO ₃ H	CH ₃ NO ₂	RT				38	[73]
d.	1 M HCl	H ₂ O	RT	38			8	[73]
e.	H ₂ SO ₄	MeOH	reflux	13	6	10	19	[73]

Scheme 4.30: Acid catalysed cyclisation of ϵ -viniferin (adapted from references 31 & 38).

The same investigators applied a similar acid treatment to (-)-vitisin B **4.26**, which also contains an ϵ -viniferin moiety as part of its structure.⁴ Thus, (+)-vitisin A **4.109**, which includes an ampelopsin B moiety, was obtained in quantitative yield (Scheme 4.31). In the same manner, acid treatment of **4.109** produced (+)-vitisin D

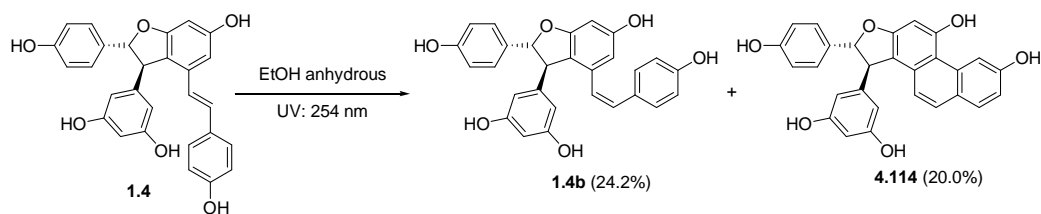
4.110 as a major product together with minor products **4.111-4.113** possessing novel skeletons incorporating ampelopsins B, D and F moieties respectively.



Scheme 4.31: Acid catalysed cyclisation of vitisin A and B (adapted from reference 4).

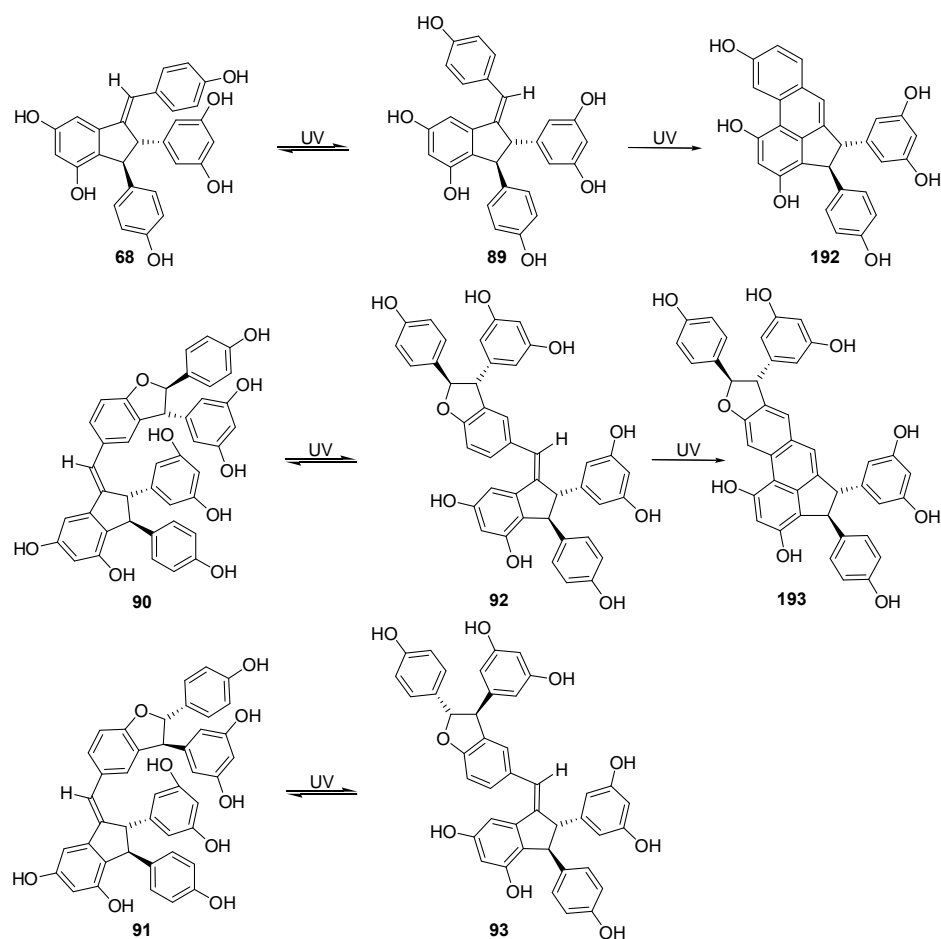
4.1.10. Stilbene photooxidation

Lin and co-workers subjected *Z*-viniferin **1.4** to ultraviolet radiation ($\lambda = 254$ nm) in ethanol resulting in (*Z*)- ϵ -viniferin **1.4b** and novel dihydrophenanthrofurans **4.114** in 24% and 20% yield respectively (Scheme 4.32).²¹ The formation of **4.114** is considered as resulting from electrocyclic ring closure of the *Z* olefin **1.4b** via phenolic hydrogen atom abstraction promoted by UV radiation.



Scheme 4.32: Photooxidation of ϵ -viniferin (adapted from reference 21).

Subjecting (-)-parthenocissin A **4.29**, a regioisomer of (-)-ampelopsin D **4.107**, to UV irradiation in methanol for 2 h generated (-)-quadrangularin A **4.6** and (+)-laetevirenol A **4.115** in 31% and 9% yield respectively (Scheme 4.33).¹⁹ It was a time-dependent reaction where in the first 20 minutes equilibration between (*E*)- and (*Z*)-isomers **4.29** and **4.6** respectively predominated, only after which compound **4.115** started to appear. Similarly, (-)-parthenocissin B **4.32** was isomerised to **4.30** by UV irradiation and later cyclised to **4.116**. (+)-Laetevirenol C **4.31** and (+)-laetevirenol E **4.33** were only isomerized to each other under UV irradiation.



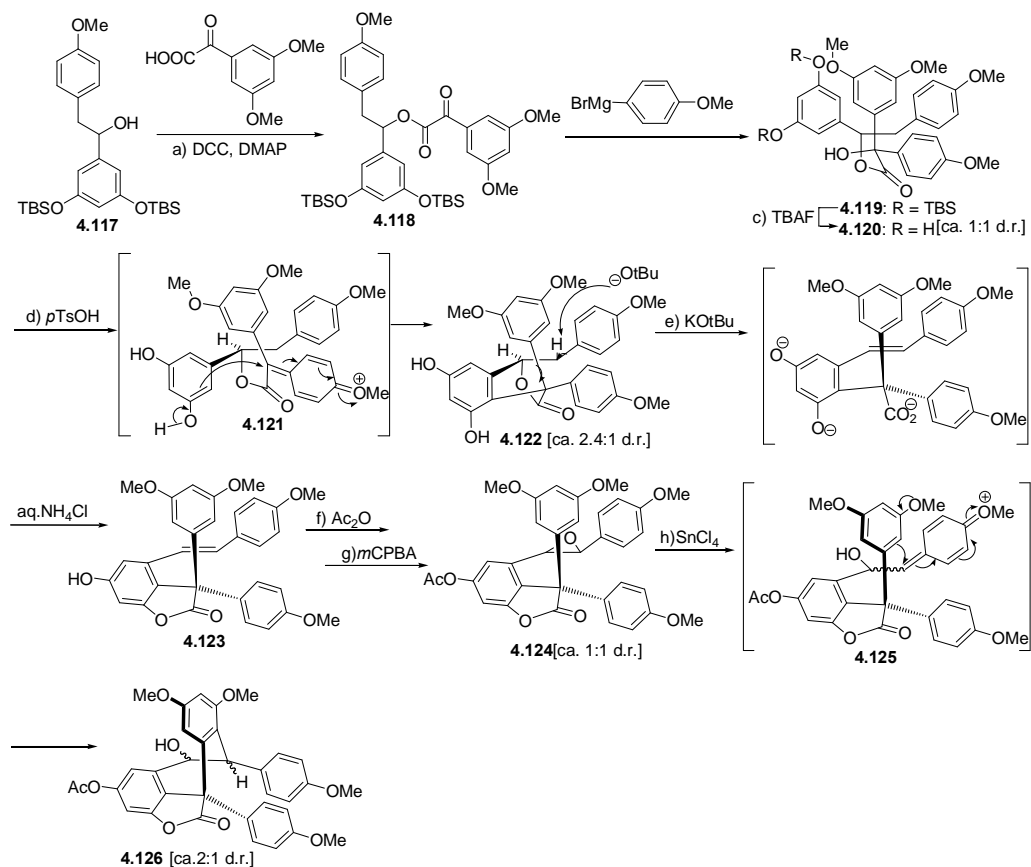
Scheme 4.33: Photooxidation of stilbene dimers and trimers (adapted from reference 19).

4.2. Non biomimetic syntheses

a) Synthesis of hopeahainol A 4.131 and hopeanol 4.132 by Nicolaou et al..

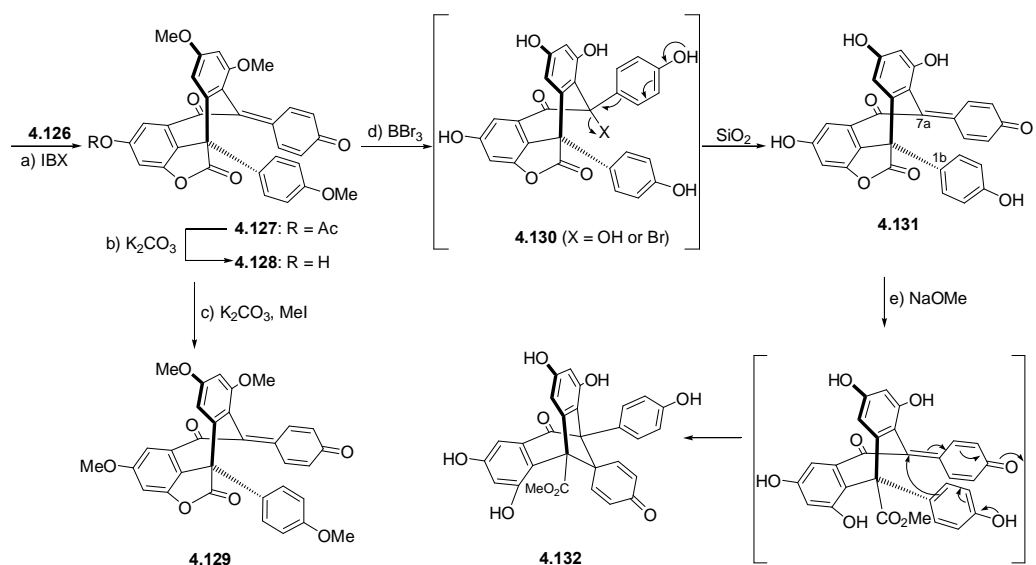
Nicolaou *et al.* (2009)³⁹ reported the total synthesis of hopeahainol A **4.131** and hopeanol **4.132** using bibenzylic alcohol **4.117** as starting building block (Scheme 4.34). **4.117** underwent esterification to form the keto ester **4.118** followed by Grignard reaction yielding bis-TBS derivative **4.119** (mixture of diastereoisomers). Protected silyl ethers of compound **4.119** was cleaved by TBAF leading to hydroxy ester mixture of diastereoisomers **4.120**, which was then subjected to *p*-TsOH in CH₂Cl₂ to produce γ -lactone **4.122** mixture of diastereoisomers in 65% yield via

reactive intermediate **4.121**. Addition of base followed by quenching by an ammonium chloride solution led to olefinic α -lactone **4.123** through anion formation, β -elimination and ring closure to afford a single isomer in 76% yield. Acetylation of the phenolic group of **4.123** and subsequent epoxidation by *m*CPBA afforded **4.124** as a mixture of diastereoisomers. Treatment of **4.124** with SnCl₄ in CH₂Cl₂ at -40 to -20°C produced intermediate hydroxy α -lactone **4.125** through epoxide ring opening followed by carbon-carbon bond formation leading to **4.126**.



Reaction	Conditions	Yield (%)
a.	2-(3,5-dimethoxyphenyl)-2-oxoacetic acid (1.5 equiv), DCC (2.3 equiv), DMAP (0.3 equiv), CH_2Cl_2 , 25°C, 12 h.	95
b.	4-methoxyphenylmagnesium bromide (0.2 M in THF, 1.3 equiv), THF, 10°C, 10 min.	
c.	TBAF (1.0 M in THF, 2.0 equiv), THF, 0°C, 30 min (1:1 mixture of diastereoisomers)	79%
d.	<i>p</i> TsOH (3.0 equiv), CH_2Cl_2 , 25°C, 48 h. (2.4:1 mixture of diastereoisomers)	65%
e.	KOtBu (1.0 M in THF, 5.0 equiv), THF, 0° to 25°C, 4h, aq NH_4Cl	76
f.	Ac_2O (1.5 equiv), DMAP (0.1 equiv), pyridine, 0° to 25°C, 1 h.	
g.	<i>m</i> CPBA (77% wt/wt, 4.0 equiv), NaHCO_3 (6.0 equiv), CH_2Cl_2 , 0°C, 30 min, (ca. 1:1 mixture of diastereoisomers)	
h.	SnCl_4 (1.0 M in CH_2Cl_2 , 1.5 equiv), CH_2Cl_2 , -40 to -20°C, 20 min, (mixture of diastereoisomers).	62%

Scheme 4.34: Construction of epoxide **4.124** and hexacyclic intermediate **4.126**.³⁹



Reaction	Conditions	Yield (%)
a.	IBX (10 equiv), DMSO, 25°C, 24 h	66
b.	NaHCO ₃ , MeOH, 25°C, 1 h, quant.	
c.	MeI (20 equiv), K ₂ CO ₃ (5.0 equiv), acetone, 80°C, 1 h	90
d.	BBr ₃ (1.0 M in CH ₂ Cl ₂ , 18 equiv), CH ₂ Cl ₂ , -78 to -20°C, 24 h	84
e.	NaOMe (1.0 equiv), MeOH, 25°C, 60 h	80

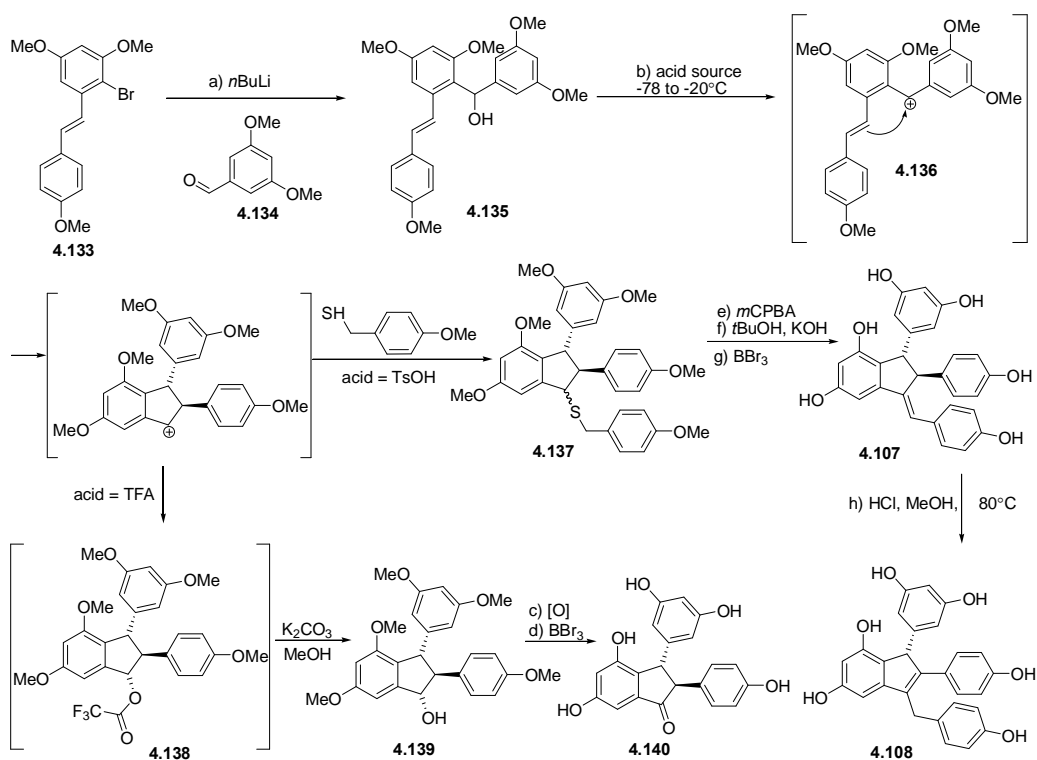
Scheme 4.35: Total synthesis of tetramethyl hopeahainol A **4.129**, hopeahainol A **4.131**, and hopeanol **4.132**.³⁹

Compound **4.126** is now ready to be converted to **4.131** by just three steps as it possesses the scaffold of hopeahainol A (Scheme 4.35). Oxidation of **4.126** by IBX transformed to keto quinoid **4.127** followed by deacetylation furnishing phenol **4.128**. The known derivative **1.129** was prepared by the methylation of **4.128** where **4.129** was spectroscopically confirmed, thus supporting the close resemblance of **4.128** to that of hopeahainol A. Subjecting **4.128** to BBr₃ in CH₂Cl₂ (-78 to -20°C) afforded **4.130** (84%) which when placed on a preparative silica gel plate for a few hours, collapses to give the target compound **4.131**. This can be rationalized by the presence of a labile group (X = OH or Br) in the intermediate **4.130**. Finally, hopeanol **4.132** too was achieved by just treating **4.131** in sodium methoxide in 80% yield. The lactone ring present in **4.131** makes interaction between C1b and C7a more difficult due to the

distance of separation, thus sodium methoxide helped bringing them closer by breaking the lactone ring.

b) Synthesis of paucifloral F 4.140, isoampelopsin D 4.108, quadrangularin A 4.6, isopaucifloral F 4.142, pallidol 1.6, ampelopsin F 1.5 and diptoindonesin A 4.152 congener by Snyder et al.

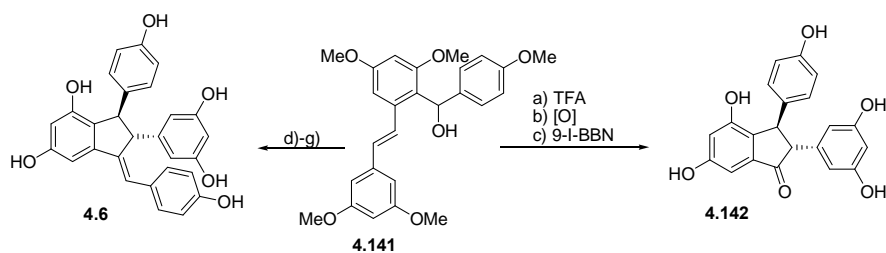
Snyder *et al.*⁴⁰ published in 2007 the synthesis of six natural oligostilbenoids with five and seven membered rings, paucifloral F **4.140**, isoampelopsin D **4.108**, quadrangularin A **4.6**, isopaucifloral F **4.142**, pallidol **1.6**, ampelopsin F **1.5** and diptoindonesin A **4.152** congener in excellent yield (Scheme 4.36). The author was of the opinion that resveratrol based natural compounds like diptoindonesin D and paucifloral F appear to be incongruent with direct resveratrol oligomerisation as they possess an odd number of aromatic rings (three instead four rings). Thus, suggesting the usage of a generalized building block with three aryl rings located in the same core structure for the construction of oligostilbenoids in a controlled manner by just modifying the reagents and reaction conditions. Biaryl alcohol **4.135** will be one of these types of building blocks obtained by reacting 3,5-dimethoxybenzaldehyde **4.134** with lithiated form of **4.133**. Treating this key precursor with TFA proceeded to carbocation species **4.136** followed by regio- and stereoselective cyclization and nucleophilic attack by TFA furnished intermediate **4.138**. Subsequent quenching of **4.138** in basic medium resulted **4.139** completing the one pot synthesis from compound **4.133**. Paucifloral F **4.140** was achieved by another additional two steps of Dess-Martin periodinane alcohol oxidation and demethylation in 84% overall yield.



Reaction	Conditions	Yield (%)
a.	nBuLi (1.0 eq), THF, -78°C, 20 min; then 150 (1.0 eq), -78° to 25°C, 4 h for 154: TFA (1.0 eq), CH ₂ Cl ₂ , -30 to -20°C, 5 h; then K ₂ CO ₃ (10 eq), MeOH, 25°C, 5 min, 75%; for 155: TsOH (1.0 eq), CH ₂ Cl ₂ , -30 to 20°C, 5 h; p-methoxy- -toluenethiol (3.0 eq), then concentration to near dryness, 25°C, 12 h	71
b.	mCPBA (3.0 eq), NaHCO ₃ (10 eq), CH ₂ Cl ₂ , 0 to 25°C, 3 h	78
c.	Dess-Martin periodinane (1.2 eq), NaHCO ₃ (5.0 eq), CH ₂ Cl ₂ , 25°C, 3 h	97
d.	BBr ₃ (1.0 M in CH ₂ Cl ₂ , 10 eq), CH ₂ Cl ₂ , 0°C, 6 h	86
e.	tBuOH/H ₂ O/CCl ₄ (5/1/5), KOH (20 eq), 80°C, 12 h	52
f.	BBr ₃ (1.0 M in CH ₂ Cl ₂ , 12 eq), CH ₂ Cl ₂ , 25°C, 6 h, 76% of 115,	13% of 4.107
g.	conc. HCl (5 eq), MeOH, 80°C, 2 h	96

Scheme 4.36: Total synthesis of three dimeric resveratrol-based natural products (**4.107**, **4.140** and **4.108**) from key building block **4.133**.⁴⁰

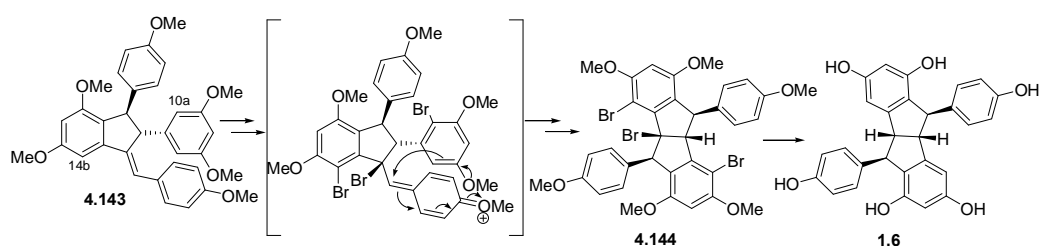
However, if **4.135** was subjected to TsOH and treated with nucleophilic *p*-methoxy- -toluenethiol, sulfide **4.137** was afforded. Subsequent Ramberg-Backlund highly selective reaction under Meyerø's modified condition and standard demethylation procedure gave the natural compound ampelopsin D **4.107** (76%). Acid treatment of **4.107** transformed it into isoampelopsin D **4.108** in 96% via olefinic isomerization.



Reaction	Conditions	Yield (%)
a.	TFA (1.0 eq), CH ₂ Cl ₂ , -30 to -20°C, 5 h; then K ₂ CO ₃ (10 eq), MeOH, 25°C, 5 min	93%
b.	Dess-Martin periodinane (1.2 eq), NaHCO ₃ (5.0 eq), CH ₂ Cl ₂ , 25°C, 3 h	98%
c.	9-I-BBN (1 M in hexanes, 10 eq), CH ₂ Cl ₂ , 40°C, 30 min	72%
d.	TsOH (1.0 eq), CH ₂ Cl ₂ , -30 to -20°C, 5h; p-methoxy-a-toluenethiol (3.0 eq), 25°C, 12 H	65
e.	mCPBA (3.0 eq), NaHCO ₃ (10 eq), CH ₂ Cl ₂ , 0 to 25 °C, 3 h	70%
f.	tBuOH/H ₂ O/CCl ₄ (5/1/5), KOH (20 eq), 80°C, 12 h	55%
g.	BBr ₃ (1.0 M in CH ₂ Cl ₂ , 12 eq), CH ₂ Cl ₂ , 25°C, 6 h	75%

Scheme 4.37: Total synthesis of three dimeric resveratrol-based natural products (**4.6** and **4.142**) from key building block **4.141** (adapted from reference 40).

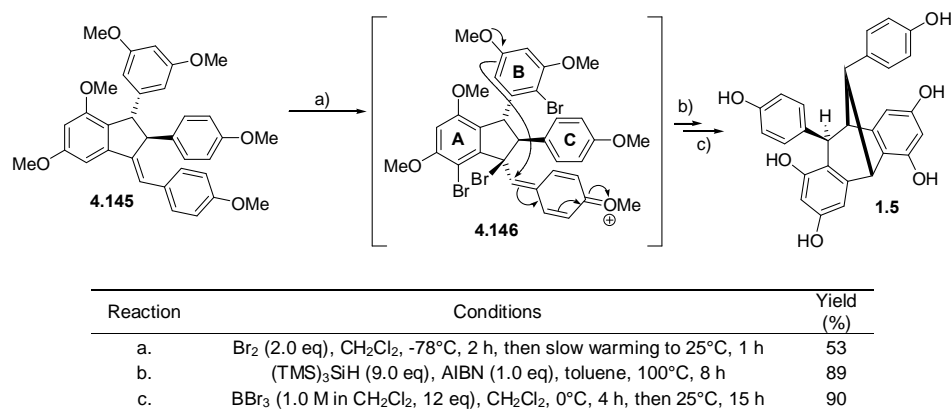
Replacing the building block **4.135** with the prepared **4.141**, which differs only by the methoxy substitution pattern, share the same chemical behaviors. Repeating the same reaction sequences on **4.141** as shown in Scheme 4.37 results in similar skeletons quadrangularin A **4.6** and isopaucifloral F **4.142** as anticipated. Thus, from the observed results, any resveratrol based compound possessing a single cyclopentane ring can be prepared from choosing the right triaryl precursors.



Reaction	Conditions	Yield (%)
a.	Br ₂ (2.0 eq), CH ₂ Cl ₂ , -78°C, 2 h, then slow warming to 25°C, 1 h	81
b.	H ₂ , Pd/C (20%, 0.2 eq), MeOH, 25°C, 24 h	76
c.	BBr ₃ (1.0 M in CH ₂ Cl ₂ , 12 eq), CH ₂ Cl ₂ , 0°C, 4 h, then 25°C, 20 h	83

Scheme 4.38: Sequential, cascade-based halogenation to access pallidol **1.6** (adapted from reference 40).

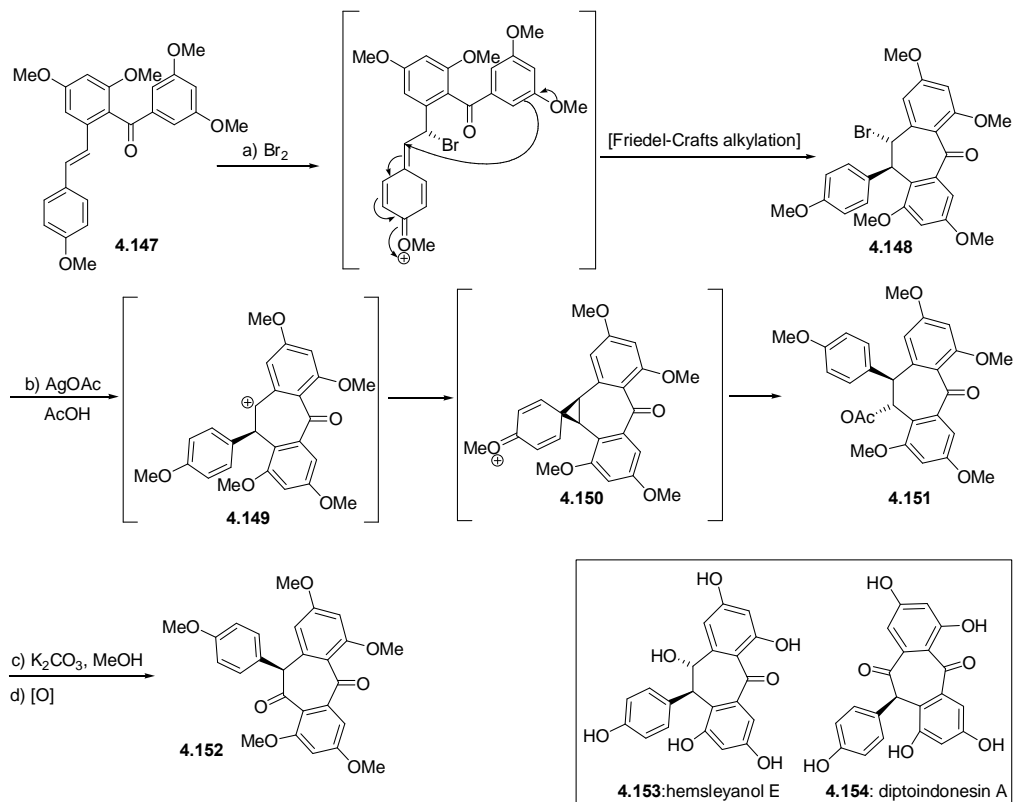
The authors⁴⁰ also described the synthesis of more complex compounds, such as pallidol **1.6** and ampelopsin F **1.5**, constructed by additional ring onto the cyclopentane core (Scheme 4.38 and 4.39). The authors have designed the chemical pathways initiated by the notion of electrophilic activation of the olefins within both ampelopsin D **4.107** and quadrangularin A **4.6**, followed by a Friedal-Crafts alkylation in order to achieve the same objective in a controlled manner. This idea is based on the use of bromine as an activating agent. As a result, subjecting permethylated quadrangularin A **4.143** to bromine at -78°C followed by slow warming to ambient temperature and resulting in highly selective cascade reaction lead to the formation of bicycle **4.144** (81%). The halogens in the intermediates play an important role due to its size in ensuring that upon ring closure, a compound will be formed stereoselectively. Hydrogenation onto Pd/C and demethylation of **4.144** accomplished **1.6** in 83% yield.



Scheme 4.39: Sequential, cascade-based halogenation to access ampelopsin F **1.5** (adapted from reference 40).

The same sequence of reactions were repeated on permethylated ampelopsin D **4.145** selectively as shown in Scheme 4.39 leading towards ampelopsin F **1.5**. In this Scheme, the three bromine atoms were replaced (intermediate **4.146**) by radical

conditions [(TMS)₃SiH, AIBN]. Obviously, the presence of halogen atoms gave access to greater molecular complexity within the resveratrol family.



Reaction	Conditions	Yield (%)
a.	Br ₂ (1.0 eq), CH ₂ Cl ₂ , -78°C, 1 h, then 25°C, 12 h	50
b.	AgOAc (3.0 eq), AcOH, 25°C, 4 h	62
c.	K ₂ CO ₃ (10 eq), MeOH, 25°C, 12 h	78
d.	Dess-Martin periodinane (1.2 eq), NaHCO ₃ (5.0 eq), CH ₂ Cl ₂ , 25°C, 1 h	99

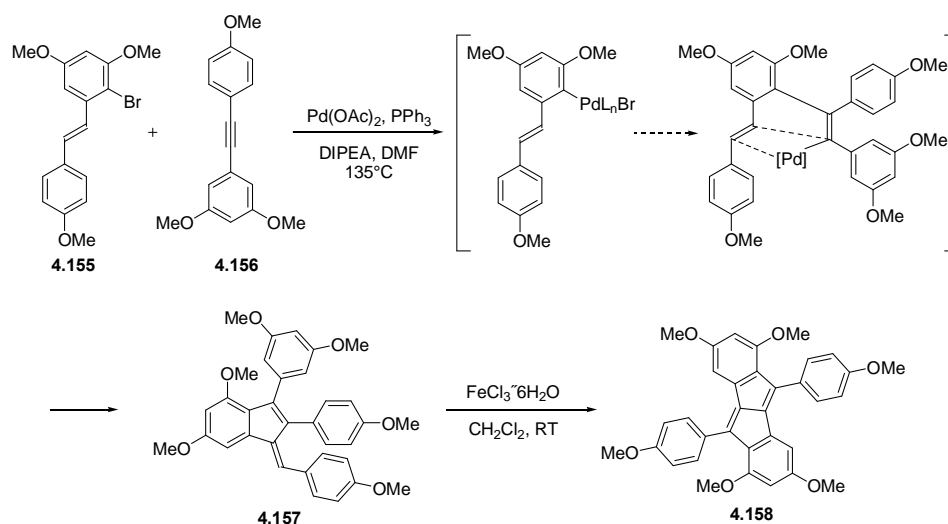
Scheme 4.40: Alternate use of key intermediate **4.147** to access the unique architectures of related nonnatural products (such as **4.152**) (adapted from reference 40).

The methylated diptoindonesin A **4.152** possessing a seven membered ring was accomplished by simply following the above described electrophilic activation/cyclization sequence. As shown in Scheme 4.40 the key precursor **4.147** resembles the oxidized form of **4.135**. Subsequent bromination and Friedal-Crafts alkylation led to **4.148**. Treating **4.148** with silver acetate in AcOH gave **4.151** (62%) via two key intermediates carbocation species **4.149** and *ortho*- and *para*-orientated

alkoxy groups in **4.150**. The migration of an aryl ring in intermediate **4.150** is due to thermodynamically favored phenonium shift which then creates an electrophilic site allowing attack by the acetate. Deacetylation of **4.151** gave a protected regioisomeric analogue of hemsleyanol E **4.153** and oxidation of the resultant alcohol produced diptoindonesin A congener **4.152**.

c) Synthesis of precursors for quadrangularin A, parthenocissin A and pallidol by Jeffrey and Sarpong.

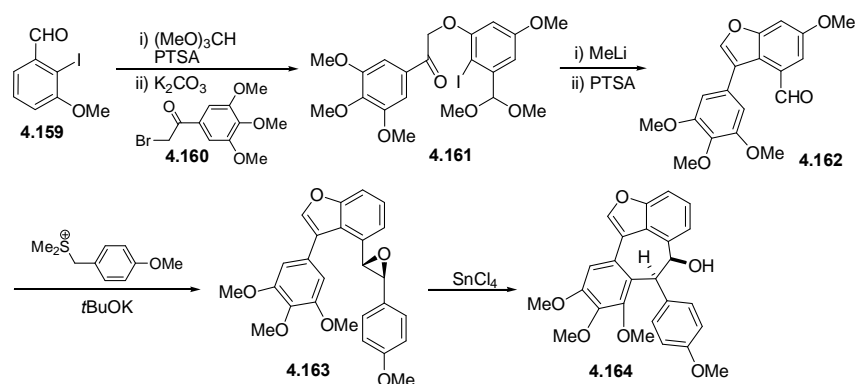
Jeffrey and Sarpong (2009)⁴¹ prepared potential precursors for natural products like quadrangularin A **4.6**, parthenocissin A **4.29** and pallidol **1.6** (Scheme 4.41). They have employed the standard Heck condition to couple bromostilbene derivative **4.155** (**4.155** was prepared by following Snyder's procedure) and tolane **4.156** via Heck/intramolecular cyclisation cascade to achieve the carbon skeleton of quadrangularin A **4.157**. Subjecting **4.157** further to a Lewis acid $\text{FeCl}_3 \cdot 6\text{H}_2\text{O}$ produced **4.158** with a carbon skeleton of pallidol through oxidative cyclisation.



Scheme 4.41: Synthesis of potential precursors for natural products.⁴¹

d) *Synthesis of malibatol A analogue by Kraus and Kim.*

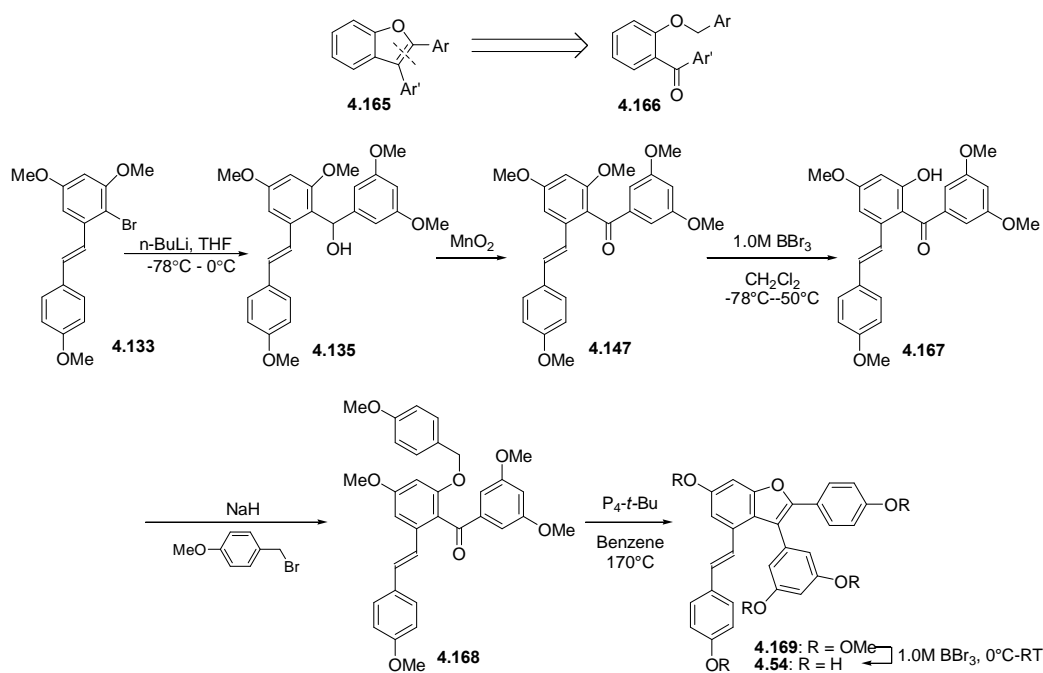
Kraus and Kim (2003)⁴² proposed a synthetic approach to malibatol A analogue from iodo aldehyde **4.159** as shown in Scheme 4.42 (**4.159** was previously prepared by Lock in 1936). Protection of aldehyde **4.159** as the acetyl and alkylation of the phenol gave ketone **4.161**. This is followed by halogen-metal exchange using alkyl lithium and treatment of PTSA, which then results in benzofuran carboxaldehyde **4.162**. Epoxidation of **4.162** continued by intramolecular cyclisation of **4.163** *via* stannic acid produced malibatol A analogue **4.164**.



Scheme 4.42: Synthesis of malibatol A analogue **4.164**.⁴²

e) *Synthesis of amurensin H 4.54 by Kraus and Gupta.*

Kraus and Gupta reported the direct synthesis of amurensin H **4.54** in year 2009.⁴³ They prepared an array of diarylbenzofurans **4.165** from benzophenones **4.166** and extended this strategy to amurensin H **4.54** (Scheme 4.43). Snyder's building block was used as their starting material **4.133**. Stilbene **4.133** was reacted with 3,5-dimethoxybenzaldehyde after the metal-halogen exchange to give **4.135**. Compound **4.135** was first oxidized, selectively demethylated and converted into benzyl ether **4.168**. Cyclization of benzyl ether **4.168** by the aid of base P₄-t-Bu at 170°C yielded methylated amurensin H **4.169** (42%). Deprotection of **4.169** successfully gave amurensin H **4.54** in 67% yield.

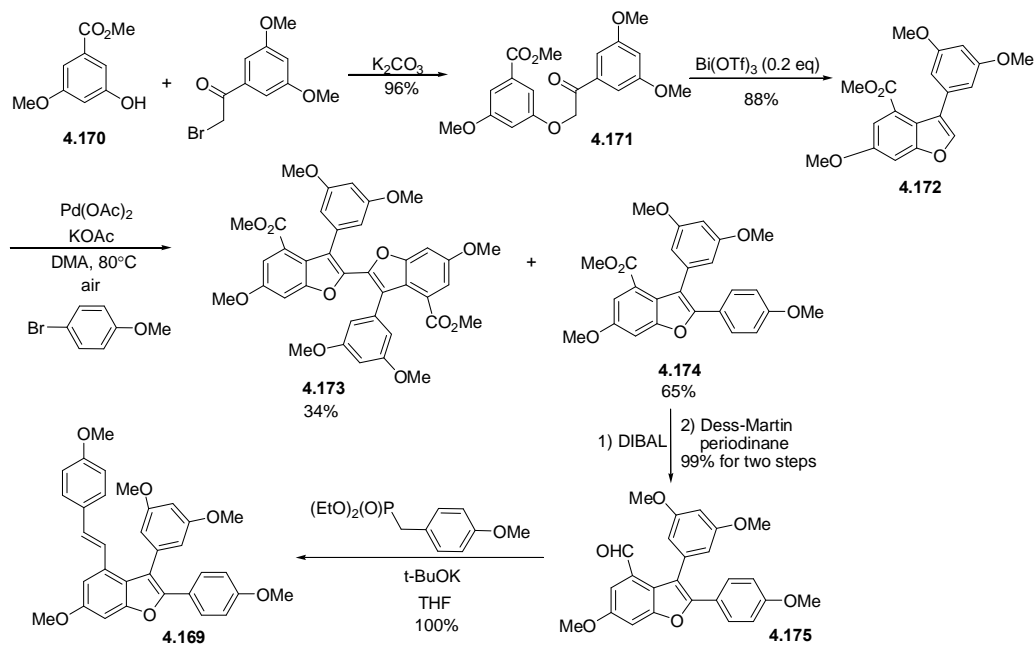


Scheme 4.43: Synthesis of amurensin H.⁴³

f) Synthesis of malibatol A **4.179**, shoreaphenol **4.178** and viniferifuran **4.169** by Kim *et al.*

Kim *et al.*⁴⁴ (2009) reported the synthesis of three oligostilbenoid analogues malibatol A **4.179**, shoreaphenol **4.178** and viniferifuran **4.169** in excellent yields. To prepare all those three oligostilbenoids, compound **4.175** seems to be the preferred precursor. In the attempt to prepare **4.175**, a sequence of reactions was carried out (Scheme 4.44). Firstly, phenol **4.170** was reacted with α -bromoketone in basic medium to accomplish ketone **4.171**. This is followed by subjecting **4.171** to Bi(OTf)₃ in refluxing dichloromethane affording a cyclized product 3-arylbenzofuran **4.172**. Among the different tested cyclodehydration conditions (BCl₃/CF₃CO₂H/InCl₃/FeCl₃/BiCl₃) Bi(OTf)₃ was found to be the best reagent affording **4.172** in 88% yield. To insert an aryl group to the benzofuran **4.172** at C2, 4-bromoanisole was reacted with **4.172** in the presence of Pd(OAc)₂, KOAc and DMA at 80°C open

atmosphere to afford arylated product **4.174** (65%) and cross-coupled product **4.173** (34%).

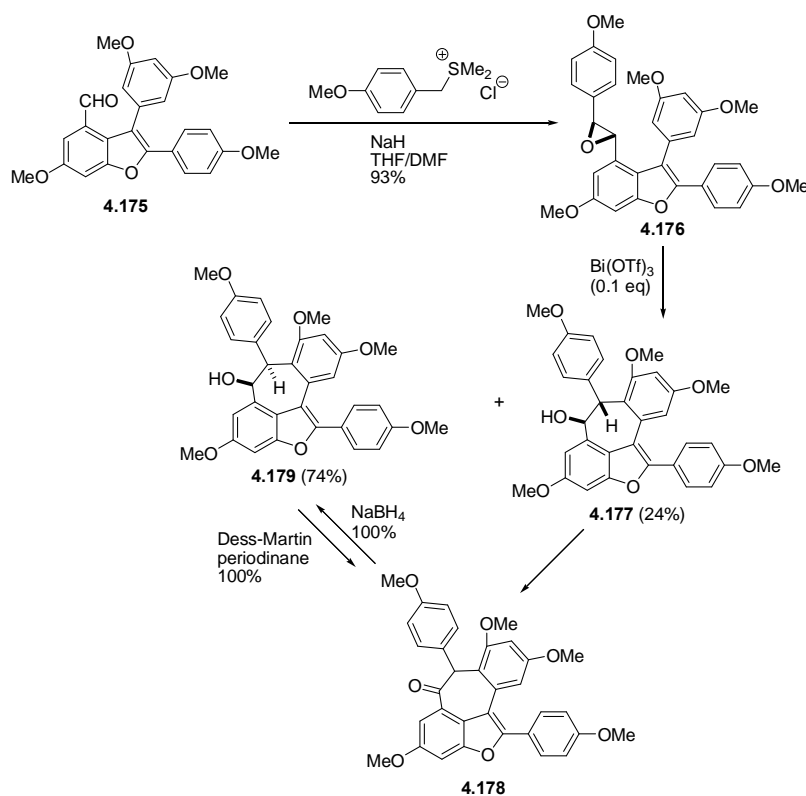


Scheme 4.44: Synthesis of viniferifuran analogue **4.169** (from Kim *et al.*).⁴⁴

Replacing 4-bromoanisole with either 4-iodoanisole or 4-methoxyphenylboronic acid showed significant reduction in the yield of **4.174** and conducting the reaction in a lower temperature was essential. The next stage was to convert the ester group in **4.174** to an aldehyde as in compound **4.175** with the help of DIBAL and Dess-Martin. Permethylated analogues of veniferan **4.169** were produced by performing Horner-Wadsworth-Emmons type olefination of **4.175** with diethyl-4-methoxybenzylphosphonate (Scheme 4.44).

The seven membered ring compounds **4.179** and **4.178** were designed to be constructed by olefinic epoxidation of **4.169** but this method ended up with a complex mixture. This led directed to a different approach where Corey-Chaykovsky protocol was used to make epoxide **4.176**. Therefore, **4.175** was reacted with dimethyl(4-methoxybenzyl)sulfonium chloride to produce the desired *trans*-epoxide **4.176**

(Scheme 4.45). The addition of $\text{Bi}(\text{OTf})_3$ to **4.176** opened the epoxide ring stereoselectively via nucleophilic attack by the neighboring aromatic group accomplishing **4.179** and **4.177** in a ratio of 3:1. Replacing $\text{Bi}(\text{OTf})_3$ with other reagents (SnCl_4 , PTSA- H_2O , PPTS, InCl_3 , $\text{CH}_3\text{CN-H}_2\text{O}$) did not render satisfactory results. Subjecting compound **4.179** or **4.177** to Dess-martin oxidation provided **4.178** in quantitative yield. However, **4.178** can be reconverted to **4.179** by sodium borohydride reduction. The conversion of **4.177** to **4.179** *via* **4.178** further confirms the stereochemical outcome.

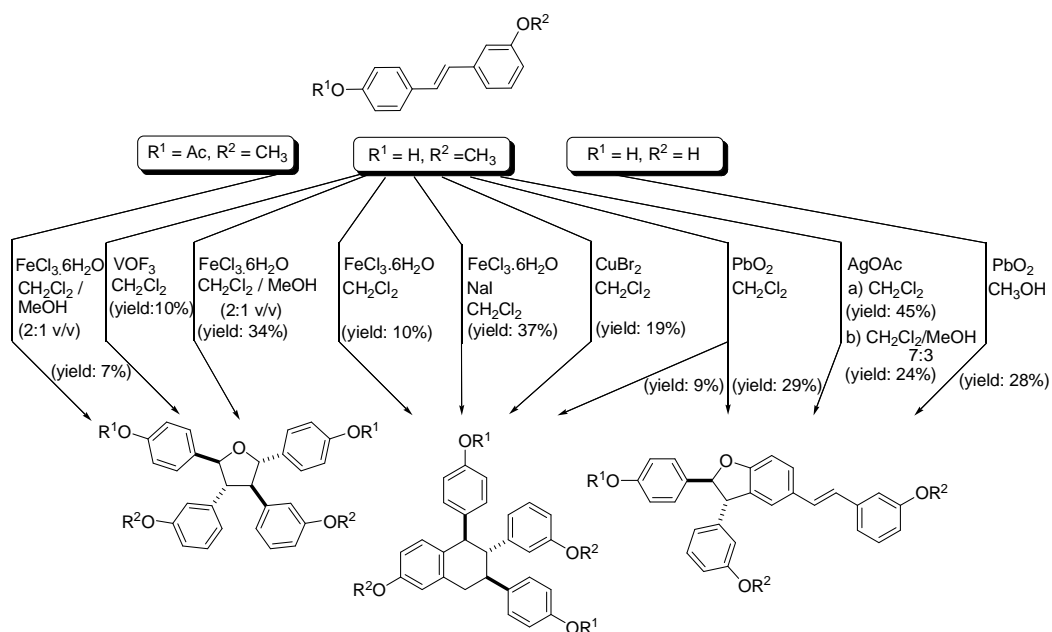
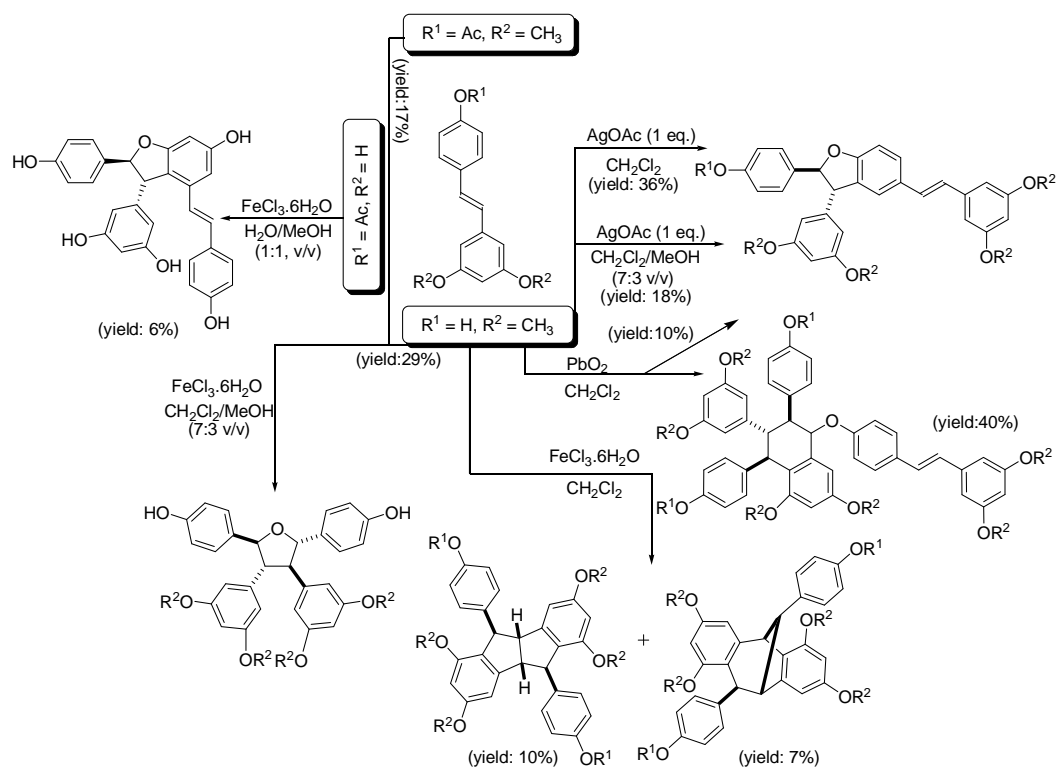


Scheme 4.45: Synthesis of malibatol A **4.179** and shoreaphenol **4.178** analogues (from reference 44)

4.3. Results and discussion

As mentioned previously in the introduction of this chapter, below is the outline of a series of one pot oxidative coupling reactions performed to prepare ten

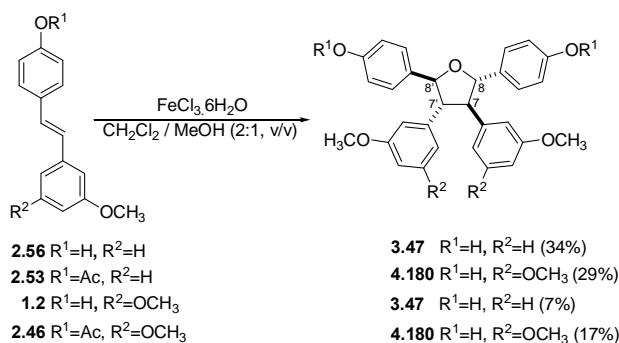
oligostilbenoid analogues with five different types of skeletons using various chemical oxidants such as $\text{FeCl}_3 \cdot 6\text{H}_2\text{O}$, $\text{FeCl}_3 \cdot 6\text{H}_2\text{O}/\text{NaI}$, AgOAc , PbO_2 , CuBr_2 and VOF_3 (Scheme 4.46). Stilbenoids with six different substitution patterns namely pterostilbene **1.2**, 3,5-dimethoxy-12-acetoxystilbene **2.46**, 3,5-dihydroxy-12-acetoxystilbene **2.52**, demethoxypterostilbene **2.56**, 3-methoxy-12-acetoxystilbene **2.53** and 3-hydroxy-12-hydroxystilbene **2.58** are selected and exposed to the above metal oxidants in different types of solvents CH_2Cl_2 , $\text{CH}_2\text{Cl}_2/\text{MeOH}$ mixture, MeOH and $\text{MeOH}/\text{H}_2\text{O}$ mixture. The analysis of these results together with those obtained by other researchers as summarized above would help to provide some rationale in terms of mechanistic issues involved in the oxidative coupling and are presented herein.



Scheme 4.46: Summary of synthesized oligostilbenoids *via* chemical oxidation

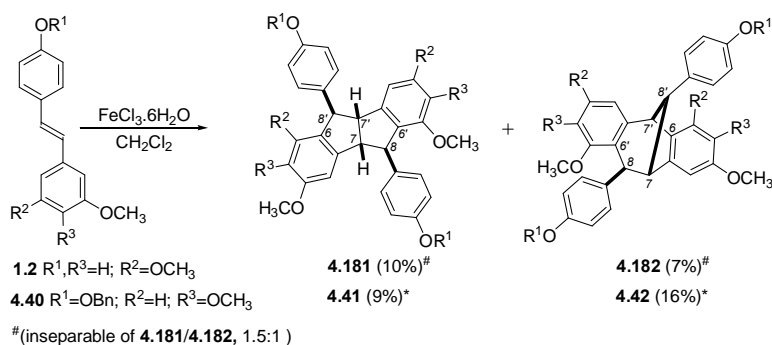
4.3.1. Oxidative coupling with Fe³⁺

Tricuspidatol A analogue **3.47** was formed from the building blocks **2.56** and **2.53**, while **4.180** was obtained from **1.2** and **2.46** in the presence of FeCl₃·6H₂O (Scheme 4.47). This reaction is, however, solvent dependent as it occurs only in a mixture of CH₂Cl₂/MeOH (7:3, v/v).



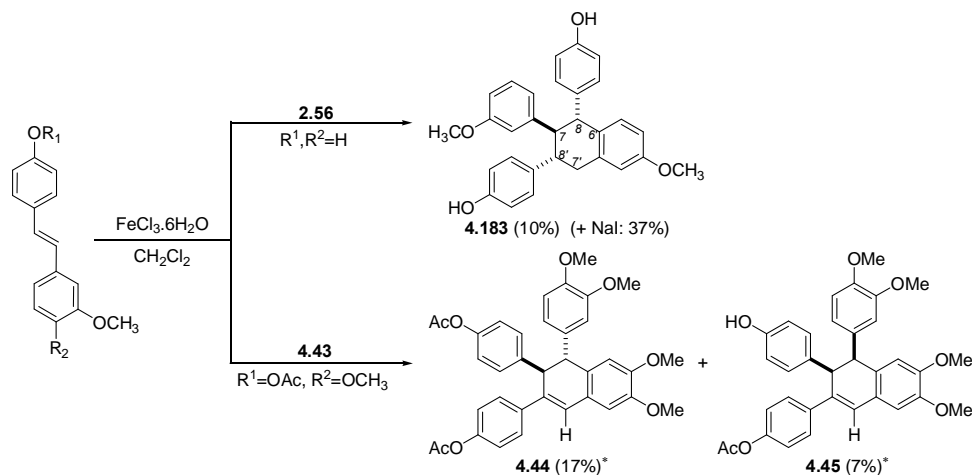
Scheme 4.47: Synthesis of tricuspidatol A analogues in FeCl₃·6H₂O/CH₂Cl₂/MeOH mixture

When this reaction was performed in pure CH₂Cl₂ we observed the formation of compounds whose structures would depend on the substitution pattern of the building blocks (Scheme 4.48). Subjecting pterostilbene **1.2** to FeCl₃·6H₂O in CH₂Cl₂ produced pallidol and ampelopsin F analogues **4.181** and **4.182** respectively in a ratio of 1.5:1 but as an inseparable mixture. When catechol substituted stilbene **4.40** was employed by one of our group members, pallidol and ampelopsin F analogues **4.41** and **4.42** respectively were obtained in an inverse proportion (Scheme 4.48).²⁵



Scheme 4.48: Generation of pallidol and ampelopsin F analogues in $\text{FeCl}_3 \cdot 6\text{H}_2\text{O} / \text{CH}_2\text{Cl}_2$ mixture (*adapted from reference 25).

In contrast, treatment of demethoxypterostilbene **2.56** with $\text{FeCl}_3 \cdot 6\text{H}_2\text{O}$ in CH_2Cl_2 (in the absence of methanol) produced the all-*trans* triaryltetralin **4.183** (Scheme 4.49), quite similar to restrytol C **4.13**. The addition of NaI to the reaction mixture increased the yield very significantly from 10 to 37%.

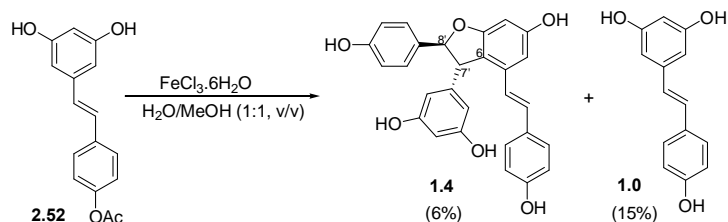


Scheme 4.49: Synthesis of tetrahydronaphthalene and dihydronaphthalene based stilbene dimers in $\text{FeCl}_3 \cdot 6\text{H}_2\text{O} / \text{CH}_2\text{Cl}_2$ mixture (*adapted from reference 26).

The above-mentioned products **4.183**, together with **4.44** and **4.45** prepared by Thomasø group (see above section 4.1.3.3, Scheme 4.16) resemble restrytol C **4.13**, a biotransformation product of **1.0** by *Botrytis cinerea*¹⁴ (see above section 4.1.2.1, Figure 4.2). However, **4.183** should be looked upon as resulting from head-to-tail

alignment of the stilbene precursors, while **4.44** and **4.45** derive from a head-to-head alignment of the monomers (for detailed mechanistic explanation, see section 4.3.5.10).

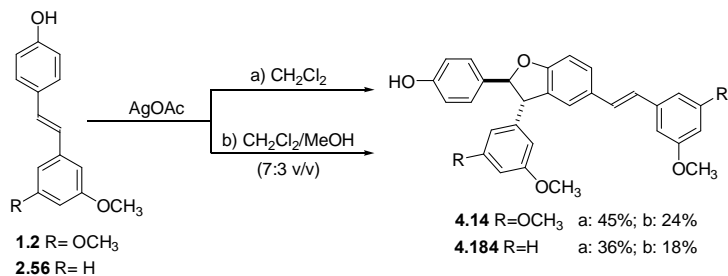
Subjecting dihydroxy-*para*-acetate stilbene **2.52** to ferric chloride dimerization in MeOH/H₂O mixture gave naturally occurring resveratrol **1.0** and -viniferin **1.4** whereby the acetoxy groups are cleaved in both cases (Scheme 4.50).



Scheme 4.50: Synthesis of -viniferin via FeCl₃·6H₂O oxidation

4.3.2. Oxidative coupling with Ag⁺

Stilbenes **1.2** and **2.56** (previously exposed to FeCl₃, see section 4.3.1) converted by means of AgOAc into δ-viniferin analogues **4.14** and **4.184** respectively (Scheme 4.51). A solvent effect was, however, observed: when the reaction is carried out in CH₂Cl₂, the yield is roughly twice the one obtained from a mixture of CH₂Cl₂/MeOH (2:1 v/v). Generally speaking, the δ-viniferin skeleton is obtained by treatment of a 12-hydroxystilbenes **1.2** and **2.56** by AgOAc, regardless of the substitution pattern or the nature of the solvent.

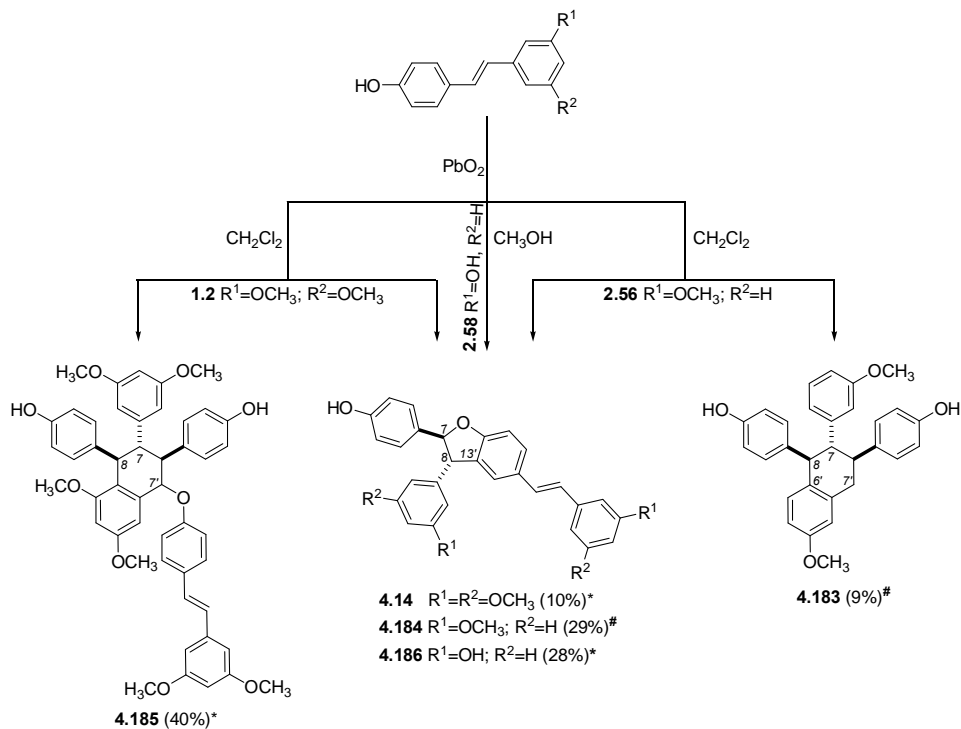


Scheme 4.51: Synthesis of δ-viniferin analogues by AgOAc oxidative coupling

It is noteworthy that 3-hydroxy-12-methoxystilbene **2.57** is not dimerised when subjected to any of the above conditions.

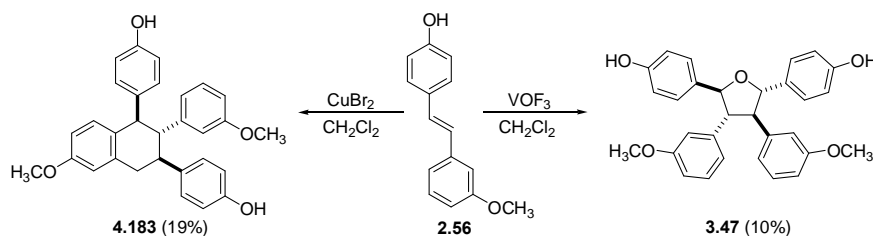
4.3.3. Dimerization with other oxidants

As a continuation of the work presented in section 4.3.2, subjecting stilbenes **1.2**, **2.56** and **2.58** to PbO_2 led to results that can be viewed as combining elements of transformations promoted by Fe^{3+} and Ag^+ oxidative coupling of the stilbenes above (Scheme 4.52). Treating demethoxypterostilbene **2.56** with PbO_2 in CH_2Cl_2 gave tetralin **4.183** (9%) and δ -viniferin analogue **4.184** (29%). Intriguingly, trimer **4.185**, which possess a tetralin moiety, together with δ -viniferin analogue **4.14** were the results of pterostilbene **1.2** oxidative coupling in the same above reaction condition in 40% and 10% yield respectively. In addition, exposure of **2.58** to PbO_2 in MeOH gave solely **4.186** (28%) as another variety of δ -viniferin analogue.



Scheme 4.52: Oxidative coupling by PbO_2 of stilbenes **1.2**, **2.58** and **2.56**

Treatment of demethoxypterostilbene **2.56** in $\text{CuBr}_2/\text{CH}_2\text{Cl}_2$ mixture produces tetralin **4.183** in 19% yield, twice the yield of tetralin obtained from PbO_2 and $\text{FeCl}_3 \cdot 6\text{H}_2\text{O}$ in CH_2Cl_2 (Scheme 4.53). Tricuspidatol A analogue **3.47** could be obtained by dimerising **2.56** in $\text{VOF}_3/\text{CH}_2\text{Cl}_2$ mixture, just like from $\text{FeCl}_3 \cdot 6\text{H}_2\text{O}/(\text{CH}_2\text{Cl}_2/\text{MeOH})$ mixture (see section 4.3.1 and Scheme 4.47).



Scheme 4.53: Tetralin and tricuspidatol A analogues as oxidative coupling products from stilbene **2.56**

4.3.4. Spectroscopic analysis

Herein, the spectroscopic data are discussed for the following compounds: δ -viniferin analogues **4.14** and **4.184**, tricuspidatol A analogue **3.47**, tetrahydronaphthalene **4.183** and finally a novel compound **4.185**. Other synthesized compounds *i.e.* ampelopsin F **4.182**, pallidol **4.181**, tricuspidatol A **4.180**, δ -viniferin **4.186** analogues as well as ϵ -viniferin **1.4** are not discussed here. The structures of these compounds were determined by comparison of their spectroscopic data with those of the other prepared analogues with established structures as described below or by comparison with the published data. See also experimental section.

4.3.4.1. δ -Viniferin analogue **4.14**

Compound **4.14** possesses a molecular formula of $\text{C}_{32}\text{H}_{30}\text{O}_6$ as deduced from the data obtained by ESI-TOF-MS in negative mode. This would correspond to a dimeric

species which would contain two stilbene monomers. The ^1H spectrum includes signals integrating for (Table 4.1):

- a) 13 aromatic protons in the range of 6.3 to 7.3 ppm.
- b) 2 olefinic protons at 6.83 (H7 ϕ) and 7.00 ppm (H8 ϕ) with *trans* coupling constants of 16.1 Hz.
- c) 2 methyne protons at 4.47 and 5.50 ppm, which correspond to protons at positions 7 and 8 respectively. These were in accordance with carbon signals observed at 57.9 and 93.1 ppm.
- d) 2 signals corresponding to two methoxy groups at 3.75 and 3.80 ppm.

The chemical shifts of protons and carbon atoms in position 7 and 8 strongly suggest the presence of a benzofuran moiety. The value of $^3J_{\text{H-7,H-8}}$ measured from ^1H NMR spectrum (8.0Hz) suggests a predominant configuration with the two H7 and H8 protons in a pseudo *trans*-axial arrangement. The HMBC correlations between C2/6 and H7 and between C10/14 and H8 allow to establish that the 3,5-dimethoxybenzene ring is bonded to C7 whereas the 4-hydroxybenzene ring is bonded to C8. The observation of olefinic proton signals indicates the presence of one stilbene moiety in this dimeric species. Therefore we can conclude that the dimeric species consists of one stilbene unit which is fused by furan ring from another unit at positions 7 and 8 to construct a diaryldihydrobenzofuran.

NOESY data indicate that H7 is spatially close from H10 and 14. Similarly, H8 is spatially close from H2 and 6. This indicates *trans*-substitution of the benzodihydrofuran ring. This was further supported by AM1 calculations (annealing method) performed on stereoisomers which shows that the *trans*-substituted isomer possesses a lower formation heat as compared to the *cis*-substituted isomer (Figure 4.4). Appendix 41 and 42 show ^1H NMR and ^{13}C NMR spectra of compound **4.14** respectively. Appendix 43 shows ESI-TOF-MS (-) spectrum of **4.14**. Therefore, **4.14**

was assigned the structure of an analogue of naturally-occurring δ -viniferin⁴⁵, *i.e.* (*E*)-tetra-*O*-methyl- δ -viniferin (Figure 4.3).

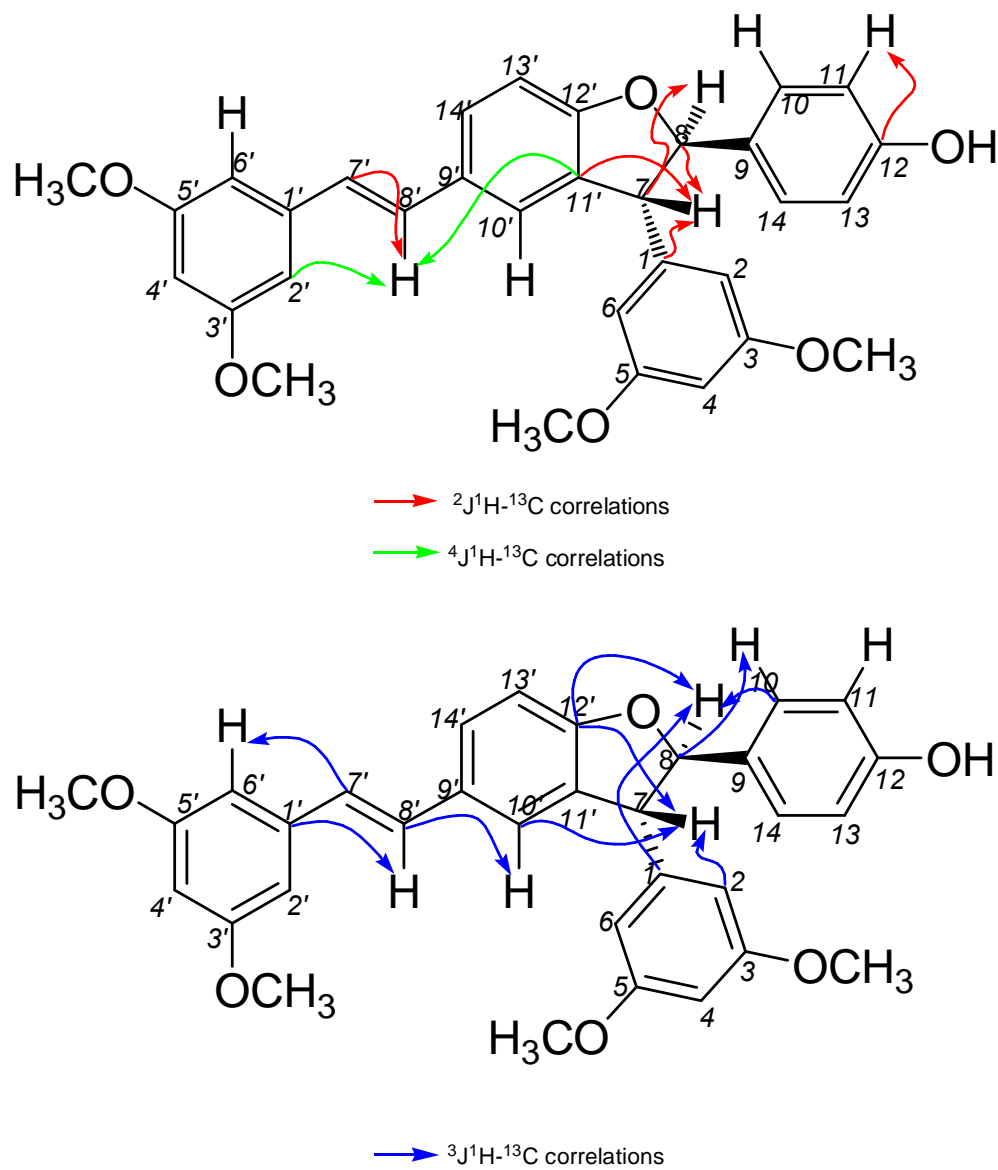
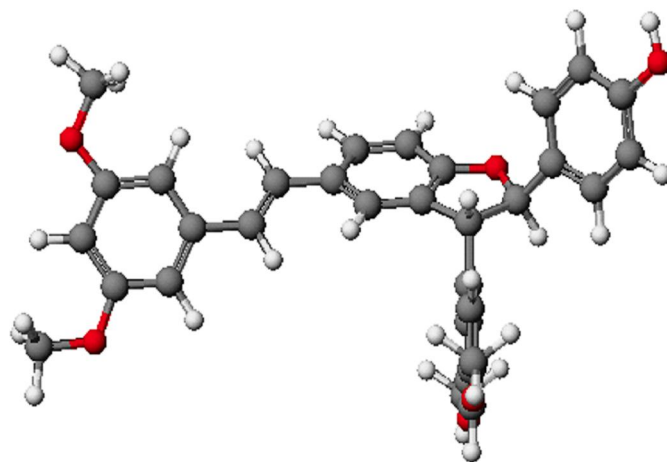
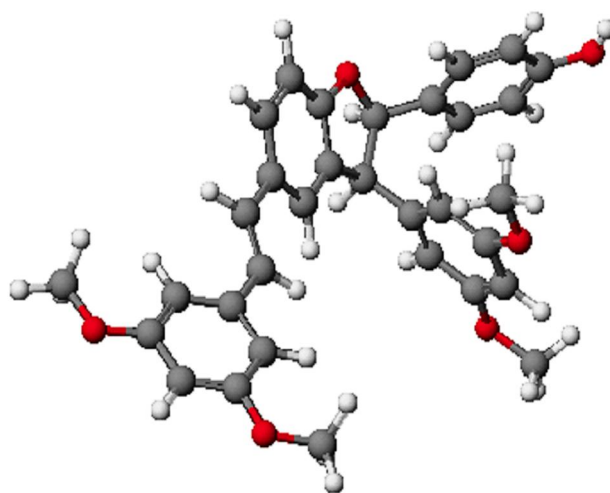


Figure 4.3: Main HMBC correlations for 4.14



Trans substituted isomer: -108.613 kcal/mol (most stable)



Cis substituted isomer: -104.961 kcal/mol

Figure 4.4: AM1 calculation for 4.14

Table 4.1: ^1H -(300 MHz) and ^{13}C -(75 MHz) NMR data **4.14**.

Carbon No.	^1H -NMR δ , ppm (J, Hz)	COSY correlations	^{13}C NMR δ , ppm	^{13}C - ^1H HMBC correlations	NOESY correlations
1	-	-	144.0	H7, H8	-
2/6	6.34 d (2.2)	4	106.5	H2/6, H4, H7	10 α , 7, 8
3/5	-	-	161.2	H2/6, H4	-
4	6.40 t (2.2)	2/6	99.1	H2/6	3/5-OMe
7	4.47 d (8.5)	8, 10 ϵ	57.9	H8, H2/6, H10 ϵ	10/14, 2/6, 8
8	5.50 (8.0) d	7	93.1	H7, H10/14	10/14, 2/6, 7
9	-	-	132.6	H11/13, H7, H8	-
10/14	7.20 d (8.8)	11/13	127.6	H10/14, H8	7, 8
11/13	6.81 d (8.5)	10/14	115.6	H11/13, H10/14, 12-OH	H2 δ /6 α , 8 α , 10 δ
12	-	-	156.0	H11/13, H10/14	-
1'	-	-	139.8	H7 α , H8 δ	-
2'/6'	6.61 d (2.2)	4 δ	104.3	H4 α , H7 α , H8 δ	11/13, 8 α , 3 δ /5 δ -OMe
3'/5 δ	-	-	161.0	-	3 δ /5 δ -OMe, 3/5-OMe
4'	6.35 t (2.2)	2 δ /6 δ	99.8	H2 δ /6 δ	-
7'	6.83 d (16.1)	8 δ	126.3	H2 δ /6 α , H8 δ	-
8'	7.00 d (16.1)	7 δ	129.1	H7 α , H10 α , H14 δ	2 δ /6 α , 11/13, 10 ϵ
9'	-	-	130.9	H7 α , H13 α , H8 α , H7 ϵ	-
10'	7.19 s	7 weak	123.2	H8 α , H14 α , H7	2/6, 11/13, 8 ϵ
11'	-	-	130.8	H8 α , H7	-
12'	-	-	159.8	H13 α , H10 α , H14 α , H7, H8	-
13'	6.91 d (8.3)	14 ϵ	109.8	-	-
14'	7.36 d (8.3)	13 δ	128.1	H8 α , H10 α , H7	11/13, 13 α , 8 ϵ
3'/5' OMe	3.8	-	55.3	H3 δ /5 δ	2 δ /6 α , 4 δ
3/5 OMe	3.75	-	55.4	H3/5	4, 4 δ

4.3.4.2. δ -Viniferin analogue 4.184

The structure below was determined using a reasoning identical as that for compound 4.14. Figure 4.5 shows the main HMBC correlations for δ -viniferin analogue 4.184 and the spectroscopic data are tabulated in Table 4.2. Appendix 44 and 45 show ^1H NMR and ^{13}C NMR spectra of compound 4.184 respectively. Appendix 46 shows ESI-TOF-MS (-) spectrum of 4.184.

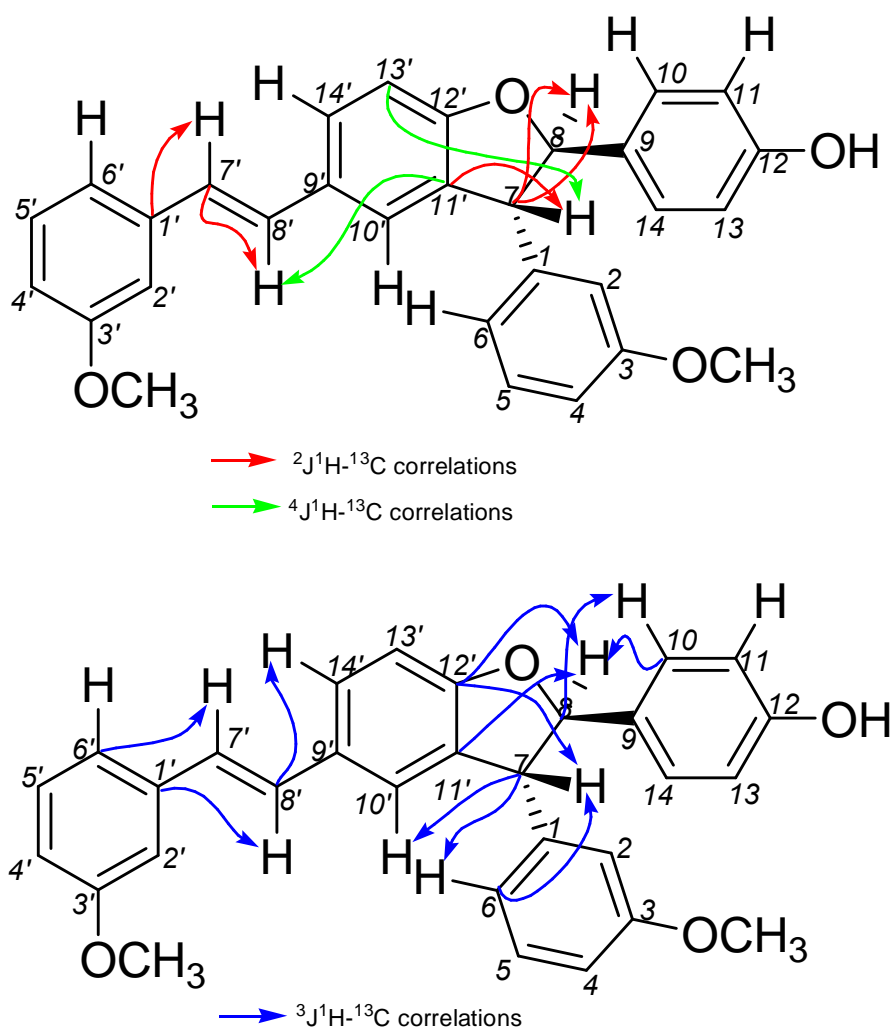


Figure 4.5: Main HMBC correlations for 4.184

Table 4.2: ^1H -(500 MHz) and ^{13}C -(125 MHz) NMR data of **4.184**

Carbon No.	^1H -NMR δ , ppm (<i>J</i> , Hz)	COSY correlations	^{13}C -NMR δ , ppm	^{13}C - ^1H HMBC correlations	NOESY correlations
1	-	-	143.1	H8, H7, H5	-
2	6.73, t (2.0)	4	114.2	H4, H6, H8	7, 8, 10 α 3-OMe
3	-	-	159.8*	-	-
4	6.84, ddd, (0.7, 2.4, 8.3)	2, 5	112.5	H5, H4, H6, H2	5, 3-OMe
5	7.26, t (7.8)	4	129.9	-	6, 4
6	6.79, dd (1.5, 7.8)	-	120.8	H5, H4, H2, H7	5, 7, 8
7	4.53, d (8.5)	8	57.6	H5, H10 α H2, H6, H8	8(weak), 2, 6, 10 α 10/14
8	5.50, d (8.5)	7	93.2	H10, H7	7 (weak), 2, 6, 10/14
9	-	-	132.6	H8	-
10/14	7.23, d (8.3)	11	127.6	H8	13/11, 7, 8
11/13	6.80, d (8.5)	10/14	115.5	H10, H11	10/14
12	-	-	155.7	H11, H10	-
1 ϕ	-	-	139.1	H7 α H8 α H5 ϕ	-
2 ϕ	6.97, t (2.0)	4 ϕ	111.4	H5 α H4 α H7 ϕ	3 ϕ -OMe
3 ϕ	-	-	159.974*	-	-
4 ϕ	6.77, dd (2.4)	2 ϕ	112.9	H5 α H2 α H6 ϕ	3 ϕ -OMe
5 ϕ	7.24, t (7.8)	6 ϕ	129.6	H6 ϕ	6 ϕ
6 ϕ	7.03, d (7.8)	5 ϕ	118.9	H5 α H10 α H6 α H2 α H7 α H4 ϕ	5 ϕ
7 ϕ	6.87, d (16.4)	8 ϕ	126.2	H8 ϕ	10 α 14 ϕ
8 ϕ	7.02, d (16.4)	7 ϕ	128.8	H14 α H7 ϕ	10 α 14 ϕ
9 ϕ	-	-	130.8 [#]	H14 α H8 α H8, H7	-
10 ϕ	7.18, bs	14 ϕ	123.1	H14 α H8 α H13 α H7	8 α 2, 7 α 7
11 ϕ	-	-	130.9 [#]	H14 α H8 α H8, H7	-
12 ϕ	-	-	159.7	H8, H7, H13, H14 α H10 ϕ	-
13 ϕ	6.92, d (8.3)	14 ϕ	109.7	H10 α 7	14 ϕ
14 ϕ	7.37, dd (1.47, 8.3)	13 ϕ /10 ϕ	127.9	H7, H8, H10 ϕ	7 α 13 α 8 ϕ
3 ϕ -OMe	3.81, s	-	159.85	H4 α H5 ϕ	4 α 2 ϕ
3-OMe	3.77, s	-	159.97	H2, H4, H6	4, 2

^{#, *} Chemical shifts with the same superscripts can be interchanged.

4.3.4.3. Tricuspidatol A analogue 3.47

Compound **3.47** possesses a molecular formula of $C_{30}H_{28}O_5$ as deduced from the data obtained by ESI-TOF-MS in negative mode. This would correspond to a dimeric species which would contain two stilbene monomers and an additional oxygen atom. The 1H NMR spectrum of compound **3.47** integrated for 8 aromatic protons and 2 methine protons, thus indicating a symmetrical dimer (Table 4.3). Appendix 47 and 48 show 1H NMR and ^{13}C NMR spectra of compound **3.47** respectively. Appendix 49 shows ESI-TOF-MS (-) spectrum of **3.47**. The symmetrical nature of this molecule was supported by the shape of the H7 and H8 proton signals, which appear as pseudo doublets, typical of AA ϕ BB ϕ systems found in symmetrical structure.

Olefinic protons of the starting material **2.56** were no longer observed, indicating that the corresponding sp^2 carbons were converted into stereogenic sp^3 centers. The chemical shifts of both the proton and the carbon at position 8 (and 8 ϕ) (5.28 and 87.5 ppm respectively) indicate a substitution of these position by an oxygen atom. As a result, this molecule derives from a symmetrical tetrasubstituted tetrahydrofuran. Analysis of the HMBC correlations was utilized to establish the connectivities of the aromatic rings to the tetrahydrofuran ring. The correlations between C2/6 and H7 and between C10/14 and H8 demonstrated that the 3-methoxybenzene ring is attached to C7 whereas the 4-hydroxybenzene ring is attached to C8. The complete analysis of COSY, HMQC and HMBC led to establish the structure of compound **3.47** as 4,4 ϕ [3,4-bis(3-methoxyphenyl)-tetrahydrofuran-2,5-diyl]-diphenol (Figure 4.6). NMR experiments were, as expected, unable to allow us to determine the type of symmetry, that is whether **3.47** possess an axis or a plane of symmetry. As crystals could not be obtained, we opted for computational AM1 calculation (annealing method) (Figure 4.7). The configuration that was found to have the lowest formation heat correspond to an all-*trans* substituted derivative, with an

axial symmetry. As a result, **3.47** was found to be an analogue of tricuspidadol A isolated from *Parthenocissus tricuspidata*.⁴⁶

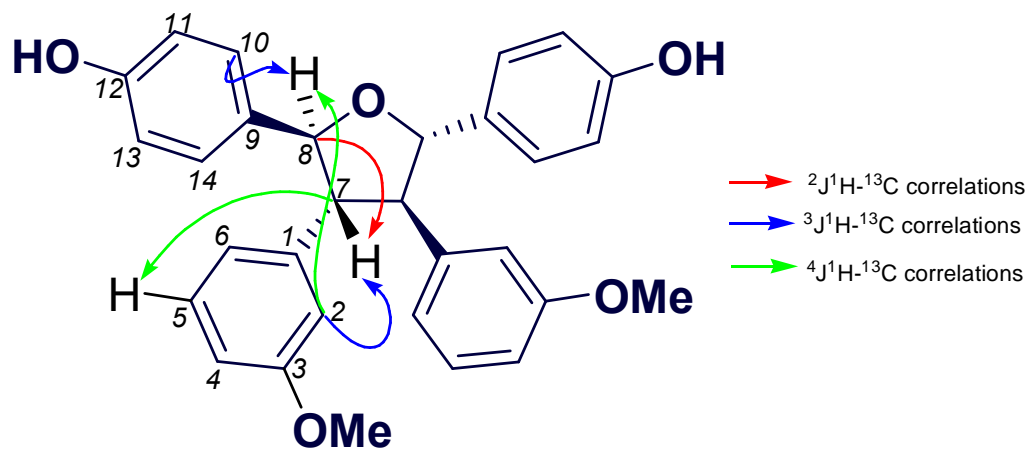
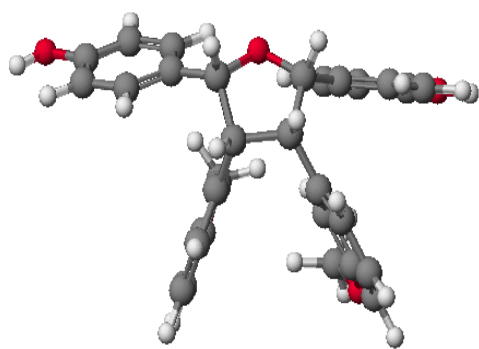
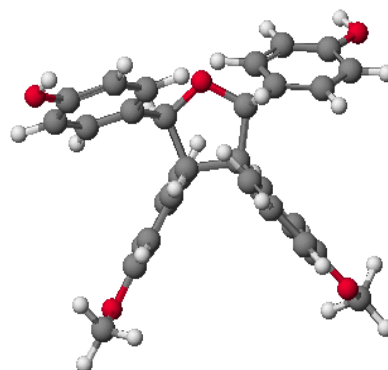


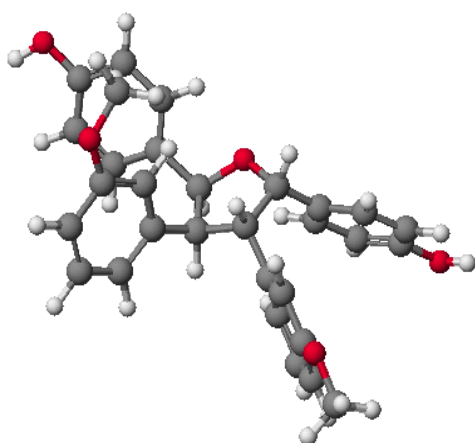
Figure 4.6: Main HMBC correlations for **3.47**



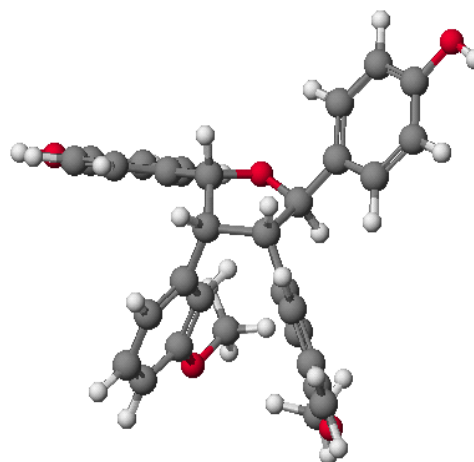
-90.213 kcal/mol



-103.640 kcal/mol (most stable)



-95.222 kcal/mol



-95.570 kcal/mol

Figure 4.7: AM1 calculation of tricuspidatol A analogue **3.47**

Table 4.3: ^1H -(300 MHz) and ^{13}C -(75 MHz) NMR data of **3.47**

Carbon No.	^1H -NMR δ , ppm (J, Hz)	COSY correlations	^{13}C -NMR δ , ppm	^{13}C - ^1H HMBC correlations	NOESY correlations
1	-	-	139.4	H7, H8, H6, H5	-
2	6.58 s	-	114.2	H7, H8, H6/4, H5	8, 7, 3-OMe
3	-	-	159.5	3-OMe, H2, H4, H5	-
4	6.68 (7.3) d	-	112.0	H2, H6, H5	3-OMe
5	7.09 (8.0) t	-	129.5	H4/6	-
6	6.69 (7.3) d	-	120.4	H7, H8, H2, H4, H5	7, 8
7	3.61 (10) AA'BB' d*	8	62.1	H7, H8, H2, H6, H5	10/14, 2, 6, 8
8	5.28 (10) AA'BB' d*	7	87.4	H7, H8, H10/14	10/14, 7, 2, 6
9	-	-	132.9	H7, H8, H11/13	-
10	7.13 (8.5) d	11/13	127.6	H8, H11/13, H10/14	7, 8
11	6.65 (8.5) d	10/14	115.4	H11/13, H10/14	12-OH
12	-	-	155.4	H11/13, H10/14	-
13	6.65 (8.5) d	10/14	115.4	H11/13, H10/14	12-OH
14	7.13 (8.5) d	11/13	127.7	H8, H11/13, H10/14	7, 8
OMe	3.65 s	-	55.2	-	2, 4
12-OH	-	-	-	-	11/13

*Actually these pseudo doublets include 6 lines each, as expected from an AA ϕ BB ϕ system in a symmetrical structure. The 10 Hz measurements corresponds to the frequency difference between the two main lines.

4.3.4.4. Tetrahydronaphthalene 4.183

Compound **4.183** possesses a molecular formula of $C_{30}H_{28}O_4$ as deduced from the data obtained by ESI-TOFMS negative mode. This would correspond to a dimeric structure that would include two interstilbene bonds. The 1H spectrum includes signals integrating for 15 aromatic protons, thus indicating that one of the aromatic rings is engaged in the interstilbene linkage (Table 4.4). Appendix 50 and 51 show 1H NMR and ^{13}C NMR spectra of compound **4.183** respectively. Appendix 52 shows ESI-TOF-MS (-) spectrum of **4.183**. Five signals, corresponding to aliphatic protons are observed between 3.0 and 4.2 ppm and are assigned to positions 7, 8, 7' and 8. The ^{13}C and DEPT spectra provided similar information: 24 aromatic carbon atoms, of which 7 are C-H, and 4 benzylic carbon atoms. At this stage, we can already conclude that a triaryltetrahydronaphthalene ring structure is present. There are two questions left to be solved, the identity of each aromatic ring and the stereochemistry of the molecule. The plane structure is readily obtained from analysis of the two dimensional homo- and heteronuclear spectra as that of 5,7-bis(4-hydroxyphenyl)-2-methoxy-6-(3-methoxyphenyl)-tetrahydronaphthalene (Figure 4.8). Given the relative inconclusiveness of the NOESY data (see Table 4.4), computational modeling (AM1, the annealing method) was carried out and the most stable conformation was determined ($-71.4 \text{ kcal.mol}^{-1}$). In this relative configuration the central ring bearing the three stereogenic centers is a distorted chair (half-chair, see Figure 4.9). Dihedral angles between hydrogen atoms of the central ring (positions 8', 7', 8 and 7) were measured and compared with coupling constants obtained for these protons (Table 4.5). These suggest that **4.183** had the relative stereochemistry shown in Figure 4.9.

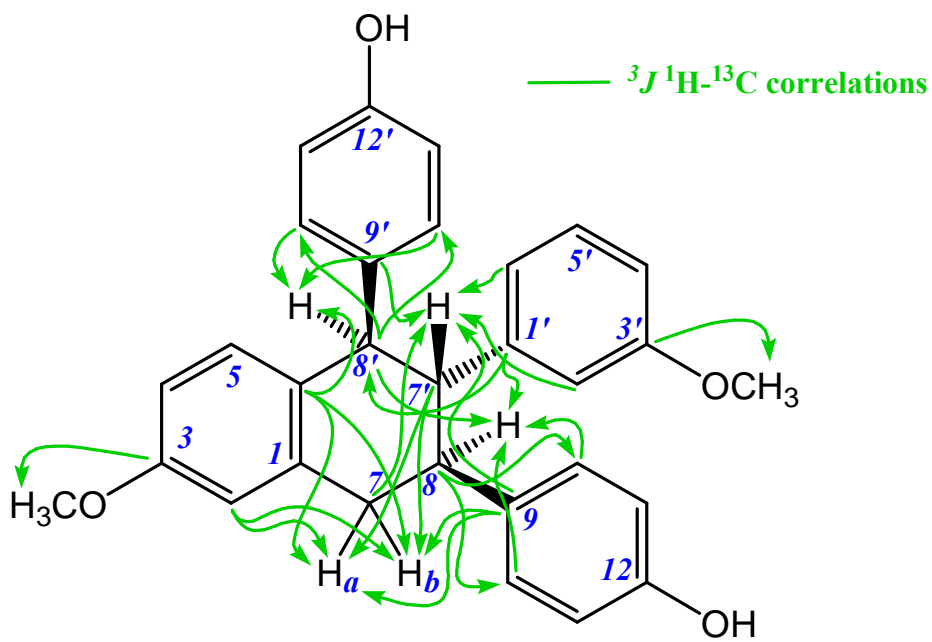
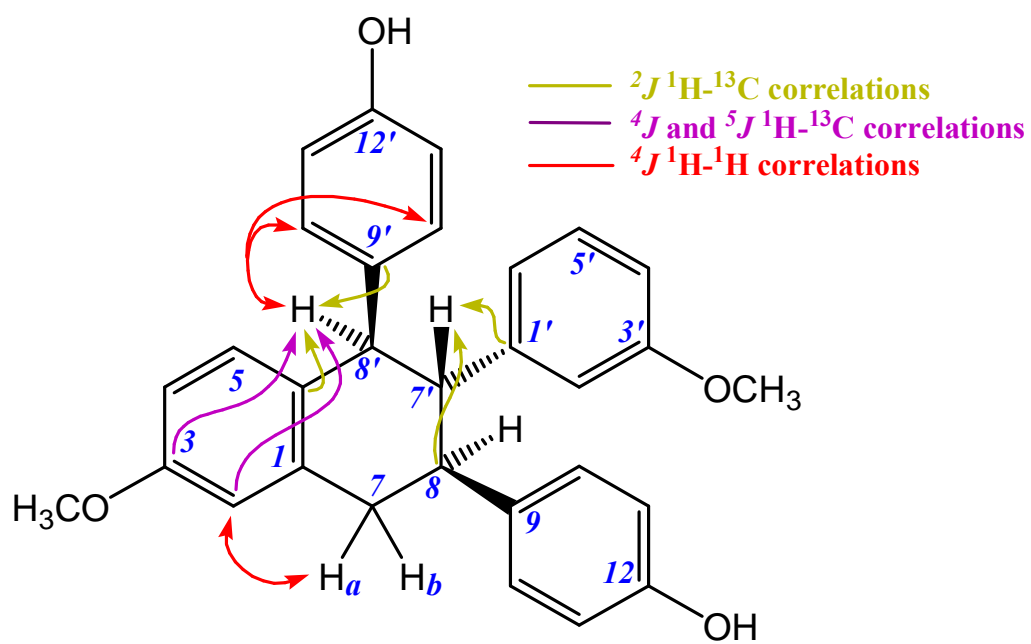


Figure 4.8: Main HMBC and long range COSY correlations for 4.183

Table 4.4: ^1H -(500 MHz) and ^{13}C -(125 MHz) NMR data of **4.183**

Carbon No.	^1H -NMR δ , ppm (<i>J</i> , Hz)	^{13}C -NMR δ , ppm	^{13}C - ^1H HMBC correlations	NOESY correlations
1	-	138.1	H5, H7b, H8	-
2	6.66, d (2.7)	112.7 ^A	H4, H5, H7a, H7b, H8 ϕ	7a (weak), 7b, 3-OCH ₃
3	-	157.6	H2, H4, H5, H7a, H8 ϕ 3-OCH ₃	-
4	6.63, dd (2.7, 8.8)	112.5 ^A	H2, H5	5, 3-OCH ₃
5	6.72, d (8.8)	131.2	-	4
6	-	132.5	H2, H4, H7a, H7b, H8 ϕ	-
7	a: 3.23, dd (12.0, 16.4) b: 3.06, dd (4.2, 16.4)	40.5	H2, H8, H7 ϕ	2 (weak), 10/14 2
8	3.36, "t"d (12.0, 11.0, 4.2)	46.0	H7a, H7b, H10/14, H7 ϕ H8 ϕ	10/14, 2', 6'
9	-	136.6	H7a, H7b, H8, H11/13, H7 ϕ	-
10/14	6.93, d (8.5)	128.8	H8, H10/14, H11/13	8, 7a, 2', 6', 7'
11/13	6.54, d (8.5)	115.1	H10/14, H11/13	10/14, 11/13, 12-OH
12	-	153.6*	H10/14, H11/13	-
3-OCH ₃	3.77, s	55.3	-	2, 4
1'	-	144.7	H8, H5 ϕ H7 ϕ H8 ϕ	-
2'	6.32 bs	114.6	H7 ϕ	8, 10/14 (weak), 7', 8', 3 ϕ OCH ₃
3'	-	158.9	H2 ϕ H4 ϕ H5 ϕ H6 ϕ 3 ϕ OCH ₃	-
4'	6.45, dd (2.2, 7.9)	111.0	H2 ϕ H5 ϕ H6 ϕ	5', 3 ϕ -OCH ₃
5'	6.87, t (7.9)	128.6	H6 ϕ	4', 6'
6'	6.40, bd (7.9)	121.3	H2 ϕ H4 ϕ H5 ϕ H7 ϕ	8, 10/14 (weak), 5', 7', 8'
7'	3.14, "t" (11.0)	56.7	H7a, H7b, H2 ϕ H6 ϕ H8 ϕ	10'/14', 2', 6', 10'/14'
8'	4.16, d (10.5)	53.9	H8, H7', H10 ϕ /14 ϕ	2', 6', 10'/14'
9'	-	137.9	H7 ϕ H8 ϕ H11 ϕ /13 ϕ	-
10'/14'	6.70, d (8.3)	130.3	H8 ϕ H10 ϕ /14 ϕ H11 ϕ /13 ϕ	7', 8', 11 ϕ /13 ϕ
11'/13'	6.56, d (8.3)	114.9	H10 ϕ /14 ϕ H11 ϕ /13 ϕ	10 ϕ /14 ϕ 12'-OH
12'	-	153.7*	H10 ϕ /14 ϕ H11 ϕ /13 ϕ	-
3 ϕ OCH ₃	3.57, s	55.1	-	2', 4'

^A* Chemical shifts with the same superscripts can be interchanged.

Table 4.5: Computed dihedral angles and measured coupling constants for protons of the central ring of **4.183**

Protons	Angle (°)	Coupling constant (Hz)
H-8' / H-7'	159.6	10.5
H-7' / H-8	176.4	11
H-8 / H-7a	176.7	12
H-8 / H-7b	77.0	4.2

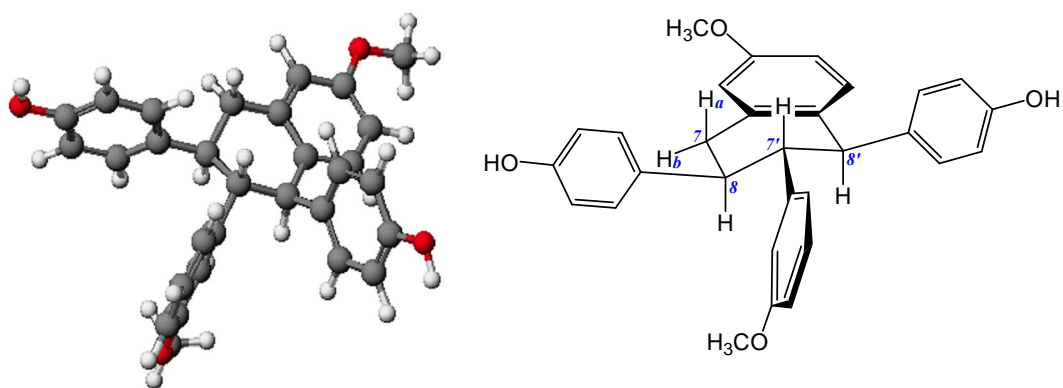


Figure 4.9: Computational model of **4.183**

4.3.4.5. Trimeric compound 4.185

Compound **4.185** possesses a molecular formula of $C_{48}H_{46}O_9$ as deduced from the data obtained by ESI-TOFMS positive mode. This would correspond to a trimeric structure that would include three interstilbene bonds. The 1H spectrum includes signals integrating for 20 aromatic protons, thus indicating that one of the aromatic rings is engaged in the interstilbene linkage (Table 4.6). Appendix 53 and 54 show 1H NMR and ^{13}C NMR spectra of compound **4.185** respectively. Appendix 55 shows ESI-TOF-MS (+) spectrum of **4.185**. Two olefinic protons at 6.96 (H-8) and 6.84 ppm (H7) with *trans* coupling constants of 16.5 Hz indicating the presence of intact stilbene unit. Three methyne protons are observed at 5.49, 3.35 and 3.22, which correspond to protons at positions 7 α , 8 ϕ and 7 δ respectively. In addition, HMBC correlation between C12 and H7 ϕ further supports that possibly one of the 12-O of the stilbene units is engaged in the interstilbene linkage (Figure 4.10). At this stage, we can already conclude that a triaryltetrahydronaphthalene ring structure is present and interlinked through an ether bond from a third stilbene unit. As observed in compound **4.183**, triaryltetrahydronaphthalene ring is thermodynamically stable when in *trans-trans* configuration. Therefore, triaryltetrahydronaphthalene moiety in compound **4.185** can be concluded having similar configuration (Figure 4.10), however, the stereochemistry at C7 δ is yet to be determined.

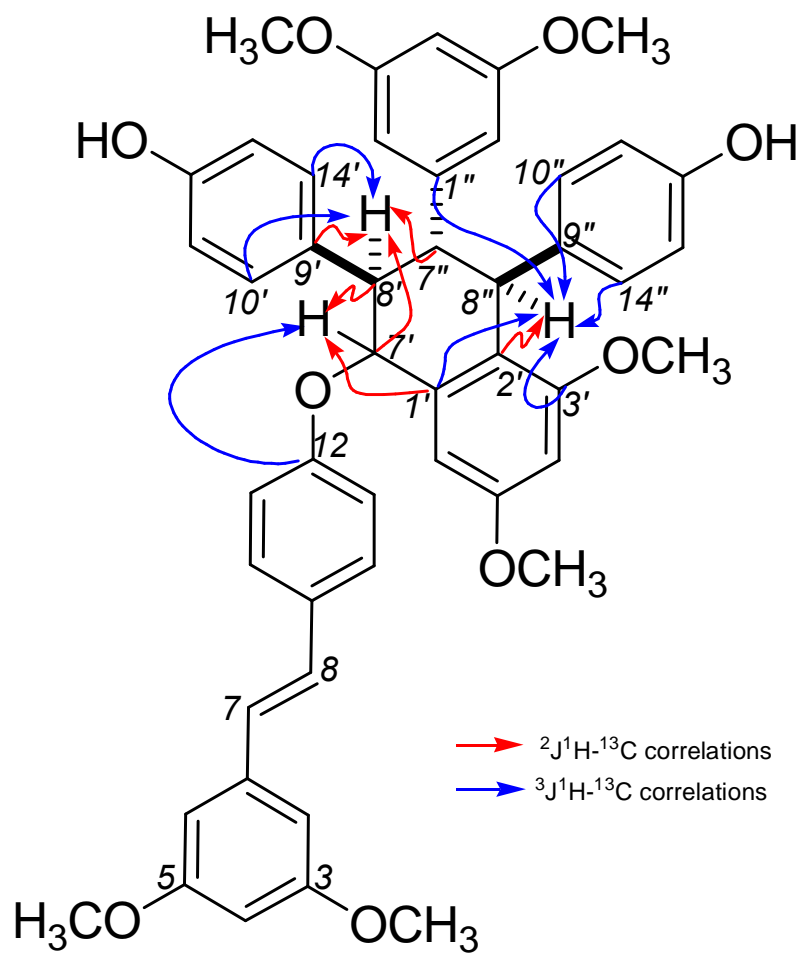


Figure 4.10: Main HMBC correlations for 4.185

Table 4.6: ^1H -(400 MHz) and ^{13}C -(125 MHz) NMR data of **4.185**

Carbon No.	^1H -NMR δ , ppm (<i>J</i> , Hz)	COSY correlations	^{13}C -NMR δ , ppm	^{13}C - ^1H HMBC correlations
1	-	-	139.7	H7, H8
2/6	6.62, d (2.3)	-	104.4	H7, H4
3/5	-	-	161.0	H2/6, H4
4	6.37, t (2.3)	-	99.7	H6/2
7	6.84, d (16.5)	H8	126.7	H2/6
8	6.96, d (16.5)	H7	128.7	-
9	-	-	130.3	H7, H11/13
10/14	7.27, d (8.7)	H11/13	127.7	-
11/13	6.66, d (8.7)	H10/14	116.4	H7, H10
12	-	-	159.9	H10/14, H11/13, H7 ϕ
1'	-	-	141.3	H7 ϕ
2'	-	-	19.8 ¹	H6 α H4 α H8 δ
6'	6.69, s	-	100.9	H4 ϕ
3'	-	-	158.3	H8 δ
5 ϕ	-	-	159.5	H4 ϕ
4'	6.41, d (2.3)	-	98.6	H6 α
7'	5.49, d (10.6)	-	82.1	H8 α H10 ϕ /14 ϕ
8'	3.35, t (10.6)	-	54.2	H6 α H7 δ
9'	-	-	132.9	H11 α H8 ϕ
10'/14'	6.79, d (8.7)	H11 ϕ /13 ϕ	129.5	H8 ϕ
11'/13'	6.45, d (8.7)	H10 ϕ /14 ϕ	114.89*	H10 ϕ /14 ϕ
12'	-	-	153.7	H10 ϕ /14 α H11 ϕ
1 δ	-	-	146.3	H8 δ , H7 δ
2 δ /6 δ	6.01, d (1.8)	-	106.7	H4 δ , H7 δ , H8 δ
3 δ /5 δ	-	-	160.2	
4 δ	6.15, t (2.3)	-	98.1	H6 δ /2 δ
7 δ	3.22, dd (11.4, 6.8)	-	56.8	H6 δ /2 δ , H8 δ , H8 ϕ
8 δ	4.45, d (6.9)	-	47.4	H10 δ /14 δ , H7 δ
9 δ	-	-	139.2	H11 δ , H8 δ , H7 δ
10 δ /14 δ	6.75, d (8.7)	H11 δ /13 δ	128.5	H8 δ
11 δ /13 δ	6.65, d (8.7)	H10 δ /14 δ	114.85*	-
12 δ	-	-	53.4 ¹	H10 δ /14 δ , H11 δ
3/5 OMe	3.81, s	-	55.4	-
3'OMe	3.50, s	-	55.6	-
5 ϕ OMe	3.73, s	-	55.4	-
3 δ /5 δ OMe	3.59, s	-	55.2	H4 δ , H2 δ

- Assignments of chemical shifts with the same superscript are interchangeable

4.3.5. Mechanistic considerations

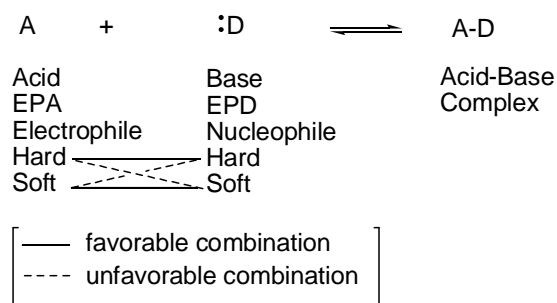
In this section we will discuss mechanistic aspects of stilbene dimerisation with emphasis on some commonly obtained skeletons. This discussion will not be restricted to the mechanism related to the formation of stilbene oligomers obtained in this study, but will also cover reactions used by previous workers but not convincingly explained. However, before examining specific cases, some general remarks on one-electron oxidants used by the various workers seem appropriate.

Metal ions (M^+), which are oxidants, can also be seen as Lewis acids due to their electron acceptor properties. In the early 1960s Ralph Pearson introduced the hard and soft acid and base (HSAB) principle, which, in a nutshell, correlates the properties of acid and bases with their charge densities.⁴⁷ We believe that there is a relationship between the hardness/softness of the metal ions and the kind of dimerisation product obtained from stilbenoids. Very different dimerisation products are obtained depending on whether the starting stilbene is exposed to a hard acid (*i.e.* Fe^{3+}) one electron oxidant or a soft acid (*i.e.* Ag^+) oxidant. Interestingly enough, $Pb(IV)$, considered as a borderline acid, yields products that could be seen as characteristic intermediate in their behavior between the two extremes. It was also realized that the type of solvent and ligands coordinating to the metals influenced the hardness or softness of the metal. As a result we believe we can present a general explanation for the observations made by the various investigators involved in oligostilbene chemistry. This will be followed by a discussion for some important structural types related to the hardness/softness of the oxidant, solvent and substituents influence the final outcome of the dimerisation. Two approaches can be considered, either stilbene radical or radical cation reacting with its native stilbene or two stilbene

radicals or radical cations reacting to with each other in an appropriate orientation leading towards stilbene dimers. We have chosen the first approach throughout the mechanistic discussion, even though we are aware of some arguments in favor of the latter (Ebersøn and Steckhan work and Thomas group's bisindoline synthesis would appear to point to radical-radical or radical cation-radical cation pathway^{48,49,50}).

4.3.5.1. HSAB Principle

According to Lewis, acids are electron pair acceptors (EPA) while bases are electron pair donors (EPD) as shown in the following equilibrium (Scheme 4.54).⁵¹



Scheme 4.54: Acid base complex formation.⁵¹

The Lewis acid/base complex is formed via an overlap between a doubly occupied orbital of the donor D and a vacant orbital of the acceptor A. This acid/base approach was extended by Pearson who divided Lewis acids and bases into two groups, hard and soft, according to their electronegativity and polarizability, known as principle of hard and soft acids and bases (HSAB concept, Table 4.7). Hard acids and hard bases are those derived from small atoms with high electronegativity and generally of low polarizability. Soft acids and bases are usually derived from large atoms with low electronegativity and are usually polarizable. A safe rule is that the

hardness of Lewis acids increases with increasing positive oxidation state and vice versa for the softness of acids. The hardness or softness of Lewis acids of a given element in a fixed oxidation state is also affected by the other groups/ligands attached to it. Groups which transfer negative charge to the central atom will increase the softness of that atom since such transfer of charge is equivalent to a reduction of the oxidation state. The groups which most easily transfer negative charge will be the soft bases, particularly if negatively charged. In general, hard acids prefer to coordinate to hard bases and soft acids to soft bases. There are also some exceptions where hard reacts with soft and soft with hard.

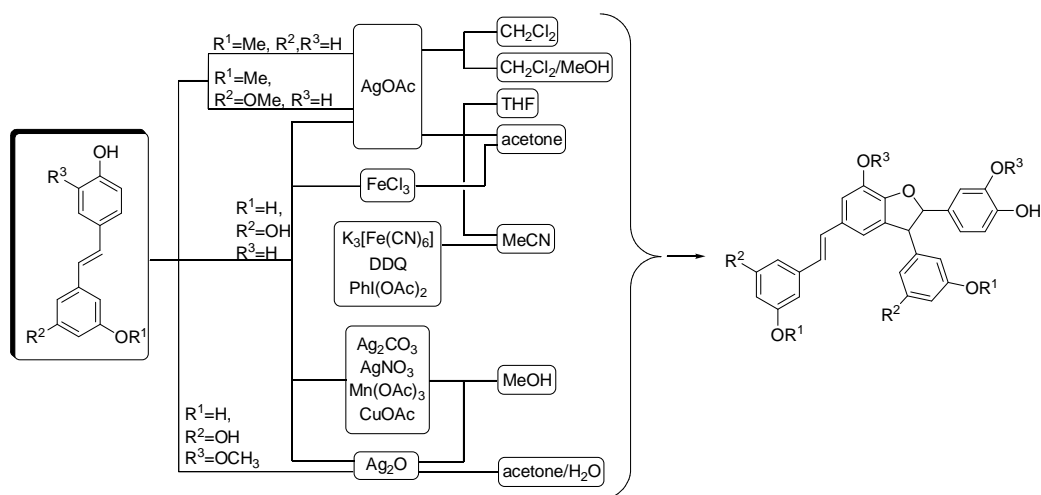
Table 4.7: Hard, borderline and soft acids and bases.⁵²

Bases (Nucleophiles)	Acids (Electrophiles)
	<i>Hard</i>
<p>H₂O, OH⁻, F⁻ CH₃CO₂⁻, PO₄³⁻, SO₄²⁻ Cl⁻, CO₃²⁻, ClO₄⁻, NO₃⁻ ROH, RO⁻, R₂O NH₃, RNH₂, N₂H₄</p>	<p>H⁺, Li⁺, Na⁺, K⁺ Be²⁺, Mg²⁺, Ca²⁺ Al³⁺, Ga³⁺ Cr³⁺, Co³⁺, Fe³⁺ CH₃Sn³⁺ Si⁴⁺, Ti⁴⁺ Ce³⁺, Sn⁴⁺ (CH₃)₂Sn²⁺ BeMe₂, BF₃, B(OR)₃ Al(CH₃)₃, AlCl₃, AlH₃ RPO²⁺, ROPO²⁺ RSO²⁺, ROSO²⁺, SO₃ I⁷⁺, I⁵⁺, Cl⁷⁺, Cr⁶⁺ RCO⁺, CO₂, NC⁺ HX (hydrogen bonding molecules)</p>
	<i>Borderline</i>
<p>C₆H₅NH₂, C₅H₅N, N₃⁻, Br⁻, NO₂⁻, SO₃²⁻, , N₂</p>	<p>Fe²⁺, Co²⁺, Ni²⁺, Cu²⁺, Zn²⁺, Pb²⁺, Sn²⁺, B(CH₃)₃, SO₂, NO⁺, R₃C⁺, C₆H₅⁺</p>
	<i>Soft</i>
<p>R₂S, RSH, RS⁻, I⁻, SCN⁻, S₂O₃²⁻, R₃P, R₃As, (RO)₃P CN⁻, RNC, CO C₂H₄, C₆H₆ H⁻, R⁻</p>	<p>Cu⁺, Ag⁺, Au⁺, Tl⁺, Hg⁺ Pd²⁺, Cd²⁺, Pt²⁺, Hg²⁺, CH₃Hg⁺, Co(CN)₅²⁻ Tl³⁺, Tl(CH₃)₃, BH₃ RS⁺, RSe⁺, RTe⁺ I⁺, Br⁺, HO⁺, RO⁺ I₂, Br₂, ICN, etc. trinitrobenzene, etc. chloroanil, quinones, etc. tetracyanoethylene, etc. O, Cl, Br, I, N, RO, RO₂ M⁰ (metal atoms) bulk metals CH₂, carbenes</p>

Most solute/solvent interactions can be classified as generalized Lewis-acid/base reactions. The application of the HSAB concept to solutions leads to the rule stating that hard solutes dissolve in hard solvents and soft solutes dissolve in soft solvents. For instance, small hard cations of high oxidation state will be preferably solvated by hard electron pair donors (EPD) solvents like H₂O or ROH. In principle, relative to the gas state, all ions become softer in the solute state as the result of solvation.

4.3.5.2. Oxidative coupling with soft acids

Based on the Pearson's definition of soft ions; AgOAc, Ag₂O, Ag₂CO₃, AgNO₃, CuOAc, DDQ and PhI(OAc)₂ can be categorized straight forwardly as soft reagents. Some reagents are made of a hard acid (Fe³⁺) and soft ligands (CN⁻) and/or are used in soft solvents (acetone/MeCN) such as K₃[Fe(CN)₆]/MeCN complex and FeCl₃/acetone complex. These combinations lead to complexes that can be considered as soft. It is remarkable to observe that all these soft reagents produce stilbene dimers with the δ -viniferin skeleton when resveratrol **1.0** is employed (Scheme 4.55).



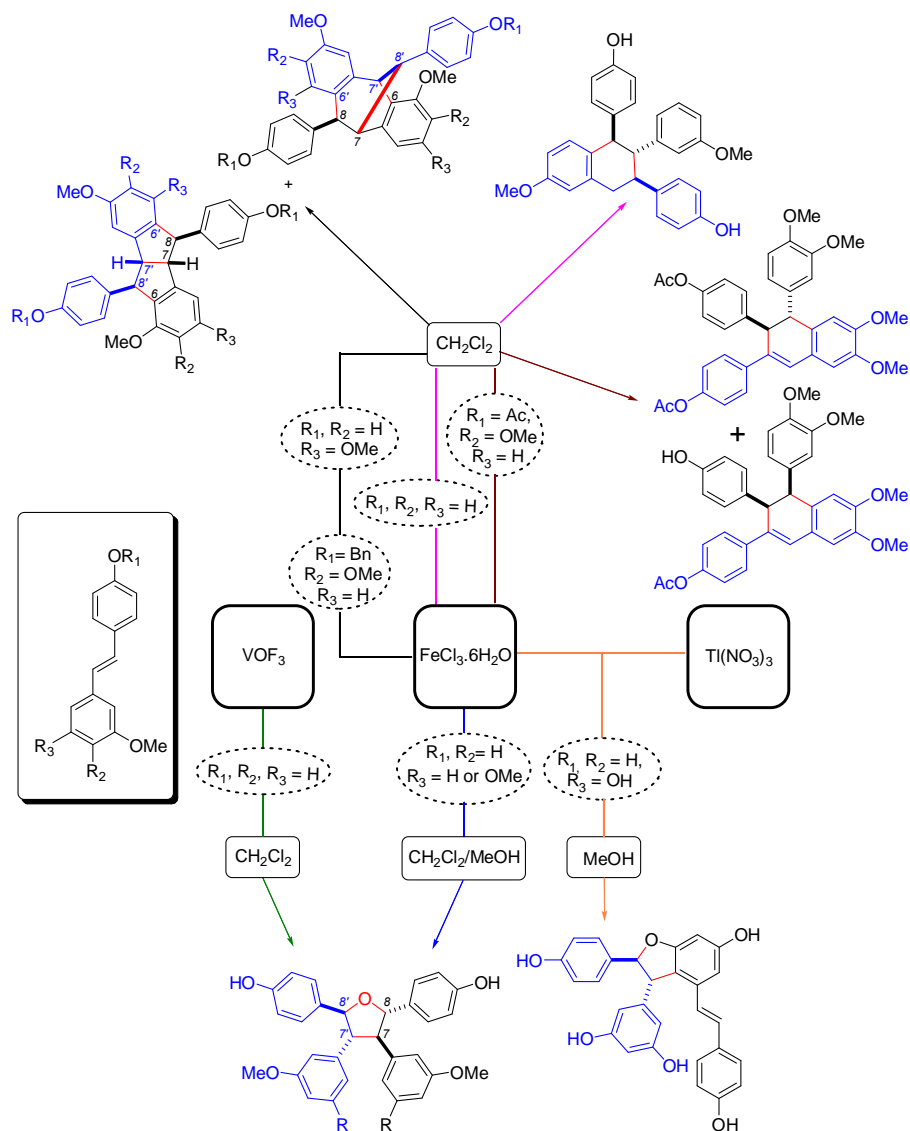
Scheme 4.55: Single electron oxidation with soft acid treatment stilbene incorporating a C12-OH group.

However, there is an exception: when piceatannol **4.46** is used as a substrate, a dioxane type stilbene dimer is obtained where the catechol group is engaged in cyclodimerization.

4.3.5.3. Oxidative coupling with hard acid single electron oxidants

When the substitution pattern of the starting stilbene is favorable, Fe^{3+} , a hard acid according to Pearson, produces ϵ -viniferin and not δ -viniferin. Fe^{3+} ion in combination with different solvents gives hard complexes $\text{FeCl}_3 \cdot 6\text{H}_2\text{O}/\text{CH}_2\text{Cl}_2$, $\text{FeCl}_3 \cdot 6\text{H}_2\text{O}/(\text{CH}_2\text{Cl}_2/\text{MeOH})$ and $\text{FeCl}_3 \cdot 6\text{H}_2\text{O}/(\text{MeOH}/\text{H}_2\text{O})$ complexes (Scheme 4.56). Subjecting different 12-OH stilbenes without free OH group in position 3 and/or 5 (*i.e.* with OMe or H) to $\text{FeCl}_3 \cdot 6\text{H}_2\text{O}/\text{CH}_2\text{Cl}_2$ affords pallidol, ampelopsin F and tetralin type skeletons, while $\text{FeCl}_3 \cdot 6\text{H}_2\text{O}/(\text{CH}_2\text{Cl}_2/\text{MeOH})$ complex gives only tricuspidatol A type skeleton. Hard oxidants like VOF_3 behave similarly. $\text{Tl}(\text{NO}_3)_3$, a combination of soft acid (Tl^{3+}) and hard base (NO_3^-), is considered as a hard to borderline reagent as well when used in hard solvent MeOH. ϵ -Viniferin **1.4** is

obtained from resveratrol **1.0** only when treated by $\text{Ti}(\text{NO}_3)_3/\text{MeOH}$ and $\text{FeCl}_3 \cdot 6\text{H}_2\text{O}/(\text{MeOH}/\text{H}_2\text{O})$ complexes (see section 4.1.5 and 4.1.3.1).



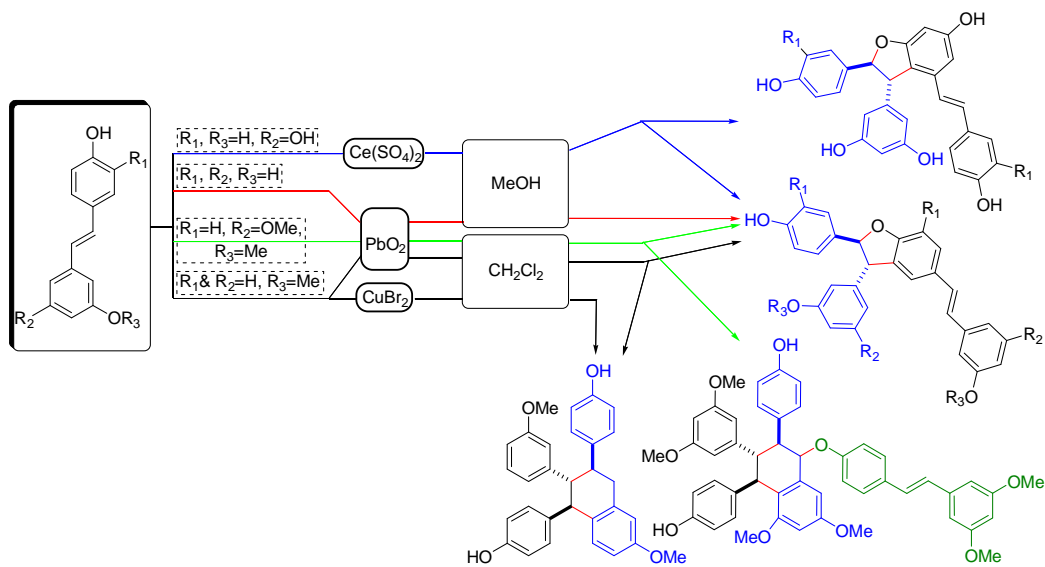
Scheme 4.56: Stilbene dimer skeletons produced by hard acid treatment of various stilbene starting materials.

4.3.5.4. Oxidative coupling with borderline acids

According to the HSAB principle, $\text{Pb}(\text{IV})$ or $\text{Ce}(\text{IV})$ derivatives can be considered as borderline acids. Treatment of *para*-hydroxystilbenes with PbO_2 shows mixed results that include both δ -viniferin and tetralin skeletons, otherwise obtained

with soft and hard acids respectively. $\text{Ce}(\text{SO}_4)_2$ converted resveratrol **1.0** into both ϵ - and δ -viniferins (Scheme 4.57).

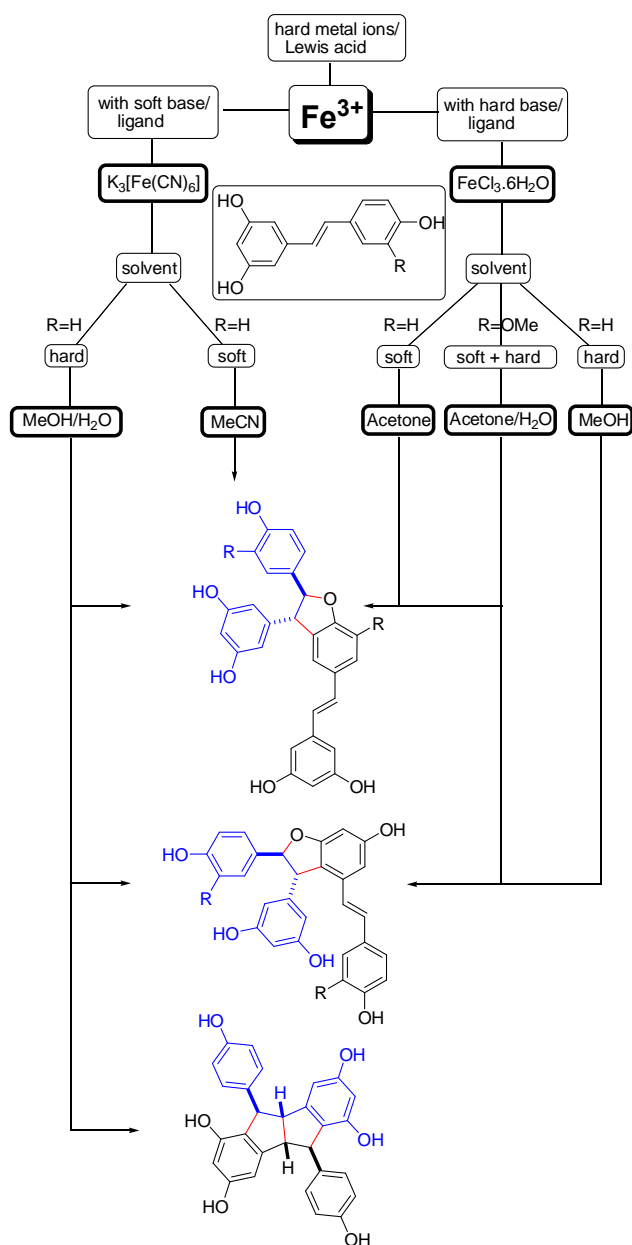
Occasionally some metals such as Cu(II) or Mn(III), which could be classified as borderline, behave either as hard or soft reagents depending on the type of combination they are part of. This is further discussed in the next section.



Scheme 4.57: Stilbene dimer skeletons produced by treatment of stilbenes with borderline acids.

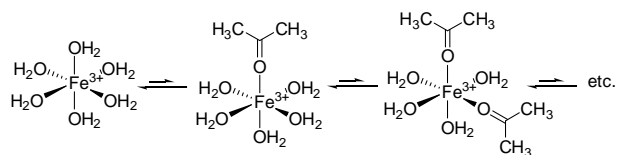
4.3.5.5. Effect of solvents and ligands on oxidants (metal ions) properties

Some observations made independently by Takaya *et al.*,⁷ Huang *et al.*,²² Sako *et al.*²³ and Yao *et al.*²⁴ do not seem to be consistent at first sight. They subjected resveratrol **1.0** and/or isorhapontigenin **1.1** to two different Fe^{3+} salts, *i.e.* $\text{FeCl}_3 \cdot 6\text{H}_2\text{O}$ and $\text{K}_3[\text{Fe}(\text{CN})_6]$ in various solvents (MeCN, MeOH, MeOH/water, acetone, acetone/water) and obtained various combinations of pallidol, ϵ - and δ -viniferins skeletons (Scheme 4.58). These structures, according to the above explained principles, should originate either from hard or soft acids.



Scheme 4.58: Treatment of resveratrol and isorhapontigenin by $\text{FeCl}_3 \cdot 6\text{H}_2\text{O}$ and $\text{K}_3[\text{Fe}(\text{CN})_6]$ in various solvents (adapted from references 7, 22-24).

Attention should be given to the ligands and the solvent, which can also be classified as hard and soft.⁴⁷ For example, acetone is considered as a soft solvent. Fe^{3+} will exchange partially its water ligands for acetone (Scheme 4.59). The resulting complex softens and induces reactions leading towards δ -viniferin skeletons.



Scheme 4.59. Acetone/water exchange in Fe^{3+} complexes.

The actual hardness/softness of the system results from the combination of all components. In $\text{FeCl}_3 \cdot 6\text{H}_2\text{O}$ used in MeOH, all components, *i.e.* the metal, the ligands and the solvent are considered as hard. As a result, ϵ -viniferin is obtained. On the other hand, when Fe(III) is complexed to cyanide ions (soft ligands) as in $\text{K}_3[\text{Fe}(\text{CN})_6]$ and used in MeCN (a soft solvent), only δ -viniferin is generated, just like with Ag(I) based reagents. Combinations of soft ligands with hard solvent or hard ligands with soft solvent would yield mixtures of viniferins and occasionally pallidol. Indeed, when isorhapontigenin **1.1** was treated by $\text{FeCl}_3 \cdot 6\text{H}_2\text{O}$ in a mixture of acetone and water (3:2; v/v), soft and hard solvents respectively, both types of viniferin derivatives were obtained.²⁴ This contrasts with the treatment of **1.0** by $\text{FeCl}_3 \cdot 6\text{H}_2\text{O}$ in pure acetone yielding δ -viniferin only.⁷

It may not be very easy to always predict how a reagent would behave. Borderline Mn(III) and Cu(II) in $\text{Mn}(\text{OAc})_3/\text{MeOH}$ and $\text{Cu}(\text{OAc})_2/\text{MeOH}$ respectively act like soft acids, inducing the formation δ -viniferin **1.3** when resveratrol **1.0** is used.²³ In contrast, CuBr_2 in CH_2Cl_2 functions like a hard acid, converting 12-hydroxystilbene into tetralin type scaffold. More examples of reagent and solvent combinations would be required to draw a complete set of rules.

4.3.5.6. δ -Viniferin analogues formation via AgOAc promoted oxidative coupling

Silver acetate, a soft Lewis acid, is able to back-bond to olefins (soft acid-soft base/ligand interaction).⁵³ Figure 4.11a shows electron donation from filled orbital of an olefin to a vacant d-orbital of a metal while the back-bonding is the back donation of electrons from the filled d-orbital metal to the antibonding π^* -orbital of the olefin as shown in Figure 4.11b. Both types of donations are in a synergy and weaken the π -bonding in the olefin.

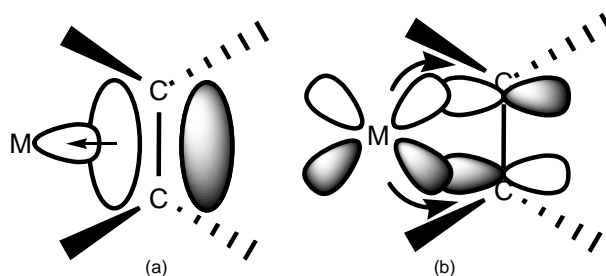
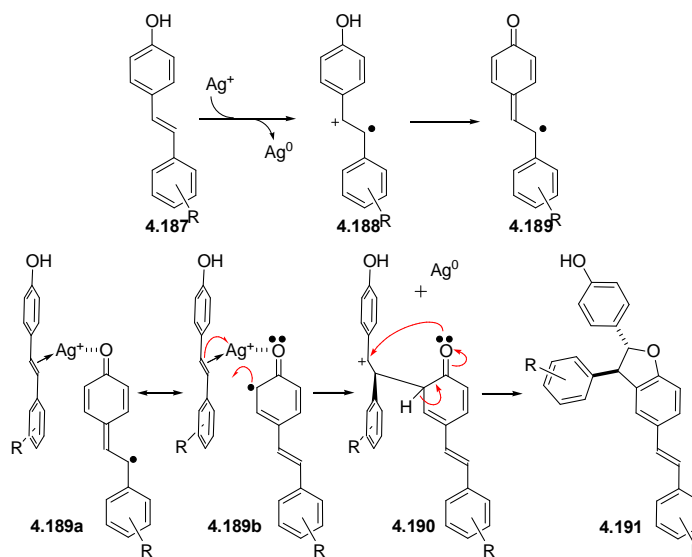


Figure 4.11: Metal-olefin bonding model.⁵³

Silver ion is also known to form complexes via coordination interaction with the oxygen atom of carbonyls.⁵⁴⁻⁵⁷ When applied to the dimerisation of 12-OH stilbenes **4.187** by the soft acid Ag^+ , the above principles lead to the following mechanism. Oxidation of a 12-hydroxystilbene leads to radical cation **4.188** which, after loss of a proton from the hydroxyl group, gives rise to stable quinone methide radical **4.189** (Scheme 4.60). Ag^+ simultaneously back-bonds the olefinic bridge of a native stilbene and coordinates the carbonyl of the quinone methide radical. However, it is unlikely that the two stilbenoids orientate themselves randomly. Van der Waals forces should maintain the two stilbenoids into a T-shape arrangement **4.189a** and

4.189b (refer to Chapter 5 section 5.6. Ag^+ ion impacts on its coordination with stilbene as well as its alignment with stilbene units).



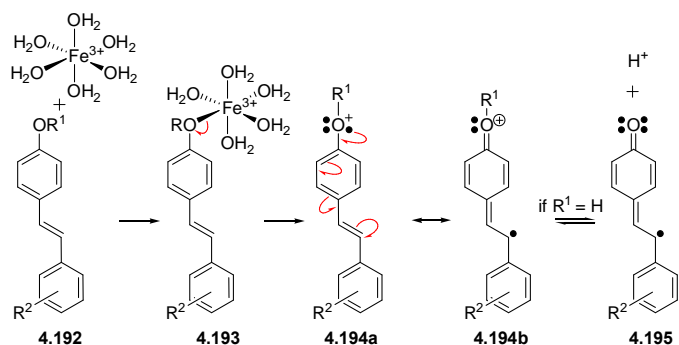
Scheme 4.60: Oxidation of 12-OH-stilbenes and alignment of the reacting species leading to δ -viniferin type dimers.

The above would only be correct for stilbenes with at least one free *para*-hydroxyl. The observed regioselectivity of this reaction arises from the fact that stable quinone methide species cannot be obtained from the 3- or 3,5-oxygenated ring. The lower yields observed for this reaction when a mixture of $\text{CH}_2\text{Cl}_2/\text{MeOH}$ is used as solvent instead of pure CH_2Cl_2 is probably due to competing solvation of silver ion and/or stilbenes by MeOH.

4.3.5.7. δ -Viniferin analogues formation via FeCl_3 oxidative coupling

ϵ -Viniferin analogues are obtained in significant yields from action of $\text{FeCl}_3 \cdot 6\text{H}_2\text{O}$ on either resveratrol or isorhapontigenin (both with hydroxy groups in positions 3 and 12) in CH_3OH . In contrast to the above, Fe^{3+} is a hard Lewis acid, and so are the oxygen atoms of phenolic and phenoxy groups. Therefore, when in presence

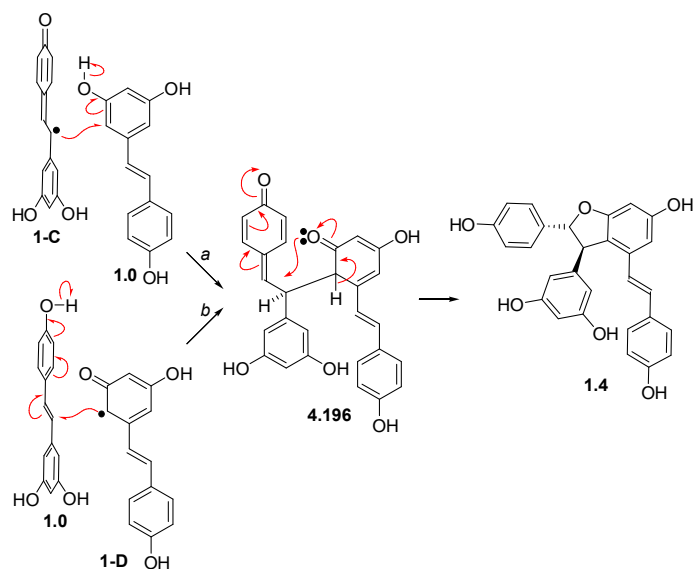
of one another, these species preferably interact (Scheme 4.61, species **4.192**). However, in order for the oxygen atom of the hydroxyl/alkoxyl to coordinate with the ferric complex, one molecule of water should be displaced from its coordination (species **4.193**). Then oxidation of the stilbene can take place (species **4.194a** and more stable resonance form **4.194b**). In the case of resveratrol **1.0** or isorhapontigenin **1.1**, oxidation may occur at any of the three hydroxyls. It would however occur preferentially at the *O*-12 as the resulting radical would be better stabilized over an extended conjugated system through the formation of a quinone methide radical such as **4.195** (refer Chapter section 5.4.3 (a) and (b) H atom transfer (HAT) mechanism and BDE calculations).



Scheme 4.61: Oxidation of *para* oxygenated stilbenes by FeCl₃·6H₂O.

The oxidized species, the quinone methide radical which is known to be planar⁵⁸ (refer to Chapter 5 section 5.4.3.1, conformational studies), will then react with a native stilbene or with another oxidized species. Since stilbenes are conjugated π -systems, non-covalent interactions such as Van der Waals and electrostatic interactions are believed to be involved in the stabilization of this system. Another important factor to consider in this reaction is the fact that CH₃OH, like other oxygenated solvents would solvate the starting material. We propose that solvated stilbenes are expected to arrange through T-shape alignment in a way similar to that

described in the previous section (Scheme 4.62). The resorcinol moiety of the native stilbene should approach at right angles to the ethylene radical bridge of the oxidized species, as can be easily seen even with simple Dreiding models. This perpendicular alignment is responsible for the stereoselectivity of the reaction. If we consider resveratrol **1.0**, two oxidized species could be considered, **1-C** and **1-D** (see section 4.1.2.1, Scheme 4.5). Each of these species could react with a native resveratrol species to form intermediate species **4.196** [note that i) **1-C** is more stable than **1-D** and that path *a* is more likely than path *b*; ii) **1-C** and **1-D** could well react on each other leading to the same intermediate **4.196**]. Intermediate **4.196** (Scheme 4.62) will undergo a ring closure by nucleophilic attack on C8 from the oxygen of the carbonyl leading to ϵ -viniferin **1.4**.

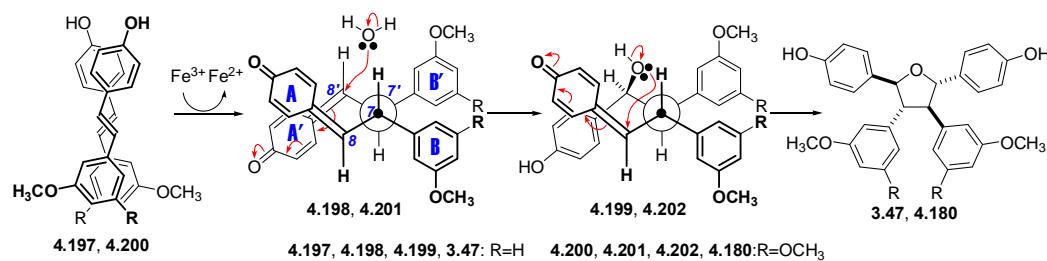


Scheme 4.62: Mechanism of the formation of ϵ -viniferin **1.4** from resveratrol **1.0**.

4.3.5.8. Tricuspidatol-A like formation via FeCl_3 oxidative coupling

The addition of limited amounts of MeOH to $\text{FeCl}_3 \cdot 6\text{H}_2\text{O} / \text{CH}_2\text{Cl}_2$ as reaction mixture (or the usage of VOF_3 as oxidizing agent) has some significant impact on the reaction outcome as analogues of tricuspidatol A are obtained (Scheme 4.63). The first

bond to be established between the two stilbene units is a C7-C7 σ . If intuition may lead to believe that head-to-tail would be a preferred arrangement, computational work on stilbene in gas phase showed that there are little differences between these two types of alignments (refer to Chapter 5, section 5.5.2, Comparison of stability between head-to-head and head-to-tail alignments of stilbenes). Gas phase alignments are likely to be different from the state of affair in solution in the presence of an oxidizing agent (pending further calculation that will include solvent effect). Therefore other parameters, such as substitution pattern or solvent may play a role in the favored alignment. It is believed that two quinone methide radicals approach in a head-to-head manner from the same faces *Re/Re* or *Si/Si* leading to intermediate **4.198/4.201** [NOTE: The designation for *Re* or *Si* face for stilbene is based on the Cahn-Ingold-Prelog system. An enantiotopic face of a trigonal atom is designated *Re* if the ligands of the trigonal atom appear in a clockwise sense in order of priority numbers when viewed from the side of the face. The opposite arrangement is termed *Si*]. We believe that this approach could be due to an enhanced stabilization of the native stilbenes (before oxidation) by the solvent CH₃OH, which holds the two 12-hydroxyls *via* hydrogen bonding with maximum interaction while CH₂Cl₂ helps to stabilize the conjugated system of this pair through π - π interaction. Thus, the cavity produced between the two rings A and A' in **4.198/4.201** allows a molecule of water to enter and acts as a nucleophile. Water originates from the FeCl₃.6H₂O complex after being displaced by MeOH, or from the reduction of VOF₃ when this reagent is used.



Scheme 4.63: Proposed mechanism of the formation of tricuspidatol A analogues **3.47** and **4.180**.

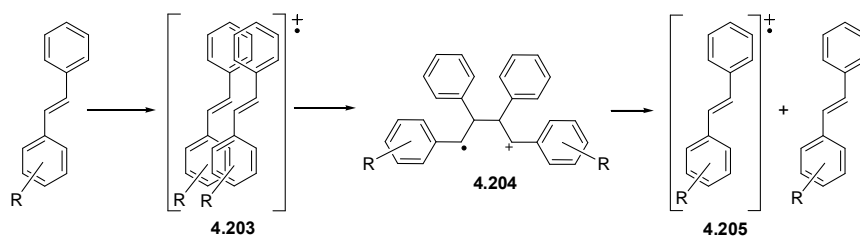
From the literature however, tricuspidatol A was not obtained when resveratrol was treated with $\text{FeCl}_3 \cdot 6\text{H}_2\text{O}$ in CH_3OH solely. A head-to-head alignment may simply not be possible due to the higher difference in electronegativity of resorcinolic hydroxy groups than that of methoxyls, resulting in a net repulsion between the two resorcinolic rings (ring B and B \emptyset).

4.3.5.9. Pallidol and ampelopsin F analogues formation via FeCl_3 oxidative coupling

Typically, pallidol and ampelopsin F analogues are obtained simultaneously upon treatment of stilbenes with 3,4- or 3,5-dialkoxy groups and 12-OH or 12-OR substituents with $\text{FeCl}_3 \cdot 6\text{H}_2\text{O}$ in CH_2Cl_2 . This solvent, aprotic and moderately dipolar, is not much likely to solvate stilbenes and/or coordinate with Fe^{3+} . As a result, the self arrangement of stilbenoid species is expected to be significantly different from the T-shape alignment described above.

Takamuku and co-workers have studied the dimerisation of substituted stilbenes using pulse and γ -ray radiolysis in 1,2-dichloroethane or butyl chloride.^{58,60} Transient species were studied by UV-vis. spectrophotometry. They proposed a radical cation attack on another native stilbene to produce a second radical cation. They

suggested that stilbene radical cation associates itself with its native stilbene to form a π -type dimer radical cation such as **4.203** Scheme 4.64). These π -type dimer radical cations would result of the overlap of π -electrons between two benzene rings of a stilbene radical cation and its native stilbene. These π -type dimer radical cations convert to dimeric radical cation **4.204**. Since this study was conducted in absence of oxidative reagent, they logically could not obtain a dimeric molecule (which requires the abstraction of a second electron) and the radical cation finally decomposes upon heat up into thermodynamically more stable stilbene radical cations **4.205** and its native stilbenes. It would seem reasonable to conclude that a spectrophotometric analysis would hardly be able to distinguish among various possible alignments in species **4.203**



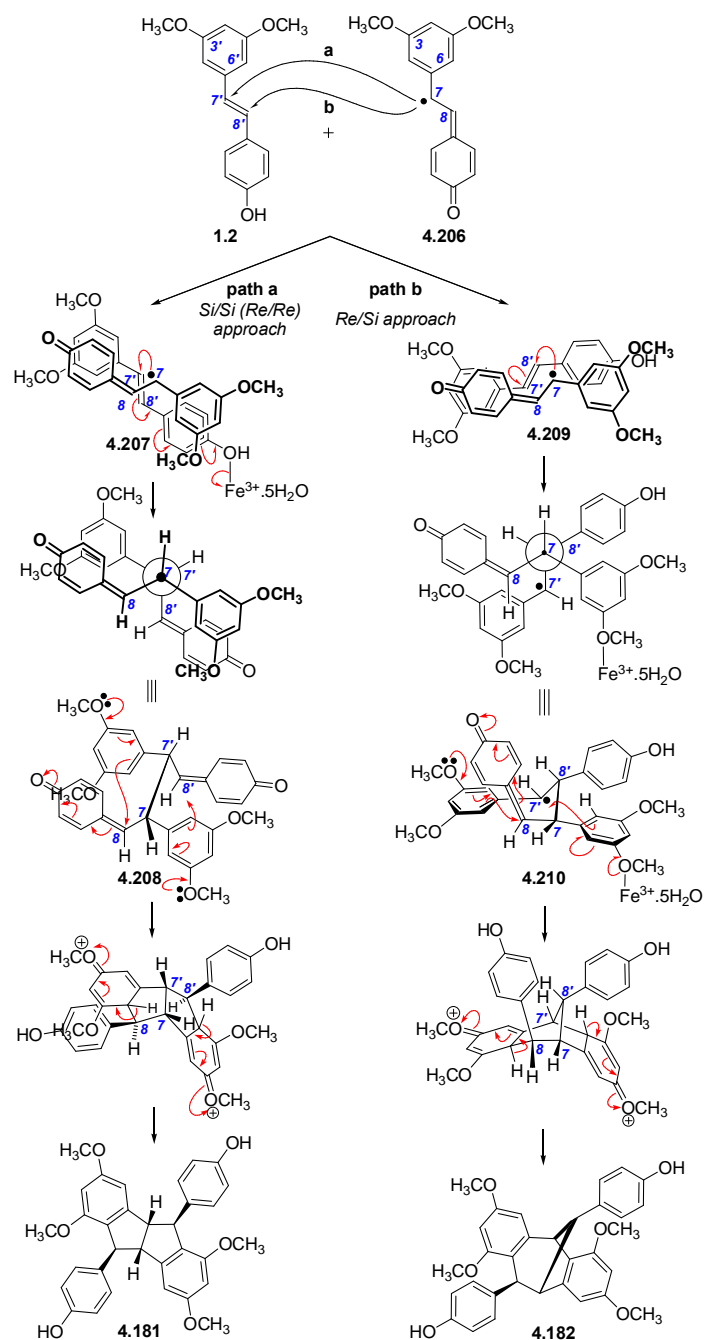
Scheme 4.64: Proposed transient species upon single electron oxidation of stilbenes (adapted from reference 58).

From the above concepts, it can be inferred that the driving forces holding together the quinone methide radical and the native stilbene or two quinone methide radicals are believed to be π - π interactions in addition to hydrogen bonding.^{58, 60} (refer to Chapter 5 section 5.5.1, Contribution of hydrogen bonding and π - π interactions in *para* hydroxy-substituted stilbenes alignment). The nearly symmetrical nature of stilbenes conceivably leads to two types of alignments, head-to-head and head-to-tail. When the dimerisation reaction is carried out in pure CH_2Cl_2 on pterostilbene **1.2** as a substrate, head-to-tail alignment would seem to be the preferred arrangement (Scheme

4.65). Additionally, both species can approach each other either from their opposite faces (*Re/Si* interaction) (refer to Chapter 5 section 5.5.3, Calculation results on various *Re/Si* approaches of pterostilbene units) or from the same faces (*Re/Re* or *Si/Si* interaction) (refer to Chapter 5 section 5.5.4, Calculation results on various *Re/Re* approaches of pterostilbene units) leading to different reaction products. When the approach is *Re/Si*, the stacking is such that the lone electron of the quinone methide radical **4.209** located on the C7 attacks the C8' of the native stilbene (path b) (refer to Chapter 5 section 5.5.9.1, Pterostilbene- pterostilbene radical). Yet, when the approach is *Re/Re* (or *Si/Si*), then the lone electron on C7 of **4.207** is in a better position to attack the C7' of **1.2** (path a). This would be followed by the delocalization of the lone electron throughout the ring and the subsequent activation of the 12-OH for removal of an electron by FeCl₃.6H₂O (**4.207**). Once the C7-C7 ϕ or C7-C8 ϕ bond is established (**4.208** and **4.210** respectively), two additional bonds are created by nucleophilic attack of the electron-rich C6 and C6' onto C8 and C7' or C8 and C8' respectively to generate the fused ring systems. Standard re-aromatization leads to pallidol analogue **4.181** or to ampelopsin F analogue **4.182**. As a result, whether **4.181** or **4.182** is produced depends on which faces (*Re/Re-Si/Si* or *Re/Si-Si/Re*) the two species approach each other as well as whether a C7-C7 ϕ or C7-C8 ϕ bond is formed first.

Pallidol and ampelopsin F analogues **4.41** and **4.42** respectively were also obtained from 3,4-dimethoxy-12-benzyloxystilbene **4.40** reacted in similar conditions as reported by Weber ϕ s group. These analogues were, however, obtained in inverse proportion compared to those deriving from pterostilbene **1.2**. One possible explanation is as follows. Pterostilbene **1.2** has one free hydroxyl and possibly a permanent dipole larger than that of **4.40** but significantly lower than resveratrol **1.0**. Dissolving **1.2** in CH₂Cl₂, with a dielectric constant of 9.08, may result in substrate/solvent interactions slightly stronger than substrate/substrate interactions.

The anti-parallel *Re/Re* (or *Si/Si*) alignment provides less overlap between two stilbenes than a parallel *Re/Si* alignment (refer to chapter 5 Table 5.4 and 5.6). The former arrangement would allow an enhanced interaction between the solvent and the stilbene as compared to the latter. Due to the favorable intermolecular interaction between the solvent and solute molecules, a *Re/Re* (or *Si/Si*) alignment would be favored and produce pallidol analogue **4.181** in yield slightly higher than the yield of ampelopsin F analogue **4.182** (*Re/Si* alignment). The impact of the substrate/solvent vs. substrate/substrate interactions is further exemplified by the outcome of unnatural stilbene **4.40** when subjected to the same reaction conditions in CH₂Cl₂.



Scheme 4.65: *Re/Si* and *Re/Re* (or *Si/Si*) approaches of reacting stilbenes leading to pallidol and ampelopsin F analogues respectively in one-pot reaction.

Fully protected stilbene **4.40** possesses a smaller permanent dipole than pterostilbene **1.2** and interstilbene Van der Waals forces are expected to be relatively stronger than in **1.2**, resulting in more species being aligned in a *Re/Si* than *Re/Re* mode. Indeed,

ampelopsin F analogue **4.42** is obtained in almost twofold higher yield than pallidol analogue **4.41**.

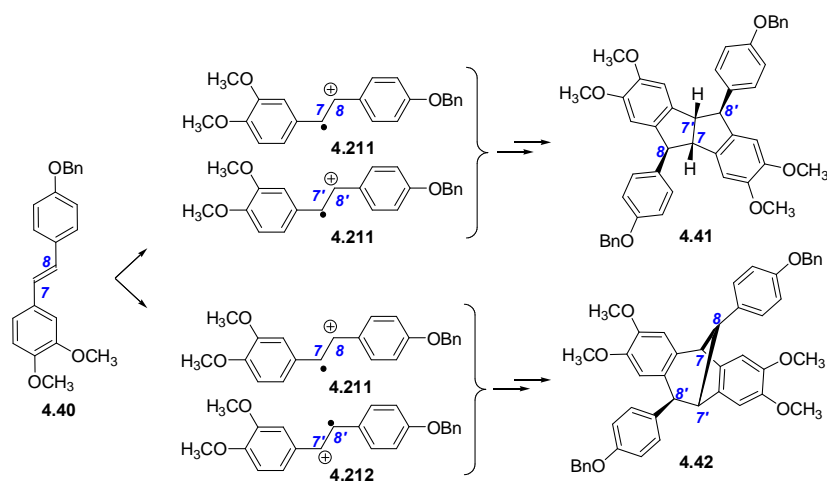
In an earlier publication,²⁵ Weberø group proposed a slightly different mechanism, which was, however, not without flaws. More specifically, the formation of pallidol analogue **4.181** was explained through an intermediate bearing a lone electron on C8ø a seemingly unlikely event as explained above. A second difficulty arose from the second oxidation barely explained as a loss of a hydrogen atom. The above presented mechanism attempts to address these issues. Notably, it is proposed that the second oxidation takes place through the coordination of Fe³⁺ with π -type dimer radical cation **4.207** or radical cation **4.210**.

When Niwaø group subjected resveratrol **1.0** (with three free OHs and a large permanent dipole) to borderline complex K₃[Fe(CN)₆] in a mixture of protic solvents CH₃OH/H₂O (2:1 v/v) with high dielectric constants (MeOH: ϵ = 33; H₂O: ϵ = 80), one could expect some competition between substrate/solvent hydrogen bonding and substrate/substrate hydrophobic interactions. Since hydrogen bonds between CH₃OH and hydroxyls of resveratrol are stronger than hydrophobic interactions, T-shape alignment dominates due to the formation of a shell of bound solvent molecules surrounding the substrate. For similar reasons, *Re/Re* (or *Si/Si*) outweigh *Re/Si* alignments. Indeed, the reaction outcome is mainly directed by T-shape alignments leading to two types of skeletons, *i.e.* δ -viniferin (22%) and ϵ -viniferin (22%) and to a lesser extent by *Re/Re* approach, which yields only one type of skeleton, pallidol in 16% yield (see Scheme 4.58, section 3.11.4).

Other mechanistic interpretation could be considered as well. An alternative approach advocated by Thomasø group on the occasion of the conversion of aminostilbenes into bisindolines considers the reaction of two radical cations,⁵⁰ or

more likely, in most cases, a radical-radical combination that will be presented as well below.

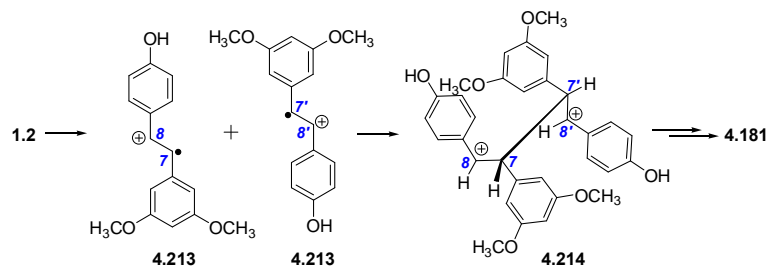
An alternative theory to the formation of both ampelopsin F and pallidol analogues would be based on the hypothesis of the formation of radical cations for stilbenes with catechol substitution. Considering the example of stilbene **4.40** leading to **4.41** and **4.42** respectively, radical cation species **4.211** or **4.212** are readily formed as the carbenium ions are equally stabilized in both the species (Scheme 4.66) (refer Chapter 5 section 5.4.3.2 spin density).



Scheme 4.66: Obtention of pallidol and ampelopsin F analogues from 4,12-dioxygenated stilbene **4.40**.

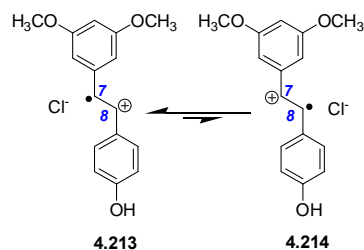
As reported above, pterostilbene **1.2**, in spite of having the resorcinol substitution pattern, produces the pallidol and ampelopsin F analogues **4.181** and **4.182** respectively. It is proposed that pterostilbene **1.2** on exposure to FeCl_3 would generate radical cation **4.213** leading ultimately to **4.181** in a way similar to the sequence **4.207/4.208** presented above (compare species **4.214** in Scheme 4.67 below with **4.208** in Scheme 4.65) (refer to Chapter 5 section 5.5.9.2, Pterostilbene radical ó pterostilbene radical). A similar mechanism would equally apply to the formation of

pallidol **1.6** from resveratrol **1.0** by Niwa's group⁷ and its analogue **4.37** from isorhapontigenin **1.1** by Lin's team²⁴.



Scheme 4.67: Radical cation intermediates en route to pallidol analogue **4.181** from pterostilbene **1.2**.

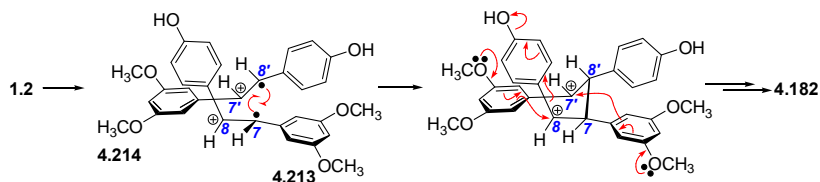
To account for the formation of the ampelopsin F analogue **4.182**, rearrangement of the radical cation **4.213** into **4.214** is proposed, both radical cations being in equilibrium (Scheme 4.68) (refer Chapter 5 section 5.4.3.2 spin density).



Scheme 4.68: equilibrium between stable **4.213** and unstable **4.214** radical cations.

Several examples of alkene radical cation rearrangements are recorded in an excellent review by Crich *et al.*⁶¹ Although a less stable carbocation has now been generated,⁶² the radical (SOMO) can now interact with the hydroxy lone pair doubly vinylogously (through the aromatic ring) with concomitant lowering of the energy of the radical, which is not unexpected given related literature precedents.⁵² With the rearranged radical cation **4.214**, a combination of **4.213** and **4.214** leading to compound **4.182** of the ampelopsin F type is generated (Scheme 4.69). The yield ratio

2:1 in favor of the pallidol skeleton might well reflect the equilibrium concentration of the radicals **4.213** and **4.214**.



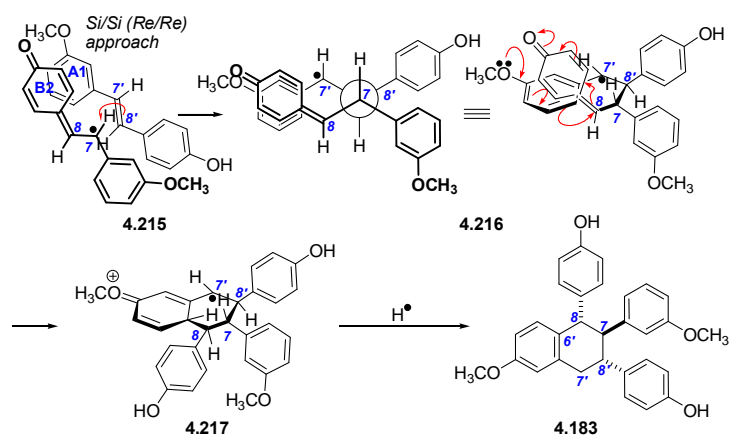
Scheme 4.69: Formation of ampelopsin F analogue **4.182** from pterostilbene **1.2** through the addition of radical cations **4.213** and **4.214**.

It is noticeable that 12-hydroxy-3-methoxystilbene **2.56** does not yield any ampelopsin F nor pallidol type compounds. This can be rationalized by suggesting not all stilbenes having 3,5-oxy or 3-oxy substituents promote the radical cation rearrangement. The equilibrium between the proposed radical cations analogous to **4.213** and **4.214** must lie substantially to the left in favor of the carbocation species that can be stabilized by resonance (Scheme 4.68). It is possible that the rearrangement becomes significant when the resorcinol ring is made sufficiently electron rich by its substituents. This hypothesis should be tested.

In summary, we have presented here two conceptions on how stilbene dimerisation leading to two polycyclic scaffolds might occur. Opinions diverge on the viability and availability of radical cations that are not stabilized by resonance, the types of reacting species (radical/radical vs. radical/native species), the influence, if any, of supramolecular spontaneous arrangements (molecular stacking and solvation). As often the case, the truth may lie somewhere in the middle. We have undertaken some computational studies using quantum mechanics in an attempt to shed some light on this issue.

4.3.5.10. Tetralin analogues formation via FeCl₃ oxidative coupling

The formation of tetralin derivative **4.183** from unsymmetrical demethoxypterostilbene **2.56** can be explained by a slight variation of the mechanism of formation of **4.181** and **4.182** from **1.2** presented on Scheme 3.51 above. The first bond to be established would be the C7-C8', with the quinone methide radical approaching a native stilbene in a head-to-tail *Re/Re* or *Si/Si* manner (Scheme 4.70) (refer to Chapter 5 section 5.5.9.3, Demethoxypterostilbene-demethoxypterostilbene radical). This alignment **4.215** would be different from **4.207** as the substituent pattern is different, leading to the positioning of the dipoles at slightly different locations. As a result the C7-C8' bond could form easily leading to intermediate **4.216**. A ring closure mechanism similar to the one above leads to intermediate **4.217** followed by the formation of **4.183**. It is noteworthy that there is a significant increase in yield when NaI is added to the reaction mixture (from 10 to 37%). I⁻ is a reducer able to facilitate the final reduction step. Compound **4.183** differs from **4.182** just by the absence of a C7-C6' bond as well as an inverted stereochemistry at C8. Disconnection of this bond from compound **4.182** would lead to a triaryltetralin with a *trans-cis* configuration, while **4.183** is of *trans-trans* configuration, thus supporting a different relative orientation of the stilbene units stacked prior to the formation of **4.183**.



Scheme 4.70: Mechanism of the formation of tetralin **4.183** from demethoxypterostilbene **2.56**.

One would like to rationalize the differences in reaction products originating from stilbene **2.56** as opposed to symmetrical stilbene **1.2** differing by only one methoxy group at C5 position. The formation of tetralin **4.183** can possibly be described from another perspective as follows. Pairs of unsymmetrical stilbenes **2.56** can be aligned in four different *Re/Re* (or *Si/Si*) orientations with the methoxy groups being positioned *syn* (alignments A and B) (refer to Chapter 5 section 5.5.5, Calculations results on various *Re/Re* approaches of dimethoxy pterostilbene units with two methoxy groups aligned *syn* to each other) and *anti* (alignments C and D) (refer to Chapter 5 sec 5.5.6, Calculations results on various *Re/Re* approaches of dimethoxy pterostilbene units with two methoxy groups aligned *anti* to each other) to each other (Figure 4.12). In contrast, symmetrical stilbene **1.2** can align in only one *Re/Re* (or *Si/Si*) orientation. An increase in the number of possible alignments means that the system is increasingly disordered. The entropy would increase resulting in negative Gibbs energy. When π -type dimer radical **4.215** forms the C7-C8 bond, the degrees of freedom of rings A1 and B2 are enhanced due to the formation of a cavity (species **4.216**), thus further increasing the entropy of the system. This could explain

why C7-C7 bond is not formed in **4.215** as observed in pallidol formation and, in contrast, why tetralin type skeleton was not observed in pterostilbene oxidative coupling. Stilbene **4.40**, just like pterostilbene **1.2**, did not dimerise into a tetralin skeleton. This observation supports the above presented hypothesis as the presence of bulky benzyloxy substituent in **4.40** restricts the freedom of movement, thus decreasing the entropy of the system. The oxidative coupling reaction using **2.56** as a substrate can therefore be considered as kinetically driven, while substrates **1.2** and **4.40** produce oxidative products (ampelopsin F and pallidol analogues) that are probably thermodynamically favored (refer to Chapter 5 section 5.5.9.4, Demethoxypterostilbene radical δ demethoxypterostilbene radical).

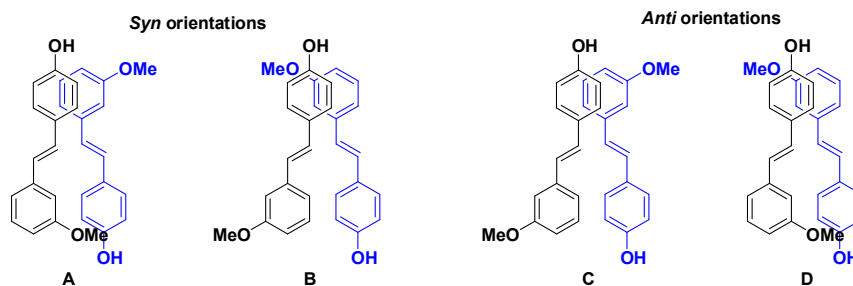
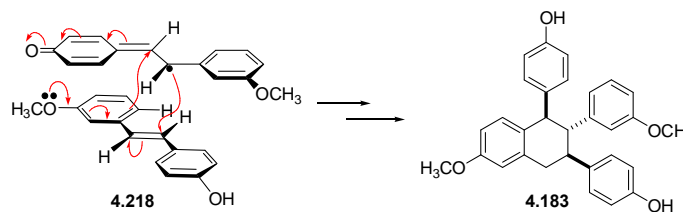


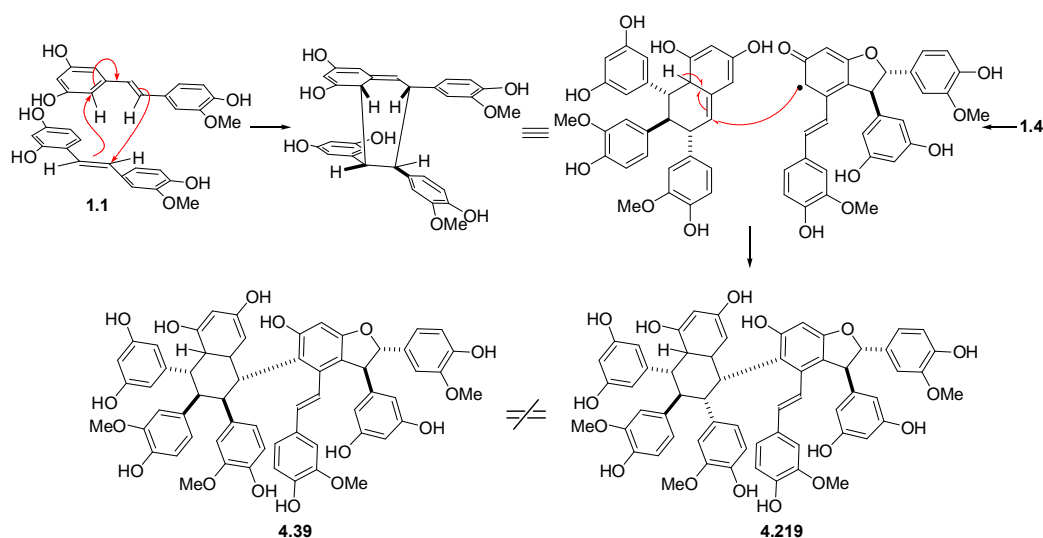
Figure 4.12: Four different *Re/Re* (or *Si/Si*) alignments for **2.56**.

As an alternative to the above mechanism, the formation of tetralin **4.183** could also be described as a radical Diels Alder type reaction represented by arrangement **4.214** (Scheme 4.71).



Scheme 4.71: Tetralin **4.183** formation *via* Diels Alder cycloaddition.

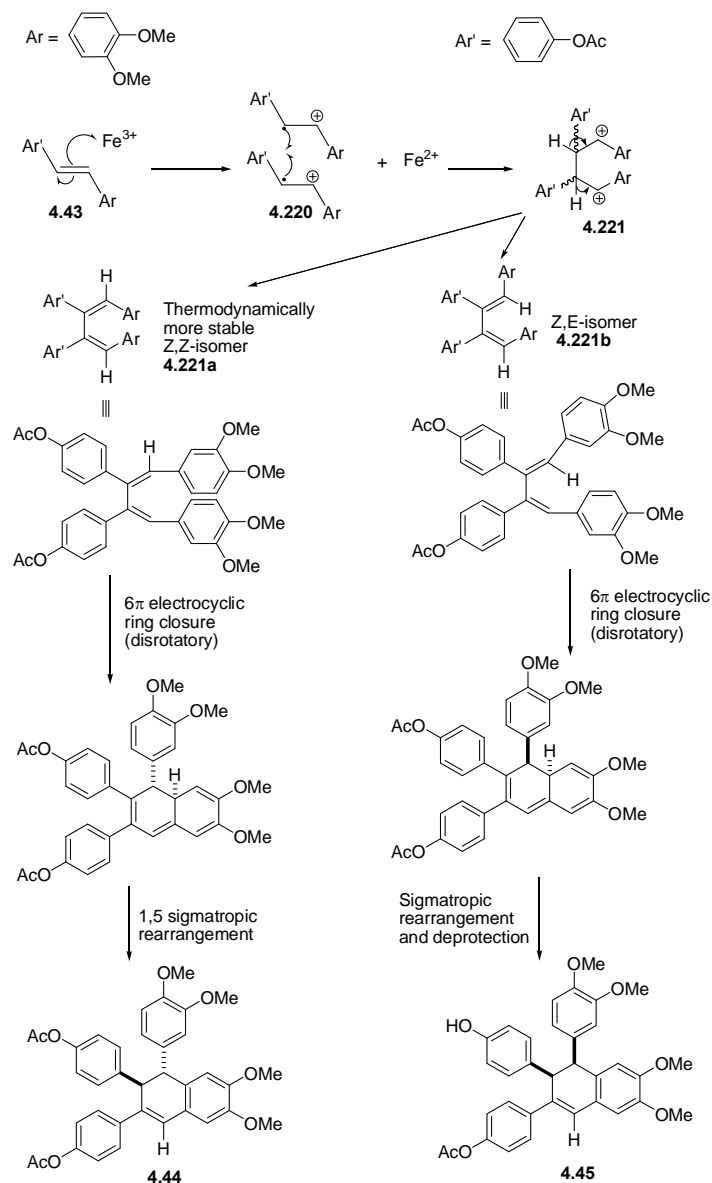
We already made reference to Lin's tetramer **4.39** (see section 4.1.3.2) for which he accounted for the tetralin portion by proposing a 4+2 Diels Alder cycloaddition of two stilbene monomers (isorhapontigenin **1.1**) as in Scheme 4.72.²⁴ Several remarks could be formulated. Lin's Diels Alder mechanism leads to compound **4.219** with a stereochemistry different from that of the published structure **4.39**. The reported NOE data would equally well support an all *trans* tetralin moiety, which, from a thermodynamic view point, would be the favored species. Next, the normal or conventional Diels Alder reaction between an electron-rich diene and an electron-rich dienophile is rather unexpected in this context. In addition, the outlined mechanism leaves many questions unanswered regarding the details. It would be more reasonable to rationalize Lin's reaction as being of the radical cation or radical type as proposed in Scheme 4.70. Finally, with an isolated yield of 0.36%, this transformation is hardly significant.



Scheme 4.72: Revised mechanism for the formation of a stilbene tetramer *via* a Diels-Alder cycloaddition of isorhapontigenin **1.1** (modified from reference 24).

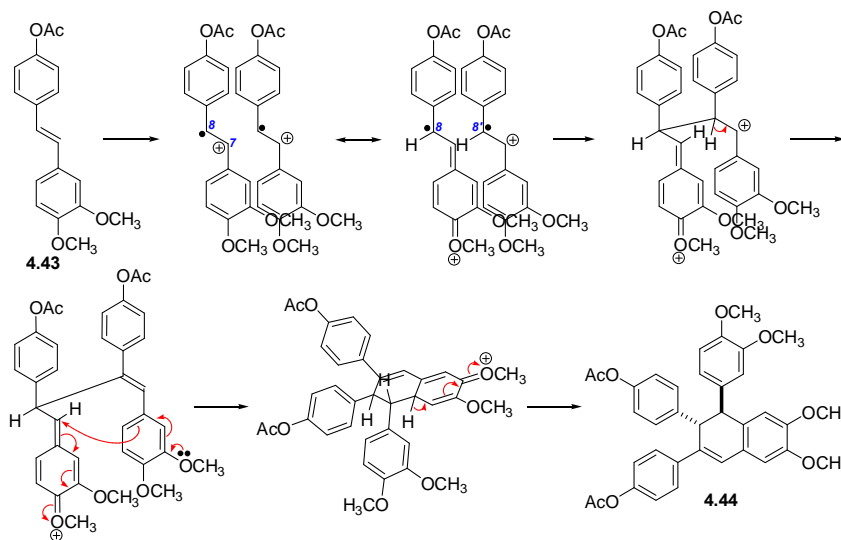
As far as the formation of restrytol C analogues **4.44** and **4.45** is concerned (section 4.1.3.3), Thomas *et al.* rationalized it as follows.²⁶ First, the oxidation of the

olefinic bond of **4.43** by $\text{FeCl}_3 \cdot 6\text{H}_2\text{O}$ in CH_2Cl_2 would produce radical cationic species **4.220** (Scheme 4.73). Consecutively, the coupling of two such radical cationic species would give **4.221** that readily converts into (*Z,Z*) or (*Z,E*) dienes (**4.221a** and **b** respectively). Combination of 6π electrocyclic ring closure and sigmatropic rearrangements to each diene would produce *anti* and *syn* stilbene dimer isomers **4.44** and **4.45** respectively.



Scheme 4.73: Mechanism of formation of restrytol C analogues **4.44** and **4.45** (adapted from reference 26).

However, since physical models suggest an extremely strained arrangement would be obtained for **4.221a** and **b**, a non-pericyclic mechanism as depicted in Scheme 4.74 may be a more viable option.



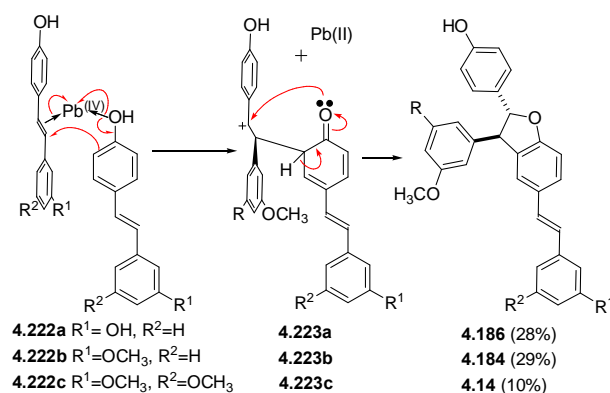
Scheme 4.74: Alternative mechanism of formation of restrytol C analogue **4.44**.

4.3.5.11. Trimer with tetralin scaffold formation via PbO_2 oxidative coupling

Based on the reactions outcomes obtained from PbO_2 oxidative coupling as reported in section 4.3.3, the mechanistic issues can be understood as follows. PbO_2 , having a large size combined to a high charge density corresponding to its +4 oxidation state, can be considered as a borderline reagent. PbO_2 is also considered as a strong oxidant with a standard redox potential $E^\circ(\text{Pb}^{4+}/\text{Pb}^{2+}) = 1.69\text{V}$.⁶³ As a result, it is possible to conceive the formation of three different complexes between stilbenes and $\text{Pb}(\text{IV})$ with two coordination sites arising from the metal (Scheme 4.75 and 4.76):

- $\text{Pb}(\text{IV})$ coordinating to two *para* hydroxyls from two stilbenes of **2.58**, **2.56** and **1.2** leading to complex **4.228a**, **4.228b** and **4.228c** respectively. In this complex, stilbenes are coordinated in such a way that there will be little interaction between them if any.
- $\text{Pb}(\text{IV})$ coordinating to two methoxy groups from the resorcinolic ring of two

pterostilbene **1.2** units leading to complex **4.224**; in this manner, the complex can be stabilized through hydrogen bonding between units (in the case of stilbene **2.56**, for which ring B is not as electron rich as in **1.2** for example, this complex might be difficult to form). iii) A mixed coordination where Pb(IV) coordinates to the olefinic bond (soft ligand) of one stilbene (**2.58**, **2.56**, **1.2**) and to the *para* hydroxyl (hard ligand) of the second stilbene unit **2.58**, **2.56** and **1.2** giving **4.222a**, **4.222b** and **4.222c** respectively.



Scheme 4.75: Formation of δ -viniferin skeleton *via* PbO₂ oxidative coupling

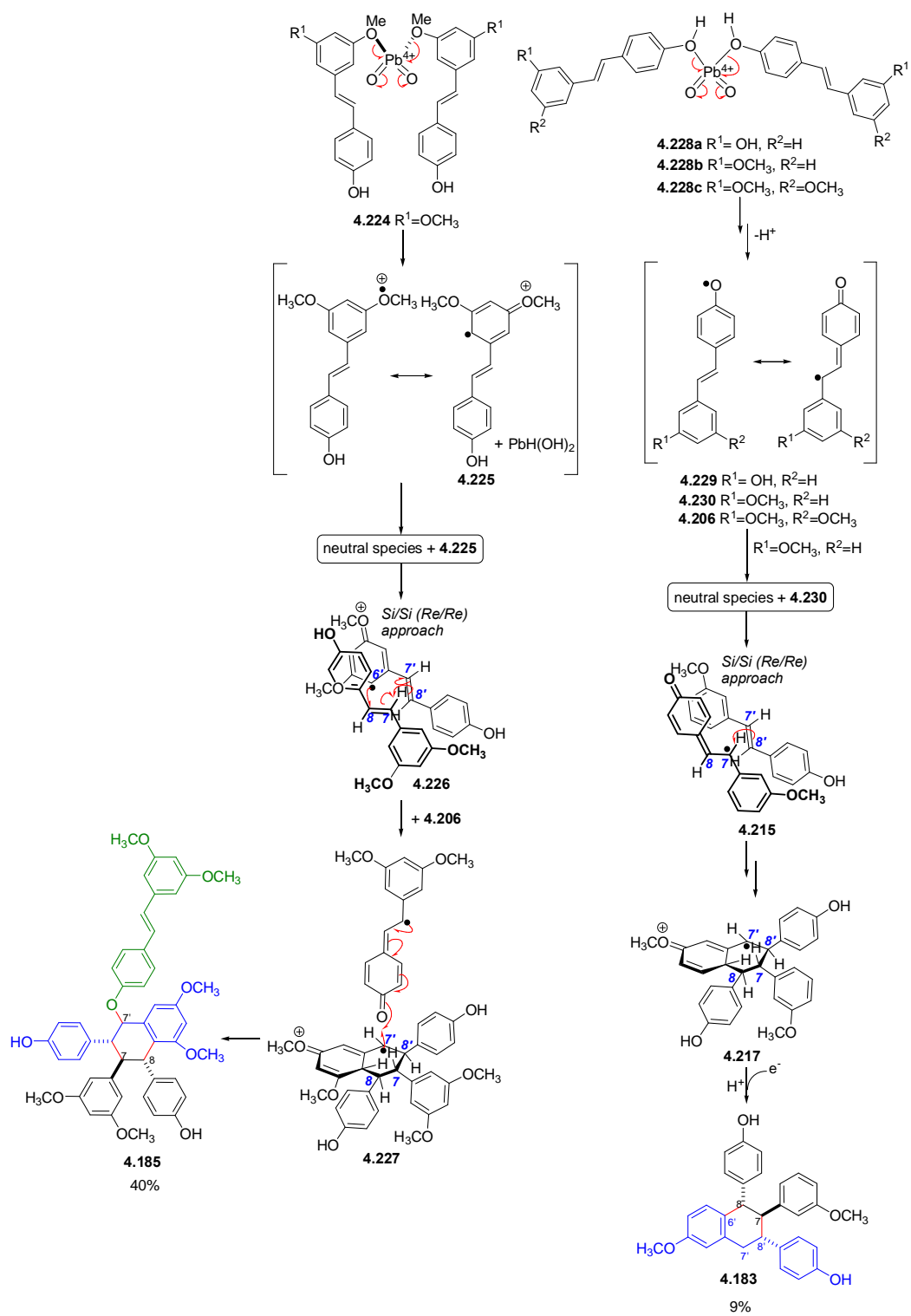
After oxidative electron transfer, complex **4.228a**, **4.228b** and **4.228c** will release radical **4.229**, **4.230** and **4.206** respectively after the lost of proton while complex **4.224** produces radical **4.225**, which are more reactive (less stable) than **4.206**. In complex **4.222a**, **4.222b** and **4.222c**, Pb(IV) coordinates to the stilbene in a manner somewhat similar to the proposed stilbene-silver complex **4.189a** (refer to section 4.3.5.6.8 and Scheme 4.60). The first oxidized stilbene species will undergo a concerted movement of electrons involving the C7 of the second stilbene unit followed by an electron transfer to lead forming complex **4.223a**, **4.223b** and **4.223c** respectively. Complex **4.223** will then be cyclised *via* carbonyl nucleophilic attack to yield δ -viniferin analogues (**4.186**, **4.184** and **4.14**). Stilbene **2.56** would be able to

generate one kind of radical species, **4.230** from complex **4.228b** and depending on the coordination pattern and alignment, δ -viniferin analogue **68** produced in 29% yield suggesting that complex **4.222b** is favored. In comparison, tetralin **4.183** was formed in only 9% yield from the same reaction, where a neutral species and a quinone methide radical are involved. These two species approach in a *Re/Re* manner (**4.215**) comparable to their alignment in the presence of $\text{FeCl}_2 \cdot 6\text{H}_2\text{O}$ (refer to section 4.3.5.10 and Scheme 4.70).

However, this was not the case for pterostilbene **1.2** when it was subjected to PbO_2 where the yield of trimer **4.185** (incorporating a tetralin scaffold) is higher than the yield of δ -viniferin analogue **4.14**. Furthermore, pterostilbene in presence of $\text{FeCl}_2 \cdot 6\text{H}_2\text{O}$ did not produce any tetralin like skeleton, suggesting that one could think of the occurrence of an additional different new radical species **4.225**, which has a different reactivity than **4.206**. This species **4.225**, possessing a reactive radical at $\text{C6}\alpha$ then establishes a first bond with C8 of the olefinic bond of another neutral species from complex **4.226** where they are aligned in a same *Re/Re* manner, followed by cyclodimerization to give species **4.227** with a lone electron located at $\text{C7}\alpha$. This species can spontaneously be attacked by the freely available quinone methide radical to form trimer **4.185**. Thus, the reaction equilibrium is shifted more towards the formation of complex **4.226** than **4.222c**. The stereochemistry at $\text{C7}\alpha$ of the trimer is yet to be determined. Further experiments can be conducted in order to confirm the presence of radical at C7 in **4.227** by means of radical traps.

On the other hand, subjecting stilbene **2.58** in MeOH to PbO_2 produces only δ -viniferin analogue **4.186** in 28% yield (Scheme 4.75) as opposed to compounds **2.56** and **1.2** which produce both δ -viniferin and tetralin type skeletons in $\text{PbO}_2/\text{CH}_2\text{Cl}_2$ (Scheme 4.76). This further confirms the hypothesis that (as described in

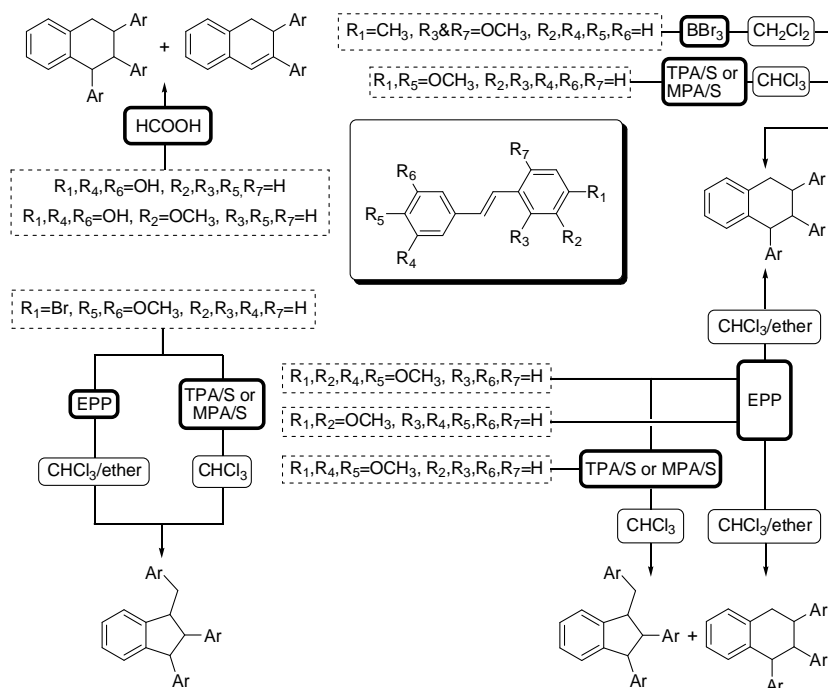
the previous section) MeOH, a protic solvent, solvates polar stilbene and prevent the stilbenes from coming closer in a parallel displaced manner (*Re/Re* approach), refer to section 4.3.5.9, Chapter 4. Thus, complex **4.222a** is probably preferred due to the T-shape alignment.



Scheme 4.76: Formation of tetralin skeleton *via* PbO_2 oxidative coupling

4.3.5.12. Tetralin and indane scaffolds formation catalysed by Brønsted acids

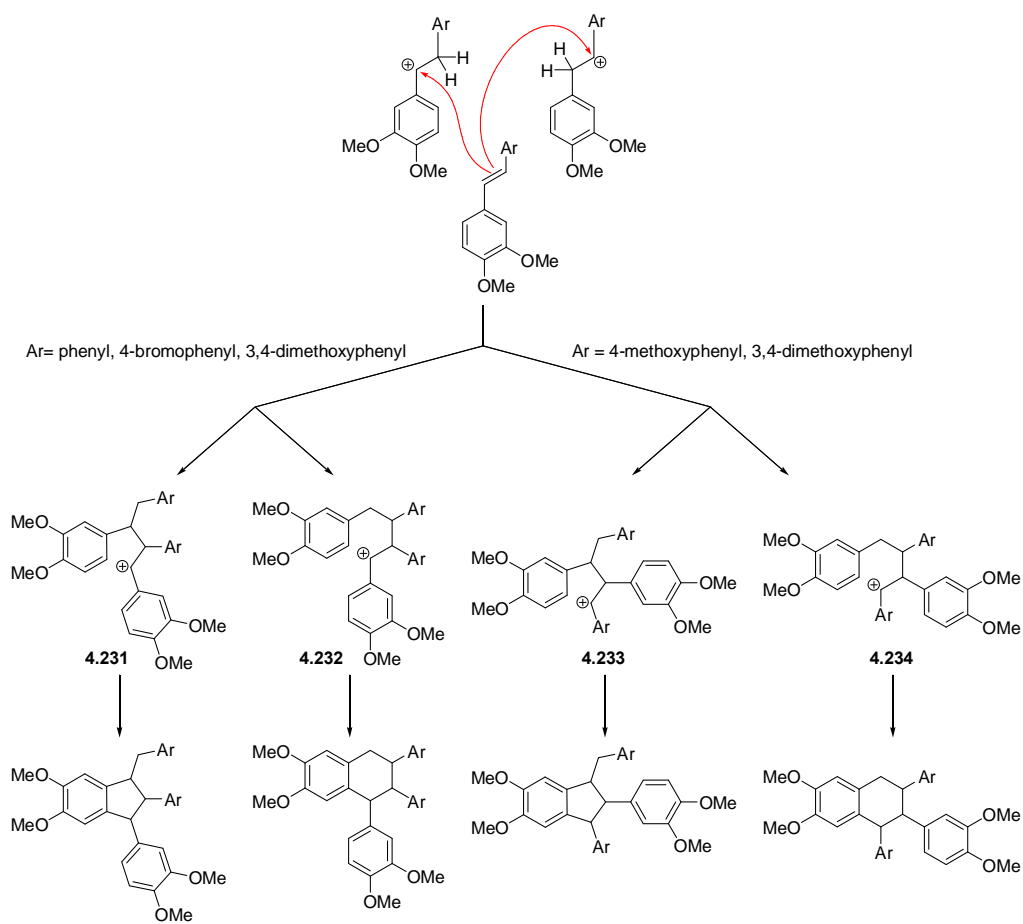
Four groups, namely Li *et al.*,³³ Aguirre *et al.*,³⁵ Li and Ferreira³⁶ and Alesso *et al.*³⁷ have carried out stilbenoid dimerisation in HCOOH, EPP, BBr₃, MPA/S and TPA/S respectively to produce tetralin and/or indane type skeletons as summarized in Scheme 4.77.



Scheme 4.77: Acid catalysed stilbene dimerisation products (adapted from references 33, 35-37).

Li *et al.* have proposed a 4+2 Diels Alder cycloaddition of two stilbene monomers in rationalizing the tetralin type skeleton formation as mentioned above (see section 4.1.8.1).³³ Other authors prefer a mechanism involving a dimeric carbocation species such as **4.231-4.234** (Scheme 4.78). These acid reagents would protonate a stilbene monomer producing an sp³ hybridized carbocation instead of a planar quinone methide sp² hybridized radical. This carbocation would react with a native stilbene to produce tetralin and/or indane skeletons. Aguirre *et al.* clarified that the final products depend on the stability of the intermediate cations as summarized in

Scheme 4.78.³⁵ The initial cation would bear the positive charge either on C7 or C8 depending on how the stabilizing influence substituents on both aromatic rings. A native stilbene would induce a nucleophilic attack on it, which then may result in two different dimeric carbocations. As a result, two regioisomeric indanes and two regioisomeric tetralins can possibly be obtained when unsymmetrical stilbenes are used, notwithstanding the possibility of formation of diastereoisomers. This proposed mechanism slightly differs from the mechanisms proposed above for metal mediated oxidation that would generate stilbene radical cations (converted into radicals if a quinone methide formation is possible). Considering species **4.231-4.234**, if Ar = phenyl, and 4-bromophenyl then dimeric carbocation **4.231** and **4.232** will be preferred over **4.233** and **4.234** due to the positively charged species linked to the electron donor 3,4-dimethoxyphenyl group contributing to a greater stability of the positive charge (Scheme 4.78). However, if the aryl group is substituted by electron donor like 4-methoxyl then species **4.233** and **4.234** would be formed. When results of all contributors are considered together, it seems that the ring size formed in cyclodimerization is dependent as well on electron-donating or withdrawing properties the aryl group. Strong electron donor substituents favor the formation of tetralin type skeleton, whereas electron withdrawing substituents induce the generation of indane type skeleton. The indane type skeleton was not obtained in metal oxidant like FeCl₃.6H₂O while the tetralin type was possible. This could support the hypothesis of the formation of a planar stilbene radical/quinone methide radical aligning through π - π interactions instead of stilbene cation in the presence of acid.



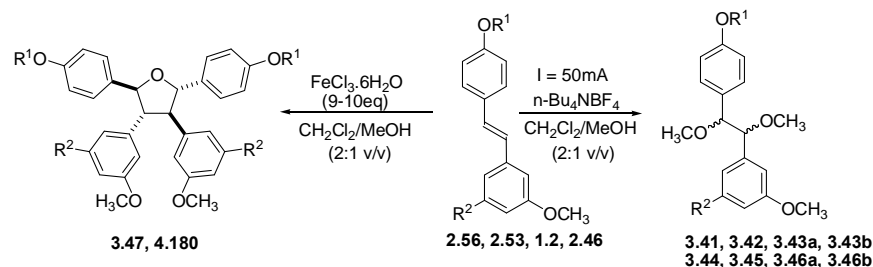
Scheme 4.78: Various pathways leading to indane and tetralin skeletons through acid-catalysed dimerisation of 3,4-dimethoxystilbenes (adapted from reference 35).

4.3.5.13. Comparison of anodic versus $\text{FeCl}_3 \cdot 6\text{H}_2\text{O}$ oxidation of stilbenes

It has been observed that the application of constant current electrolysis (CCE) to stilbene derivatives (see Chapter 3) **2.56**, **2.53**, **1.2** and **2.46** in $\text{CH}_2\text{Cl}_2/\text{MeOH}$ mixture produces monomeric stilbenoid adducts as a result of solvent addition (Scheme 4.79). On the other hand, when stilbene **2.56** is subjected to CCE in pure CH_2Cl_2 , a dimeric product tricuspidatol-A analogue **3.47** is obtained (Scheme 4.80).

It is noteworthy that when chemical oxidation is performed either in CH_2Cl_2 or $\text{CH}_2\text{Cl}_2/\text{MeOH}$ mixture onto the above stilbenes, only dimeric/trimeric species are obtained rather than any other solvent addition products. Despite of the various

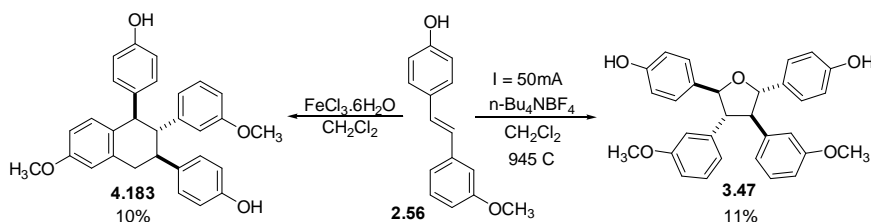
chemical oxidants being used, only $\text{FeCl}_3 \cdot 6\text{H}_2\text{O}$ oxidation has close results to that of anodic oxidation. Tricuspidatol-A type skeletons were only possible to be obtained through $\text{FeCl}_3 \cdot 6\text{H}_2\text{O}$ oxidation of some of the stilbene derivatives like **2.56**, **2.53**, **1.2** and **2.46**, when carried out in $\text{CH}_2\text{Cl}_2/\text{MeOH}$ mixture (Scheme 4.79). *Para* acetylated stilbenes **2.53** and **2.46**, give rise to lower yields (7% and 17% respectively) of tricuspidatol-A type skeleton, whereas *para* hydroxylated stilbenes **2.56** and **1.2** produce the same tricuspidatol-A type skeleton in higher yields (34% and 29% respectively). In contrast, when the above $\text{CH}_2\text{Cl}_2/\text{MeOH}$ mixture is replaced by pure CH_2Cl_2 in comparison to the anodic oxidation, tetralin type skeleton was obtained from stilbene **2.56** (Scheme 4.80).



Yield (%)	Product	Oxidant	Starting Material	Product	Yield (%)
34	3.47 $\text{R}^1, \text{R}^2 = \text{H}$	$\text{FeCl}_3 \cdot 6\text{H}_2\text{O}$	2.56 $\text{R}^1, \text{R}^2 = \text{H}$	3.41 & 3.42 $\text{R}^1, \text{R}^2 = \text{H}$ pure diastereoisomers	23 & 28
7	3.47 $\text{R}^1, \text{R}^2 = \text{H}$	$\text{FeCl}_3 \cdot 6\text{H}_2\text{O}$	2.53 $\text{R}^1 = \text{Ac}, \text{R}^2 = \text{H}$	3.43a & 3.43b $\text{R}^1 = \text{Ac}, \text{R}^2 = \text{H}$ mixture of diastereoisomers	23
29	4.180 $\text{R}^1 = \text{H}, \text{R}^2 = \text{OMe}$	$\text{FeCl}_3 \cdot 6\text{H}_2\text{O}$	1.2 $\text{R}^1 = \text{H},$ $\text{R}^2 = \text{OMe}$	3.44 & 3.45 $\text{R}^1 = \text{H}, \text{R}^2 = \text{OMe}$ pure diastereoisomers	10 & 10
17	4.180 $\text{R}^1 = \text{H}, \text{R}^2 = \text{OMe}$	$\text{FeCl}_3 \cdot 6\text{H}_2\text{O}$	2.46 $\text{R}^1 = \text{Ac},$ $\text{R}^2 = \text{OMe}$	3.46a & 3.46b $\text{R}^1 = \text{Ac}, \text{R}^2 = \text{OMe}$ mixture of diastereoisomers	17

Scheme 4.79: Comparison of stilbene derivatives electrochemical oxidation with $\text{FeCl}_3 \cdot 6\text{H}_2\text{O}$ oxidation in a mixture of $\text{CH}_2\text{Cl}_2/\text{MeOH}$.

There are a few possible aspects to be considered based on the above comparisons. Chemical oxidations ($\text{FeCl}_3 \cdot 6\text{H}_2\text{O}$) of **2.56**, **2.53**, **1.2** and **2.46** go through one electron oxidation with fixed potential yielding only dimerised products (tricuspidatol-A/tetralin analogues) either in nucleophilic or non nucleophilic solvent. On the contrary, when the current is kept constant and therefore, an increasing potential, thus, favoring two consecutive electron oxidation processes. As a result, monomeric stilbenoid adducts are obtained in the presence of nucleophilic solvent.



Scheme 4.80: Comparison of stilbene derivatives electrochemical oxidation with $\text{FeCl}_3 \cdot 6\text{H}_2\text{O}$ oxidation in CH_2Cl_2 .

The fact that different dimeric products are obtained by $\text{FeCl}_3 \cdot 6\text{H}_2\text{O}$ and anodic oxidations of **2.56** in the same non nucleophilic solvent (CH_2Cl_2) could possibly explained in the following manner. Even though both reaction conditions result in one electron oxidation, this is not sufficient to explain the different reaction outcome being obtained. One should also consider the strength of external magnetic field generated during the constant current electrolysis (CCE). This might be the cause of distortion in the initial stilbene alignment, which then lead to a new alignment corresponding to a different dimerised product *via* radical coupling. Since the potential continuously increases during CCE, many other by-products could also be formed especially due to solvent oxidation. These by-products could also influence the final reaction outcome. Alternatively, conducting anodic oxidation at a suitable controlled

potential is probably a better way to eliminate undesired by-products and enhance the formation of dimeric species.

4.4. Conclusion

As seen in the literature review, the classical phenolic oxidative coupling is applied to describe the mechanism involved in stilbene oligomerisation. This approach is globally correct but not sufficient to understand the apparent inconsistencies in the formation of various skeletons in different reaction conditions. As a result, an in-depth analysis of the outcome of stilbene oxidative coupling obtained in this study as well as by other investigators led us to derive two key different hypotheses. The first hypothesis considers the interactions between the metal oxidant (in combination with the solvent) and the stilbene through the application of Pearson's principle of Hard and Soft Acid Base (HSAB principle). Accordingly, solvent-metal oxidant combinations can be categorized into hard, soft and borderline acids and interact either with oxygenated substituent (hard base) or with olefinic bond (soft base). The second hypothesis derives from the fact that stilbenoids are fully conjugated π -systems and may therefore interact non-covalently through π - π interactions and hydrogen bonding (in presence of phenolic groups). These interactions would play an important role in the self assembly of stilbenoids prior to the phenolic radical coupling which then would determine the type of skeleton produced. These interactions would be expected to be profoundly influenced by the solvent, substitution pattern and metal oxidant coordination as all these factors tend to alter the electronic distribution in the system.

At this junction, these hypotheses, no matter how attractive they may sound, remain what they are, *i.e.* hypotheses. In an attempt to validate them, computational calculations were undertaken and the results are discussed in the next chapter.

4.5. Experimental section

All reagents used were commercial products and were used without further purification. Preparative thin layer chromatography (PTLC) was performed on silica gel plates with a fluorescent indicator that was visualized with light at 254 nm (Merck). Flash chromatography was performed using a Master Personal⁺ from Argonaut Inc. connected to a fraction collector Teledyne ISCO[®]-Retriever 500. Infra red (IR) spectra were recorded on a Perkin Elmer 1600 series FTIR, while ultra violet (UV) spectra were recorded on a Varian Cary 50 Conc. NMR spectra (¹H and ¹³C, 2D homo and heteronuclear) were recorded on a Bruker Avance 300, Jeol JNM-LA400, or Jeol ECA 500. High-resolution MS experiments were performed using a JEOL JMS-700TZ time-of-flight mass spectrometer.

4.5.1. Oligomerisation of 12-hydroxy-3,5-dimethoxystilbene 1.2

4.5.1.1. Preparation of 4.14/4.185

a) AgOAc oxidation in CH₂Cl₂

To a solution of **1.2** (50 mg, 0.2 mmol) in CH₂Cl₂ (10 mL) was added AgOAc (33 mg, 0.2 mmol) and the mixture was stirred for 24h at room temperature. The reaction mixture was concentrated and subjected to preparative silica-gel TLC (two plates) using ethyl acetate-hexane (3:7) as mobile phase to give **4.14** (18 mg, 36%).

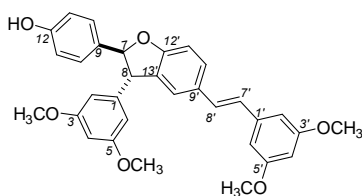
b) AgOAc oxidation in a mixture of CH₂Cl₂/MeOH

To a solution of **1.2** (50 mg, 0.2 mmol) in a mixture of CH₂Cl₂/MeOH (7:3, v/v) was added AgOAc (33 mg, 0.2 mmol) and the mixture was stirred for 48 h at room temperature. The reaction mixture was concentrated and subjected to preparative

silica-gel TLC (two plates) using ethyl acetate-hexane (3:7) as mobile phase to give **1.2** (10 mg, 18%).

c) PbO₂ oxidation

To a solution of **1.2** (50mg, 0.2mmol) in CH₂Cl₂ (10 mL) was added PbO₂ (47 mg, 0.2 mmol) and the mixture was stirred for 24h at room temperature. The reaction mixture was concentrated and subjected to preparative silica-gel TLC (two plates) using ethyl acetate-hexane (3:7) as mobile phase to give **4.14** (5 mg, 10%) and **4.185** (20 mg, 40%).



δ -Viniferin analogue **4.14**

UV: ($\lambda_{\max}^{\text{MeOH}}$): 310 nm.

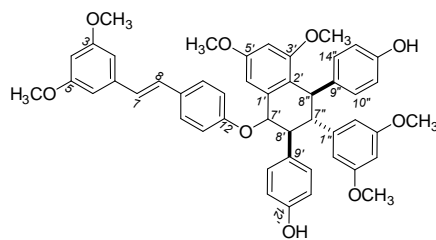
IR(film) ν_{\max} : 3392, 2924, 2851, 1594, 1204, 960 cm⁻¹

ESI-TOF-MS(-): [M-H]⁻; m/z 509.1964 measured, 509.1964 calculated for C₃₂H₂₉O₆,

m/m = 0 ppm

¹H NMR (CDCl₃, 500MHz) 6.34 (d, 1 H, *J* = 2.2 Hz, H2/6), 6.40 (t, 1 H, *J* = 2.2 Hz, H4), 4.47 (d, 1 H, *J* = 8.5 Hz, H7), 5.50 (d, 1 H, *J* = 8.0 Hz, H8), 6.81 (d, 1 H, *J* = 8.5 Hz, H11/13), 6.61 (d, 1 H, *J* = 2.2 Hz, H2 ϕ /6 ϕ), 6.83 (d, 1 H, *J* = 16.1 Hz, H7 ϕ), 7.00 (d, 1 H, *J* = 16.1 Hz, H8 ϕ), 7.19 (s, 1 H, H10 ϕ), 6.91 (d, 1 H, *J* = 8.3 Hz, H13 ϕ), 7.36 (d, 1 H, *J* = 8.3 Hz, H14 ϕ), 3.80 (s, 3 H, 3 ϕ /5 ϕ OMe), 3.75 (s, 3 H, 3/5OMe).

¹³C NMR (CDCl₃, 125 MHz) 144.0 (C1), 106.5 (2/6), 161.2 (3/5), 99.1(4), 57.9 (7), 93.1 (8), 132.6 (9), 127.6 (10), 115.6 (11/13), 156.0 (12), 139.8 (1 ϕ), 104.3 (2'/6'), 161.0 (3'/5 ϕ), 99.8 (4'), 126.3 (7'), 129.1 (8'), 130.9 (9'), 123.2 (10'), 130.8 (11'), 159.8 (12 ϕ), 109.8 (13'), 128.1 (14 ϕ), 55.3 (3'/5'OMe), 55.4 (3/5OMe).



Trimer 4.185

ESI-TOF-MS(+): [M+H]⁺; m/z 767.3199 measured, 767.3215 calculated for C₄₈H₄₇O₉,

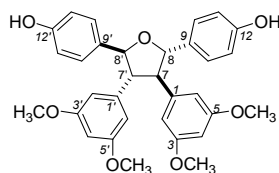
m/m = 2.1 ppm

¹H NMR (CDCl₃, 400 MHz): 6.62 (d, 2 H, J = 2.3 Hz, H2/6), 6.37 (t, 1 H, J = 2.3 Hz, H4), 6.84 (d, 1 H, J = 16.5 Hz, H7), 6.96 (d, 1 H, J = 16.5 Hz, H8), 7.27 (d, 2 H, J = 8.7 Hz, H10/14), 6.66 (d, 2 H, J = 8.7 Hz, H11/13), 6.69 (s, 1 H, H6), 6.41 (d, 1 H, J = 2.3 Hz, H4), 5.49 (d, 1 H, J = 10.6 Hz, H7), 3.35 (t, 1 H, J = 10.6 Hz, H8), 6.79 (d, 2 H, J = 8.7 Hz, H10/14), 6.45 (d, 2 H, J = 8.7 Hz, H11/13), 6.01 (d, 2 H, J = 1.8 Hz, H2/6), 6.15 (t, 1 H, J = 2.3 Hz, H4), 3.22 (dd, 1 H, J = 11.4, 6.8 Hz, H7), 4.45 (d, 1 H, J = 6.9 Hz, H8), 6.75 (d, 2 H, J = 8.7 Hz, H10/14), 6.65 (d, 2 H, J = 8.7 Hz, H11/13), 3.81 (s, 6 H, 3/5 OMe), 3.50 (s, 3 H, 3 OMe), 3.73 (s, 3 H, 5 OMe), 3.59 (s, 6 H, 3/5 OMe).

¹³C NMR (CDCl₃, 100 MHz): 139.7 (1), 104.4 (2/6), 161.0 (3/5), 99.7 (4), 126.7 (7), 128.7 (8), 130.3 (9), 127.7 (10/14), 116.4 (11/13), 159.9 (12), 141.3 (1), 119.8 (2), 100.9 (6), 158.3 (3), 159.5 (5), 98.6 (4), 82.1 (7), 54.2 (8), 132.9 (9), 129.5 (10/14), 114.89/114.85 (11/13), 153.7 (12), 146.3 (1), 106.7 (2/6), 160.2 (3/5), 98.1 (4), 56.8 (7), 47.4 (8), 139.2 (9), 128.5 (10/14), 114.89/114.85 (11/13), 153.4 (12), 55.4 (3/5 OMe), 55.6 (3 OMe), 55.4 (5 OMe), 55.2 (3/5 OMe).

4.5.1.2. Preparation of 4.180

To a solution of **1.2** (0.47 g, 1.8 mmol) in a mixture of CH₂Cl₂/MeOH (19:9 mL) was added FeCl₃.6H₂O (5 g, 18 mmol) and the mixture was stirred for 72 H at room temperature. The reaction mixture was quenched with brine solution and extracted with ethyl acetate. The organic phase was dried over anhydrous sodium sulfate, and evaporated under reduced pressure. The reaction mixture was concentrated and subjected to centrifugal chromatography (silica gel 60 PF₂₅₄ containing gypsum for preparative layer chromatography) using ethyl acetate-hexane (3:7) as mobile phase to give **4.180** (0.14g, 29%).



Tricuspidatol A analogue 4.180

¹H NMR: (CDCl₃, 400 MHz): 7.14 (2 H, d, J = 8.2 Hz, H10/14), 6.67 (2 H, d, J = 8.2 Hz, H11/13), 6.24 (1 H, d, J = 2 Hz, H4), 6.23 (2 H, br s, H2/6), 5.25 (1 H, d, J = 8.5 Hz, H8), 3.63 (6 H, s, OCH₃), 3.56 (1 H, d, J = 8.5 Hz, H7).

See Appendix 56 for ¹H NMR spectrum of compound **4.180**. The structure of **4.180** was determined by comparison of its spectroscopic data with those of compound **3.47**.

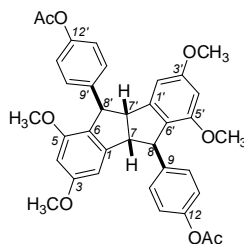
4.5.1.3. Preparation of 4.181 & 4.182

To a solution of **1.2** (0.69 g, 3 mmol) in CH₂Cl₂ (140 mL) was added FeCl₃.6H₂O (0.74 g, 3 mmol) and the mixture was stirred for 48h at room temperature. The reaction mixture was concentrated and subjected to flash column chromatography on a Flashmaster Personal⁺ on a Isolute[®] SPE silica cartridge using ethyl acetate-hexane (3:7) as mobile phase to give a inseparable mixture of **4.181** and **4.182** in a

ratio of 1.5:1 respectively (112 mg). In the hope of separating derivatives of **4.181** and **4.182**, acetylation of this mixture was carried out (see below).

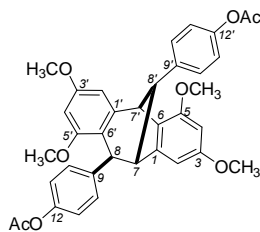
Acetylation of **4.181** & **4.182** into **4.181a** & **4.182a**

To a mixture of **4.181** & **4.182** (112 mg) in pyridine (4 mL) was added acetic anhydride (5.0 mL) and the mixture was stirred for 24 h at room temperature. The reaction mixture was quenched with brine solution and extracted with ethyl acetate. The organic phase was dried over anhydrous sodium sulfate, and evaporated under reduced pressure. The reaction mixture was subjected to preparative silica-gel TLC (five plates) using ethyl acetate-hexane (3:7) as mobile phase to give another inseparable mixture of **4.181a** and **4.182a** (103 mg) in a ratio of 1.5:1 respectively.



Pallidol analogue **4.181a**

¹H NMR: (CDCl₃, 400 MHz): 7.15 (4 H, d, J=8.4Hz, H10/14), 6.95 (4 H, d, J=8.4Hz, H11/13), 6.65 (2 H, d, J=1.8, H6), 6.25 (2 H, d, J=1.8, H4), 4.62 (2 H, s, H8), 4.03 (2 H, s, H7), 3.84 (6 H, s, OCH₃), 3.60 (6 H, s, OCH₃), 2.27 (6 H, s, COCH₃).



Ampelopsin F analogue **4.182a**

¹H NMR: (CDCl₃, 400 MHz): 7.20 (2 H, d, J=8.6 Hz, H10/14), 7.00 (2 H, d, J=8.6 Hz, H11/13), 6.90 (2 H, d, J=8.5 Hz, H10/14), 6.80 (2 H, d, J=8.5Hz, H11/13), 6.56 (1 H, d, J=2.0Hz, H6), 6.50 (1 H, d, J=2.4, H6), 6.24 (1 H, d, 2.4, H4), 6.18 (1 H, d,

J=1.7Hz, H4), 4.24 (1 H, s, H8), 4.19 (1 H, s, H7), 3.82 (3 H, s, OCH), 3.78 (3 H, s, OCH), 3.75 (1 H, s, H8), 3.74 (3 H, s, OCH), 3.45 (1 H, s, H7), 3.42 (3 H, s, OCH), 2.28 (3 H, s, COCH), 2.22 (3 H, s, COCH).

See Appendix 57 for ¹H NMR spectrum of mixture **4.181a** and **4.182a**. The structures were established by studying the NMR spectra of the mixture. The above structures were determined by comparison of their spectroscopic data with those of compounds **4.41**²⁵ and **4.42**²⁵ as well as by comparison with the published data for naturally occurring pallidol⁶⁴ and ampelopsin F.⁶⁵

4.5.2. Oligomerisation of 12-hydroxy-3-methoxystilbene **2.56**

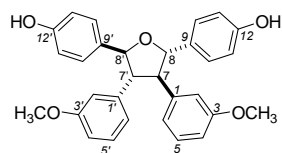
4.5.2.1. Preparation of **3.47**

a) FeCl₃.6H₂O oxidation

To a solution of **2.56** (500 mg, 2.2 mmol) in a 30 mL mixture of CH₂Cl₂/MeOH (2:1, v/v) was added FeCl₃.6H₂O (5.5 g, 0.02 mol) and the mixture was stirred for 6 days at room temperature. The reaction mixture was concentrated and subjected to preparative silica-gel TLC (ten plates) using ethyl acetate-hexane (3:7, v/v) as mobile phase to yield **3.47** (170 mg, 34%).

b) VOF₃ oxidation

To a solution of **2.56** (100 mg, 0.44 mmol) in CH₂Cl₂ (20 mL) was added VOF₃ (280 mg, 2.21 mmol) and the mixture was stirred for 72 h at room temperature. The reaction mixture was concentrated and subjected to preparative silica-gel TLC (four plates) using ethyl acetate-hexane (3:7, v/v) as mobile phase to yield **3.47** (9.7 mg, 10%).



Tricuspidadol A analogue 3.47

UV: ($\lambda_{\max}^{\text{MeOH}}$): 225, 275 nm.

IR (film) ν_{\max} : 3366, 3024, 2926, 1610, 1515, 1264, 1042 cm^{-1}

ESI-TOF-MS(-): [M-H]⁻; m/z 467.1831 measured, 467.1858. calculated for C₃₀H₂₇O₅,

m/m = -5.9 ppm

¹H NMR (CDCl₃, 500 MHz) 6.58 (s, 1 H, H2), 6.68 (d, J=7.3 Hz, H4) 7.09 (t, J= 8.0 Hz, H5), 6.69 (d, J=7.3Hz, H6), 3.61 (d, J=10 Hz, H7), 5.28 (d, J=10 Hz, H8), 7.13 (d, J= 8.5 Hz, H10), 6.65 (d, J= 8.5 Hz, H11) 6.65 (d, J= 8.5 Hz, H13) 7.13 (d, J= 8.5 Hz, H14) 3.65 (s, 3 H, OMe).

¹³C NMR (CDCl₃, 125 MHz) 139.4 (1), 114.2 (2), 159.5 (3), 112.0 (4), 129.5 (5), 120.4 (6), 62.1 (7), 87.4 (8), 132.9 (9), 127.6 (10), 115.4 (11), 155.4 (12), 115.4 (13), 127.7 (14), 55.2 (OMe)

4.5.2.2. Preparation of 4.183/4.184

a) PbO₂ oxidation

To a solution of **2.56** (100 mg, 0.44 mmol) in CH₂Cl₂ (20 mL) was added PbO₂ (330 mg, 1.33 mmol) and the mixture was stirred for 48 h at room temperature. The reaction mixture was concentrated and subjected to preparative silica-gel TLC (four plates) using ethyl acetate-hexane (3:7, v/v) as mobile phase to yield **4.183** (8.9 mg, 9%) and **4.184** (28.7 mg, 29%).

b) FeCl₃.6H₂O oxidation

To a solution of **2.56** (480 mg, 2.1 mmol) in CH₂Cl₂ (145 mL) was added FeCl₃·6H₂O (570 mg, 2.1 mmol) and the mixture was stirred for 24 h at room temperature. The reaction mixture was concentrated and subjected to preparative silica-gel TLC (ten plates) using ethyl acetate-hexane (3:7, v/v) as mobile phase to yield **4.183** (48.7 mg, 10%).

c) CuBr₂ oxidation

To a solution of **2.56** (100 mg, 0.44 mmol) in CH₂Cl₂ (20 mL) was added CuBr₂ anhydrous (198 mg, 0.88 mmol) and the mixture was stirred for 48 h at room temperature. The reaction mixture was concentrated and subjected to preparative silica-gel TLC (four plates) using ethyl acetate-hexane (3:7, v/v) as mobile phase to yield **4.183** (19.4 mg, 19%).

d) FeCl₃·6H₂O/NaI oxidation

To a solution of **2.56** (100 mg, 0.44 mmol) in CH₂Cl₂ (20 mL) was added FeCl₃·6H₂O (180 mg, 0.66 mmol) followed by NaI (600 mg, 3.98 mmol) and the mixture was stirred for 24 h at room temperature. The reaction mixture was concentrated and subjected to preparative silica-gel TLC (four plates) using ethyl acetate-hexane (3:7, v/v) as mobile phase to yield **4.183** (37 mg, 37%).

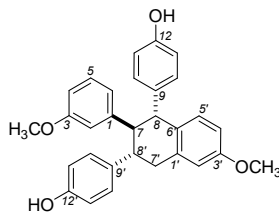
e) AgOAc oxidation in dichloromethane

To a solution of **2.56** (50 mg, 0.2 mmol) in CH₂Cl₂ (10 mL) was added AgOAc (33 mg, 0.2 mmol) and the mixture was stirred for 24 h at room temperature. The reaction mixture was concentrated and subjected to preparative silica-gel TLC (two plates) using ethyl acetate-hexane (3:7, v/v) as mobile phase to yield **4.184** (27 mg, 48%).

f) AgOAc oxidation in mixture of dichloromethane and methanol.

To a solution of **2.56** (50 mg, 0.2 mmol) in a 10 mL mixture of CH₂Cl₂/MeOH (7:3, v/v) was added AgOAc (33 mg, 0.2 mmol) and the mixture was

stirred for 48 h at room temperature. The reaction mixture was concentrated and subjected to preparative silica-gel TLC (two plates) using ethyl acetate-hexane (3:7, v/v) as mobile phase to yield **4.184** (13.4 mg, 24%).



Tetrahydronaphthalene 4.183

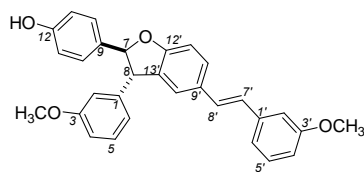
UV: (λ_{\max}^{MeOH}): 320 nm.

IR(film) ν_{\max} : 3392, 3026, 2932, 2835, 1597, 1507, 1237 cm^{-1}

ESI-TOF-MS(-): $[\text{M}-\text{H}]^-$; m/z 451.1882 measured, 451.1909 calculated for $\text{C}_{30}\text{H}_{27}\text{O}_4$,
 $m/m = -6.0$ ppm

^1H NMR (CDCl_3 , 500MHz) 6.66 (d, 1 H, $J=2.7$ Hz, H2), 6.63 (dd, 1 H, $J=2.7$ Hz, $J=8.8$ Hz, H4), 6.72 (d, 1 H, $J=8.8$ Hz, H5), 3.23 (dd, 1 H, $J=12.0$ Hz, $J=16.4$ Hz, H7a), 3.06 (dd, $J=4.2$ Hz, $J=16.4$ Hz, H7b), 3.36 ("t"d, 1 H, $J=12.0$ Hz, 11.0 Hz, 4.2 Hz, H8), 6.93 (d, 1 H, $J=8.5$ Hz, H10/14), 6.54 (d, 1 H, $J=8.5$ Hz, H11/13), 3.77 (s, 3 H, 3-OCH₃), 6.32 (bs, 1 H, H2'), 6.45 (dd, 1 H, $J=2.2$ Hz, $J=7.9$ Hz, H4'), 6.87 (t, 1 H, $J=7.9$ Hz, $J=5'$ Hz), 6.40 (bd, 1 H, $J=7.9$ Hz, H6'), 3.14 ("t", 1 H, $J=11.0$ Hz, H7'), 4.16 (d, 1 H, $J=10.5$ Hz, H8'), 6.70 (d, 1 H, $J=8.3$ Hz, H10'/14'), 6.56 (d, 1 H, $J=8.3$ Hz, H11'/13'), 3.57 (s, 3 H, 3 ϕ -OCH₃)

^{13}C NMR (CDCl_3 , 125 MHz) 138.1 (1), 112.7 (2), 157.6 (3), 112.5 (4), 131.2 (5), 132.5 (6), 40.5 (7), 46.0 (8), 136.6 (9), 128.8 (10/14), 115.1 (11/13), 153.6 (12), 55.3 (3-OCH₃), 144.7(1 ϕ), 114.6 (2 ϕ), 158.9 (3 ϕ), 111.0 (4 ϕ), 128.6 (5 ϕ), 121.3 (6 ϕ), 56.7 (7 ϕ), 53.9 (8 ϕ), 137.9 (9 ϕ), 130.3 (10'/14'), 114.9 (11'/13'), 153.7 (12 ϕ), 55.1 (3 ϕ -OCH₃)



δ -Viniferin analogue 4.184

UV: ($\lambda_{\max}^{\text{MeOH}}$): 310 nm.

IR (film) ν_{\max} : 3392, 3023, 2936, 2835, 1598 cm^{-1}

ESI-TOF-MS(-): $[\text{M}-\text{H}]^-$; m/z 449.1761 measured, 449.1753 calculated for $\text{C}_{30}\text{H}_{25}\text{O}_4$,

$m/m = 1.8$ ppm

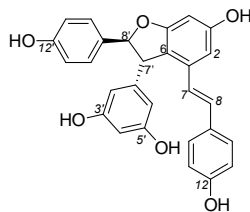
$^1\text{H NMR}$ (CDCl_3 , 500MHz) 6.73 (t, 1 H, $J=2.0$ Hz, H2), 6.84 (ddd, 1 H, $J=0.7$ Hz, $J=2.4$ Hz, $J=8.3$ Hz, H4), 7.26 (t, 1 H, $J=7.8$ Hz, H5), 6.79 (dd, 1 H, $J=1.5$ Hz, $J=7.8$ Hz, H6), 4.53 (d, 1 H, $J=8.5$ Hz, H7), 5.50 (d, 1 H, $J=8.5$ Hz, H8), 7.23 (d, 1 H, $J=8.3$ Hz, H10/14), 6.80 (d, 1 H, $J=8.5$ Hz, H11/13), 6.97 (t, 1 H, $J=2.0$ Hz, H2 ϕ), 6.77 (dd, 1 H, $J=2.4$ Hz, H4 ϕ), 7.24 (t, 1 H, $J=7.8$ Hz, H5 ϕ), 7.03 (d, 1 H, $J=7.8$ Hz, H6 ϕ), 6.87 (d, 1 H, $J=16.4$ Hz, H7 ϕ), 7.02 (d, 1 H, $J=16.4$ Hz, H8 ϕ), 7.18 (bs, 1 H, H10 ϕ), 6.92 (d, 1 H, $J=8.3$ Hz, H13 ϕ), 7.37 (dd, 1 H, $J=1.47$ Hz, $J=8.3$ Hz, H14 ϕ), 3.81 (s, 3 H, H3 ϕ -OMe), 3.77 (s, 3 H, H3-OMe).

$^{13}\text{C NMR}$ (CDCl_3 , 125 MHz) 143.1 (1), 114.2 (2), 159.8 (3), 112.5 (4), 129.9 (5), 120.8 (6), 57.6 (7), 93.2 (8), 132.6 (9), 127.6 (10/14), 115.5 (11/13), 155.7 (12), 139.1 (1 ϕ), 111.4 (2 ϕ), 159.974 (3 ϕ), 112.9 (4 ϕ), 129.6 (5 ϕ), 118.9 (6 ϕ), 126.2 (7 ϕ), 128.8 (8 ϕ), 130.8 (9 ϕ), 123.1 (10 ϕ), 130.9 (11 ϕ), 159.7 (12 ϕ), 109.7 (13 ϕ), 127.9 (14 ϕ), 159.85 (3 ϕ -OMe), 159.97 (3-OMe).

4.5.3. Oligomerisation of 2.52

4.5.3.1. Preparation of 1.4 and 1.0

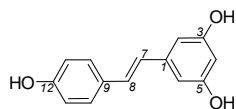
To a solution of **2.52** (40 mg, 0.15 mmol) in a 2 mL mixture of H₂O/MeOH (1:1, v/v) was added FeCl₃·6H₂O (51 mg, 0.19 mmol) and the mixture was stirred for 48 h at room temperature. The reaction mixture was concentrated and subjected to preparative silica-gel TLC (two plates) using ethyl acetate-hexane (4:6, v/v) to yield ϵ -viniferin **1.4** (2 mg, 6%) and resveratrol **1.0** (5 mg, 15%), as by product.



ϵ -Viniferin **1.4**

¹H NMR (500 MHz, deuterated acetone) δ ppm: O-H 8.17 (bs), H11/13 7.20 (d; J = 8.2 Hz; 2 H), H11/13 7.05 (d, J = 8.2 Hz; 2 H), H8 6.92 (d; J = 16.3 Hz; 1 H), H10/14 6.84 (d; J = 8.2 Hz; 2 H), H10/14 6.74 (d; J = 8.2 Hz; 2 H), H4 6.73 (s, 1 H), H7 6.72 (d; J = 16.3 Hz; 1 H), H2 6.33 (d; J = 2.7 Hz; 1 H), H2/6 6.25 (s; 2 H), H4 6.25 (s; 1 H), H8/5 5.43 (d; J = 5.5 Hz; 1 H), H7/3 4.48 (d; J = 5.5 Hz; 1 H).

See Appendix 58 for ¹H NMR spectrum of compound **1.4**. The analytical data for **1.4** matched with the previously reported data of the natural isolate.⁶⁶



Resveratrol 1.0

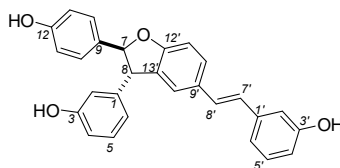
$^1\text{H NMR}$ (500 MHz, deuterated acetone) δ ppm: H14/10 7.42 (d; $J = 7.5$ Hz; 2 H), H7 7.02 (d; 16.3; 1 H), H8 6.89 (d; 16.3; 1 H), H13/11 6.84 (d; $J = 8.8$ Hz; 2 H), H6/2 6.54 (d; $J = 2.5$ Hz; 2 H), H4 6.27 (t; $J = 2.5$ Hz; 1 H).

See Appendix 59 for $^1\text{H NMR}$ spectrum of compound **1.0**. The analytical data for **1.0** matched with the previously reported data of the natural isolate.⁶⁷

4.5.4. Oligomerisation of 2.58

To a solution of **2.58** (50 mg, 0.24 mmol) in a 2 ml of MeOH was added PbO_2 (56 mg, 0.24 mmol) and the mixture was stirred for 48 h at room temperature. The reaction mixture was concentrated and subjected to preparative silica-gel TLC (two plates) using ethyl acetate-hexane (4:6, v/v) as mobile phase to yield **4.186** (13.5 mg, 28%)

4.5.4.1. Preparation of 4.186



δ -Viniferin analogue 4.186

ESI-TOF-MS(+): $[\text{M}+\text{H}]^+$; m/z 423.1581 measured, 423.1591 calculated for $\text{C}_{28}\text{H}_{23}\text{O}_4$,
 $m/m = 2.4$ ppm.

$^1\text{H NMR}$ (500 MHz, deuterated acetone) δ ppm: OH 8.33 (bs), H14 7.47 (d; $J = 8.3$ Hz; 1 H), H10 7.25 (d; $J = 8.5$ Hz; 2 H), H10' 7.26 (s; 1 H), H5 7.19 (t; $J = 7.8$ Hz; 1

H), H5 7.15 (t; J = 7.9 Hz; 1 H), H2 7.15 (s, 1 H), H8 7.14 (d; J = 16.3 Hz; 1 H), H6 7.03-7.01 (m; 1 H), H4 7.03-7.01 (m; 1 H), H7 6.99 (d; J = 16.3 Hz; 1 H), H13 6.91 (d; J = 8.3 Hz; 1 H), H11 6.86 (d; J = 8.6 Hz; 2 H), H6 6.78 (dd; J = 8.2 Hz, 1.6 Hz; 1 H), H4 (m; 1 H), H2 6.70-6.75 (m; 1 H), H8 5.49 (d; J = 8.1 Hz; 1 H), H7 4.58 (d; J = 8.1 Hz; 1 H).

See Appendix 60 for ¹H NMR spectrum of compound **4.186** and Appendix 61 for ESI-TOF-MS (+) spectrum of **4.186**. The above structure was determined by comparison of its spectroscopic data with those of compound **4.184** and **4.14**.

References

1. D. H. R. Barton, A. M. Defflorin and O. E. Edwards, *J. Chem. Soc.*, 1956, 530.
2. R. Thomas, *Nat. Prod. Rep.*, 2004, **21**, 224-248.
3. S. Sotheeswaran and V. Pasupathy, *Phytochemistry*, 1993, **32**, 1083-1092.
4. Y. Takaya, K.-X. Yan, K. Terashima, Y.-H. He and M. Niwa, *Tetrahedron*, 2002, **58**, 9265-9271.
5. K.-X. Yan, K. Terashima, Y. Takaya and M. Niwa, *Tetrahedron*, 2001, **57**, 2711-2715.
6. C. Ponzoni, E. Beneventi, M. R. Cramarossa, S. Raimondi, G. Trevisi, U. M. Pagnoni, S. Riva, and L. Forti, *Adv. Synth. Catal.*, 2007, **349**, 1497-1506.
7. Y. Takaya, K. Terashima, J. Ito, Y.-H. He, M. Tateoka, N. Yamaguchi and M. Niwa, *Tetrahedron*, 2005, **61**, 10285-10290.
8. W. Li, H. Li, Y. Li, and Z. Hou, *Angew. Chem. Int. Ed.*, 2006, **45**, 7609-7611.
9. P. Langcake and R. J. Pryce, *Chem. Commun.* 1977, 208-210.
10. Y. Hirano, R. Kondo and K. Sakai, *J. Wood Sci.*, 2002, **48**, 64-68.
11. L. M. Szewczuk, S. H. Lee, I. A. Blair and T. M. Penning, *J. Nat. Prod.*, 2005, **68**, 36-42.
12. R. Pezet, *FEMS Microbiol. Lett.*, 1998, **167**, 203-208.
13. A.-C. Breuil, M. Adrian, N. Pirio, P. Meunier, R. Bessis and P. Jeandet, *Tetrahedron Lett.*, 1998, **39**, 537-540.
14. R. H. Cichewicz, S. A. Kouzi, and M. T. Hamann, *J. Nat. Prod.*, 2000, **63**, 29-33.
15. S. Nicotra, M. R. Cramarossa, A. Mucci, U. M. Pagnoni, S. Riva and L. Forti, *Tetrahedron*, 2004, **60**, 595-600.

- 16 M. Sbaghi, P. Jeandet, R. Bessis and P. Leroux, *Plant Pathol.*, 1996, **45**, 139-144.
- 17 A.-C. Breuil, P. Jeandet, M. Adrian, F. Chopin, N. Pirio, P. Meunier and R. Bessis, *Phytopathology*, 1999, **89**, 298-302.
- 18 J. Ito and M. Niwa, *Tetrahedron*, 1996, **52**, 9991-9998.
- 19 S. He, B. Wu, Y. Pan, and L. Jiang, *J. Org. Chem.*, 2008, **73**, 5233-5241.
- 20 K.-S. Huang, M. Lin and Y.-H. Wang, *Chin. Chem. Lett.*, 1999, **10**, 817-820.
- 21 C.-S. Yao, M. Lin and Y.-H. Wang, *Chin. J. Chem.*, 2004, **22**, 1350-1355.
- 22 K.-S. Huang, M. Lin, L.-N. Yu and M. Kong, *Tetrahedron*, 2000, **56**, 13216-1329.
- 23 M. Sako, H. Hosokawa, T. Ito, and M. Iinuma, *J. Org. Chem.*, 2004, **69**, 2598-2600.
- 24 C.-S. Yao, L.-X. Zhou and M. Lin, *Chem. Pharm. Bull.*, 2004, **52**, 238-243.
- 25 S. S. Velu, I. Buniyamin, K. C. Lee, F. Feroz, I. Noorbacha, C. G. Lim, K. Awang, I. Abd. Wahab and J. F. F. Weber, *Chem. Eur. J.*, 2008, **14**, 11376-11384.
- 26 N.F. Thomas, K. C. Lee, Thomas Paraidathathu, J. F. F. Weber, K. Awang, D. Rondeau, *Tetrahedron*, 2002, **58**, 7201-7206.
- 27 L. X. Zhou and M. Lin, *Chin. Chem. Lett.*, 2000, **11**, 515-516.
- 28 K. Baba, T. Kido, K. Maeda, M. Taniguchi and M. Kozawa, *Phytochemistry*, 1992, **31**, 3215-3218.
- 29 Y. Yang, P. Bie, C. Zhang and X. Pan, *J. Chem. Res. (S)*, 2003, 266-267.
- 30 M. F. Wang, Y. Jin and C-T. Ho, *J. Agric. Food Chem.*, 1999, **47**, 3974-3977.
- 31 Y. Takaya, K.-X. Yan, K. Terashima, J. Ito and M. Niwa, *Tetrahedron.*, 2002, **58**, 7259-7265.
- 32 Z. Jin, Q. Wang, and R. Huang, *Synthetic Communications*, 2004, **34**, 119-128.

- 33 X.-M. Li, K.-S. Huang, M. Lin and L.-X. Zhou, *Tetrahedron*, 2003, **59**, 44056-4413.
- 34 L. Panzella, M. De Lucia, C. Amalfitano, A. Pezzella, A. Evidente, A. Napolitano and M. d'Alò, *J. Org. Chem.*, 2006, **71**, 4246-4254.
- 35 J. M. Aguirre, E. N. Alesso and G. Y. Moltrasio Iglesias, *J. Chem. Soc., Perkin Trans. 1*, 1999, 1353-1358.
- 36 X.-C. Li and D. Ferreira. *Tetrahedron.*, 2003, **59**, 15016-1507.
- 37 E. Alesso, R. Torviso, M. Erlich, L. Finkielstein, B. Lantano, G. Moltrasio, J. Aguirre, P. Vazquez, L. Pizzio, C. Caceres, M. Blanco, and H. Thomas, *Synth. Commun.*, 2002, **32**, 3803-3812.
- 38 M. Niwa, J. Ito, K. Terashima, T. Koizumi, Y. Takaya, and K.-X. Yan, *Heterocycles.*, 2000, **53**, 1475-1478.
- 39 K. C. Nicolaou, T. R. Wu, Q. Kang, and D. Y.-K. Chen, *Angew. Chem. Int. Ed.*, 2009, **121**, 3492-3495.
- 40 a) S. A. Snyder, A. L. Zografos, and Y. Lin, *Angew. Chem. Int. Ed.* 2007, **46**, 1-7. b) S. A. Snyder, S. P. Breazzano, A. G. Ross, Y. Lin, and A. L. Zografos, *J. Am. Chem. Soc.*, 2009, **131**, 1753-1765.
- 41 J. L. Jeffrey and R. Sarpong, *Tet. Lett.*, 2009, **50**, 1969-1972.
- 42 G. A. Kraus and I. Kim, *Org. Lett.*, 2003, **5**, 1191-1192.
- 43 G. A. Kraus and V. Gupta, *Tet. Lett.*, 2009, **50**, 7180-7183.
- 44 I. Kim and J. Choi, *Org. Biomol. Chem.*, 2009, **7**, 2788-2795.
- 45 A. C. Breuil, M. Adrian, N. Pirio, P. Meunier, R. Bessis, P. Jeandet, *Tetrahedron Lett.*, 1998, **39**, 537-540.
- 46 A. P. Lins, J. D. Felicio, M. M. Braggio, L. C. Roque, *Phytochemistry*, 1991, **30**, 3144.

- 47 a) R. G. Pearson, *Chemical hardness - Applications from molecules to solids*, Wiley-VCH, Weinheim, 1997. b) R. G. Pearson, *J. Am. Chem. Soc.* 1963, **85**, 3533-3539.
- 48 V. D. Parker and L. Ebersson, *Chem Commun.*, 1969, **108**, 340.
- 49 E. Steckhan, *J. Am. Chem. Soc.*, 1978, **100**, 3526-3533.
- 50 N. F. Thomas, S. S. Velu, J. F. F. Weber, K. C. Lee, A. Hamid. A. Hadi, P. Richomme, D. Rondeau, I. Noorbacha, K. Awang, *Tetrahedron*, 2004, **60**, 11733-11742.
- 51 C. Reichardt, *Solvents and solvent effects in organic chemistry*, 2nd edition, VCH, Weinheim, 1988.
- 52 I. Fleming. *Frontier orbitals and organic chemical reactions*, John Wiley & Sons, Chichester, pp 34-35, 1976.
- 53 C. K. Kim, K. A. Lee, C. K. Kim, B. S. Lee and H. W. Lee, *Chem. Phys. Lett.*, 2004, **391**, 321-324
- 54 J. H. Kim, B. R. Min, C. K. Kim, J. Won, Y. S. Kang, *J. Phys. Chem. B*, 2002, **106**, 2786-2790.
- 55 R. F. Sweis, M. P. Schramn, S. A. Kozmin, *J. Am. Chem. Soc.*, 2004, **126**, 7442-7443.
- 56 S. W. Youn, J. I. Eom, *J. Org. Chem.* 2006, **71**, 6705-6707; d) X. Yao, C. J. Li, *Org. Lett.* 2005, **7**, 4395-4398.
- 57 X. Yao, C. J. Li, *Org. Lett.*, 2005, **7**, 4395-4398.
- 58 T. Majima, S. Tojo, A. Ishida and S. Takamuku, *J. Phys. Chem.*, 1996, **100**, 13615-13623.
- 59 A. K. Arakaki, E. G. Orellanos, N. B. Calcaterras, J. Ottados, E. A. Ceccarellis, *J. Biol. Chem.*, 2001, **276**, 44419-44426.

- 60 T. Majima, S. Tojo, A. Ishida and S. Takamuku, *J. Org. Chem.* 1996, **61**, 7793-7800.
- 61 D. Crich, F. Brebion, D.-H. Suk. Generation of alkene radical cations by heterolysis of β -substituted radicals: Mechanism, stereochemistry and application in synthesis. [in] A. Gansäuer (Ed.). *Top. Curr. Chem.*, vol. 263 - Radicals in synthesis 1, pp 1-38, Elsevier, Amsterdam, 2006.
- 62 N. F. Thomas, K. C. Lee, T. Paraidathathu, J. F. F. Weber and K. Awang, *Tetrahedron Lett.*, 2002, **43**, 3151-3155.
- 63 Y. Maeda, T. Hashimoto, K. Satoh, D. A. Tryk and A. Fujishima, *Journal of The Surface Finishing Society of Japan*, 2003, **54**, 64-68.
- 64 M. A. Khan, S. G. Nabi, S. Prakash and A. Zaman, *Phytochemistry*, 1986, **25**, 1945-1948.
- 65 Y. Takaya, K.-X. Yan, K. Terashima, Y.-H. He and M. Niwa, *Tetrahedron*, 2002, **58**, 9265-9271.
- 66 M. Bourhis, N. Theodore, J. F. Weber, J. Vercauteren, *Polyphenols Communication 96*, Bordeaux (France), July 15-18, 1996, pp 43-44.
- 67 G. S. Jayatilake, H. Jayasuriya, E.-S. Lee, N. M. Koonchanok, R. L. Geahlen, C. L. Ashendel, J. L. Mclaughlin and C. H. Chang, *J. Nat. Prod.*, 1993, **56**, 1805-1810.